Modeling Precursor Lesions by Targeting Key Molecular Pathways in High-Grade Serous Ovarian Cancer

BY

DIMPLE ASHOK MODI
B.Pharm., University of Mumbai, India, 2009
M.S., University of Southern California, Los Angeles, 2011

THESIS

Submitted as partial fulfillment of the requirements
for the degree of Doctor of Philosophy in Pharmacognosy
in the Graduate College of the
University of Illinois at Chicago, 2016

Chicago, Illinois

Defense Committee:

Dr. Joanna E. Burdette, Chair and Advisor
Dr. Judy Bolton
Dr. Douglas Thomas
Dr. Carlos Stocco, Physiology and Biophysics
Dr. Maria Barbolina, Biopharmaceutical Sciences

TO MY GRANDPARENTS

for raising me to believe that anything is possible

and for always believing in me

ACKNOWLEDGEMENTS

Words are not sufficient to thank my advisor, Dr. Joanna E. Burdette, who is the best mentor anyone could ever ask for. Throughout this spectacular journey, Joanna has truly been a friend, philosopher and guide. She is an inspiration and I consider myself very fortunate for getting the opportunity to be trained by her. Joanna has extended unconditional support and encouragement throughout my doctorate journey, by helping me think critically and argue scientifically. There is a lot to thank her for, beyond the scientific training, and I can keep going, but honestly, words would neither be enough nor do justice.

Upon joining Joanna's lab, I became a part of the "Burdette family". Dr. Shelby King was instrumental in teaching me all the fundamental techniques during my rotation. I would like to thank Dr. Sharon Eddie for being a wonderful friend and a great sounding board. Dr. Fern Toh taught me to never give up and I thank her for her constant encouragement. I thank Subbulakshmi Karthikeyan for providing valuable perspective on balancing research and life outside the lab. Over the years, I have been fortunate to work with and learn from incredibly talented individuals - Dr. Michael Endsley, Dr. Angela Russo, Dr. Matthew Dean, Dr. Suzanne Quartuccio, Dr. Eoghainín Ó hAinmhire, Dr. Georgette Heyrman, David Davis, Daniel Lantvit, Wei-Lun Chen, Alexandria Young and Laura Rodgers. All these people have contributed in several ways to my overall development as a scientist. I thank Rosemarie and Sylvia for being the best mentees ever. Above all, I thank each of them for being the best colleagues that anyone could ask for.

ACKNOWLEDGEMENTS (continued)

I extend my gratitude to my prelim committee member, Dr. Teresa K. Woodruff for her career guidance and for inspiring me to pursue STEM outreach to schoolgirls. I would also like to thank my thesis committee members, Dr. Judy Bolton, Dr. Douglas Thomas, Dr. Maria Barbolina and Dr. Carlos Stocco for their guidance and support. Outside of my committee, I whole-heartedly thank the CPB community for providing a pleasant work atmosphere.

I am fortunate to have some amazing friends that have always been there when I needed them the most. I thank Nidhi, Sonam, Tanay, Pulkit, Chaitanya and Rahul for being my strongest support system. Finally, this journey would not be complete without thanking my parents who always believed in me and most importantly, taught me that I could achieve anything if I worked hard enough. I thank my sister, Aastha and sister-in-law, Forum for being the best cheerleaders. I sincerely thank my mother- and father-in-law for their unconditional love. Lastly, I would like to thank my husband, Yash for being my greatest strength and source of empowerment. Thanks for cheering me when my experiments failed and for keeping up with my excitement when my cells looked green (!!) or when my replicates showed statistical significance! Thank you for the support and above all, believing in me.

DAM

CONTRIBUTIONS OF AUTHORS

Chapter I is a literature review that provides background information about the field with particular emphasis on the fallopian tube as the source of origin of high-grade serous cancer and importance of understanding the regulation of PAX2 as an early marker of serous tumorigenesis. Chapter II summarizes research methods and reagents utilized to execute experiments. Majority of this chapter has been published previously[23,89,92]. Chapter III is a published manuscript for which I was one of the primary authors[23]. Dr. Tyvette Hilliard and I jointly contributed to the data and manuscript writing. Chapter IV represents a series of experiments that are currently unpublished. Figures 14D, 14E and 14F were generated by Rosemarie D. Tagare. Daniel Lantvit and David Davis contributed to figures 19B and 19C. Dr. Kiira Ratia provided the compounds used in the biological screen. Chapter V is a published manuscript for which I was the primary author[89]. Dr. Suhair Sunoqrot generated figures 25 and 28. Dr. Seungpyo Hong participated in the study design and preparation of manuscript. Chapter VI contains a comprehensive summary of my dissertation and its overall contribution to the field of study, including future implications and exploratory avenues in ovarian cancer research. Appendix “A” is a published manuscript for which I was the second author[92]. Dr. Shelby M. King, Dr. Sharon L. Eddie and I contributed to the data generation and analysis. Dr. Joanna E. Burdette participated in the design of all the studies and preparation of the manuscripts.

TABLE OF CONTENTS

TABLE OF CONTENTS (continued)

LIST OF TABLES

LIST OF FIGURES

LIST OF FIGURES (continued)

LIST OF FIGURES (continued)

LIST OF ABBREVIATIONS

3D	Three-dimensional
Amhr	Anti-Müllerian hormone receptor
BCA	Bicinchoninic acid
Brdu	Bromodeoxyuridine
CDK2	Cyclin-dependent kinase 2
Cdkn2a	Cyclin-dependent kinase inhibitor 2A
ChIP	Chromatin immunoprecipitation
CICs	Cortical inclusion cysts
CK8	Cytokeratin 8
DMSO	Dimethylsulfoxide
ECM	Extracellular matrix
EGFR	Epidermal growth factor receptor
EIN	Endometrial intraepithelial neoplasia
EOC	Epithelial ovarian cancer
EPR	Enhanced permeability and retention
ER	Estrogen receptor
FAR	Folic acid receptor
FDA	Food and drug administration
FITC	Fluorescein isothiocyanate
FSH	Follicle stimulating hormone
FSHR	Follicle stimulating hormone receptor
FSHR	Follicle stimulating hormone receptor

LIST OF ABBREVIATIONS (continued)

FTE	Fallopian tube epithelium
FUT8	Fucosyl transferase 8
G5	Generation 5
GSK3β	Glycogen Synthase Kinase 3β
HD	Homeodomain
HGSC	High-grade serous ovarian cancer
HR	Homologous repair
HTS	High-throughput screen
i.p.	Intraperitoneal
IGF	Insulin-like growth factor
IGF1R	Insulin-like growth factor receptor
IGFBP	Insulin-like growth factor binding protein
IgG	Immunoglobulin G
IR	Insulin receptor
LH	Luteinizing hormone
LHR	Luteinizing hormone receptor
MAPK	Mitogen activated protein kinase
MIS	Müllerian inhibiting substance
MME	Matrix metallo endopeptidase
MOE	Murine oviductal epithelium

LIST OF ABBREVIATIONS (continued)

MOSE	Murine ovarian surface epithelium
NP	Polymeric nanoparticles
OSE	Ovarian surface epithelium
PAGE	Polyacrylamide gel electrophoresis
PAMAM	Polyamidoamine
PARP	Poly ADP ribose polymerase
PAX2	Paired box
PBS	Phosphate buffered saline
PCOS	Polycystic ovary syndrome
PD	Paired domain
PEG-PLA	Polyethylene glycol-b-polylactide
PFA	Paraformaldehyde
PI3K	Phosphatidylinositol 3-kinase
PTIP	Pax transactivation-domain interacting protein
qPCR	Quantitative real time polymerase chain reaction
RCC	Renal cell carcinoma
s.c.	Subcutaneous
SCOUTs	Secretory cell outgrowths
SEE-FIM	Sectioning and extensively examining the fimbriated end
SEER	Surveillance, epidemiology, and end results
SRB	Sulforhodamine B

LIST OF ABBREVIATIONS (continued)

STICs	Serous tubal intraepithelial carcinomas
STILs	Serous tubal intraepithelial lesions
TCA	Trichloroacetic acid
TCGA	The cancer genome atlas
TD	Transactivation domain
VEGF	Vascular endothelial growth factor

SUMMARY

Ovarian cancer is the deadliest gynecological malignancy due to the lack of information regarding early events in cancer formation that would allow for effective prevention and therapeutic strategies. One of the major confounding issues in the field is that the epithelial subtype responsible for high-grade serous ovarian cancer (HGSC) is not known and could either be the ovarian surface epithelium (OSE) or the fallopian tube epithelium (FTE) or both. If investigators have been comparing biomarkers in cancer patients to normal OSE and this was never the source of the cancer, then all the current markers might be flawed. Developing robust models is therefore critical for establishing early pathways that are responsible for disease pathogenesis and understanding if specific targets are reflective of changes from the cell type where the cancer originates.

Primary cell culture and animal models are necessary so manipulations can be made that transition a normal cell into a transformed one, allowing the source epithelium of the cancers to be determined. Three-dimensional (3D) primary culture is superior to traditional two-dimensional (2D) systems because it recapitulates the *in vivo* physiology more accurately and allows for the culture of separate epithelium to ensure the origin can be uncovered.

“Regardless of organ site, the process of ovulation contributes to ovarian cancer through three major mechanisms: wound induced proliferative repair, hormonal stimulation from follicle stimulating hormone (FSH) and luteinizing hormone (LH), and exposure to oxidative stress from inflammation. The gonadotropins, FSH and LH, have been implicated as growth factors in ovarian cancer. The pathways activated by FSH

and LH in normal OSE grown in their microenvironment were investigated. Gonadotropins increased proliferation in both 3D ovarian organ culture and in a 2D normal mouse OSE cell line. A mouse cancer pathway qPCR array using mRNA collected from 3D organ cultures identified Akt as a transcriptionally upregulated target following stimulation with FSH, LH and the combination of FSH and LH. Activation of additional pathways, such as Birc5, Cdk2, Cdk4, and Cdkn2a identified in the 3D organ cultures, were also validated. Akt and epidermal growth factor receptor (EGFR) inhibitors blocked gonadotropin-induced cell proliferation in 3D organ and 2D cell culture. OSE isolated from 3D organ cultures stimulated with LH or hydrogen peroxide initiated growth in soft agar. Hydrogen peroxide stimulated colonies were further enhanced when supplemented with FSH. LH colony formation and FSH promotion were blocked by Akt and EGFR inhibitors. These data suggested that the gonadotropins stimulate some of the same proliferative pathways in normal OSE that are activated in ovarian cancers." [23]

Rapid advances have been made in modeling serous pathogenesis from the fallopian tube epithelium, which is proposed to be the source of origin of most serous ovarian cancers. However, the existing models fail to recapitulate the molecular basis of early precursor lesion development from the FTE. Loss of PAX2 is one of the earliest reported changes identified in the FTE that may define the transition of the normal FT epithelium into benign lesions. PAX2 is a transcription factor and an epigenetic modifier and is lost in areas of secretory cell outgrowth (SCOUTs), p53 signatures, serous tubal intraepithelial carcinomas (STICs) and serous cancer. SCOUTs progress to p53

signatures, when p53 is mutated, and may ultimately progress to STICs and HGSC. PAX2 expression remains undetectable in tumors. Little is known regarding what regulates PAX2 loss in the fallopian tube, the functional significance of its loss, and whether re-expression of PAX2 in HGSC may slow or halt tumor growth.

Combination of PAX2 loss and mutant *TP53* in murine fallopian (oviductal) epithelium (MOE) cells altered functional characteristics *in vitro* but was insufficient to drive tumorigenesis *in vivo*. These models recapitulate early benign lesions and suggest that a latency period exists between early lesions and tumor formation that may allow for intervention of prevention. *Stathmin, fut8* and *mme* were identified as possible novel targets downstream of PAX2 in MOE cells and may play a role in progression from benign to malignant lesions. Re-expression of PAX2 in PAX2-null human HGSC cells reduced tumorigenic properties via apoptosis. While HGSC cells are of unknown origin, MOE cells harboring PTEN silencing that produced peritoneal tumor explants were derived from a known source; murine oviducts. Reduced levels of PTEN negatively regulated PAX2 expression in MOE cells and stable re-expression of PAX2 reduced the pro-proliferative and pro-migratory effects from PTEN silencing. PAX2 was determined to be a direct transcriptional target of p53 whereas mutant *TP53* inhibited p53-mediated PAX2 transcriptional activation in MOE. A novel small molecule screen identified a molecule that can activate PAX2 expression in MOE cells. This molecule has the potential to be used as a preventive measure in women without genetic predisposition to HGSC. In order to accurately model pelvic serous carcinogenesis, it is critical to determine the mechanism of early precursor formation and the signals that are

downstream of key protein loss, such as PAX2. PAX2 re-expression holds potential use for both prevention and therapy of fallopian tube derived serous tumors.

Irrespective of the cell of origin, developing targeted novel drug delivery techniques are critical to ensure effective biological response to chemotherapeutic agents. “Current treatment modalities include a combination of surgery and chemotherapy, which often leads to loss of fertility in premenopausal women and a myriad of systemic side effects. To address these issues, poly(amidoamine) (PAMAM) dendrimers were designed to selectively target the follicle stimulating hormone receptor (FSHR), which is overexpressed by tumorigenic ovarian cancer cells but not by immature primordial follicles and other non-tumorigenic cells. Fluorescein-labeled generation 5 (G5) PAMAM dendrimers were conjugated with the binding peptide domain of FSH (FSH33) that has a high affinity to FSHR. The targeted dendrimers exhibited high receptor selectivity to FSHR-expressing OVCAR-3 cells, resulting in significant uptake, while showing minimal interactions with SKOV-3 cells that do not express FSHR. The selectivity of the FSH33-targeted dendrimers was further validated in 3D organ cultures of normal mouse ovaries. Immunostaining of the conjugates revealed their selective binding and uptake by ovarian surface epithelium (OSE) cells that express FSHR, while sparing the immature primordial follicles. An *in vivo* study monitoring tissue accumulation following a single i.p. injection of the conjugates showed significantly higher accumulation of FSH33-targeted dendrimers in the ovary and oviduct compared to the non-targeted conjugates. These proof-of-concept findings highlight the potential of these FSH33-targeted dendrimers to serve as a delivery

platform for anti-ovarian cancer drugs, while reducing their systemic side effects such as preventing nonspecific uptake by the primordial follicles." [89]

Overall, we need to take advantage of the emerging evidence demonstrating a series of pre-neoplastic lesions that precede HGSC in the fallopian tube. Serum biomarkers for finding HGSC early have been elusive and once diagnosed, the disease is typically metastatic and quickly becomes resistant to front line therapies. Understanding the influence of gonadotropins, high levels of insulin and IGF on the FTE cells in presence of genetic aberrations commonly observed in serous cancer will generate new hypothesis and research direction as to how fallopian tube cells drive serous cancer formation. A new approach that could block or reverse pre-neoplastic lesions or replace key proteins lost during progression is needed, especially in this type of tumor that is difficult to diagnose and detect early.

I. INTRODUCTION

A. Ovarian Cancer Statistics

Ovarian cancer continues to be the fifth leading cause of cancer related deaths among women in the world and the most lethal gynecological malignancy with the highest mortality rate[1]. The American Cancer Society predicts 22,280 new cases and 14,240 deaths from ovarian cancer in 2016[1]. As per the Surveillance, Epidemiology, and End Results (SEER) program statistics, the 5-year survival rates from 1975 to 2012 have been fairly constant, with a modest improvement of 7%[2]. When diagnosed at early stages (localized to reproductive tissues), the 5-year survival rate is 92%, however, only 15% of cases are detected at this stage. The majority of ovarian cancers (~61%) are diagnosed when the disease has metastasized to the peritoneal cavity, when the 5-year survival rate sharply drops to 27%[1-3]. The high mortality rate can be attributed to ineffective early detection strategies, ambiguous signs and symptoms, chemoresistance, and a lack of specific biomarkers.

B. Ovarian Cancer Classification

Ovarian cancer is a heterogeneous disease that is comprised of three main tumor types: i) germ cell, ii) sex cord stromal and iii) epithelial ovarian cancer (EOC), with EOC being the most common type accounting for approximately 90% of all ovarian tumors[4]. EOC is further classified into four histological subtypes based on their morphological resemblance to tissues of the female reproductive tract. These are: i) clear cell carcinomas (resembles the gestational endometrium), ii) mucinous (resembles the endocervix), iii) endometrial (resembles the endometrium) and iv)

serous (resembles the fallopian tube epithelium). Based on recent histopathological and genetic studies, EOC is divided into Type I and Type II tumors[5]. Type I tumors consist of low-grade serous, low-grade endometrioid, clear cell and mucinous carcinomas and Brenner tumors. Type II tumors include **high-grade serous**, high-grade endometrioid, malignant mixed mesodermal tumors and undifferentiated carcinomas[5]. Type I tumors are typically less aggressive than Type II tumors, however Type I tumors resist conventional chemotherapy. Type I tumors demonstrate microsatellite instability and a series of mutations (*KRAS, CTNNB1, BRAF, PTEN, ARID1A, ERBB2, PIK3CA*), but never present with *TP53* mutations. In contrast, Type II tumors, almost always present with a mutation in *TP53* and are far more aggressive than Type I tumors. Type II tumors typically respond well to chemotherapy, however, their relapse rate is significantly high, in which case the tumors are often resistant to standard chemotherapies.

High-grade serous ovarian cancer (HGSC) is the most common and the most lethal histotype of EOC (Type II). Morphologically, HGSC tumors resemble the fallopian tube epithelium and genetically, about 96-100% tumors are characterized by mutation in the *TP53* gene. About 10-15% of serous cancer cases have a germline mutation in BRCA1/2 genes[6]. Additionally, somatic mutations in BRCA1/2 genes are identified in about 7% of all ovarian cancers[7]. The risk reducing strategy for this patient cohort involves prophylactic removal of ovaries and fallopian tubes prior to disease onset.

Currently, most epithelial tumors are treated with the same frontline therapy. And although, cytoreductive surgery followed by platinum-based chemotherapy and paclitaxel agents leads to disease-free survival for a short period, the relapse rate for patients with HGSC is significantly high. The difficulty in finding sufficient “normal”

tissue to work with and a low detection rate of early serous tumors has significantly slowed down the overall understanding of disease etiology and pathogenesis. The key factor, in addition to those listed previously that contributes to the high mortality, is the uncertainty of cell of origin of HGSC, which could be the ovarian surface epithelium (OSE) or the fallopian tube epithelium (FTE) or both. A probable explanation for the lack of an early, specific biomarker could be that we were working with the wrong tissue of origin. Therefore, determining the cell of HGSC origin is key to discovering early tissue specific biomarkers, understanding disease pathogenesis and etiology.

C. Risk Factors of Ovarian Cancer

Ovarian cancer is called the "silent killer" because it lacks specific signs and symptoms that can identify the disease at an early stage. Although the majority of EOCs go undetected, there are some known factors that increase the risk of developing ovarian cancer.

i. Family History

The proportion of hereditary ovarian cancers is the highest familial cancer among all cancer types[8]. Although majority cases of ovarian cancer are sporadic, about 10-15% cases of high-grade serous cancer comprise of patients representing germline *BRCA1/2* mutations. The lifetime risk of developing ovarian cancer in women harboring a mutation in *BRCA1* or *BRCA2* is 30-70% by the age of 70, HGSC being the most common histotype[9, 10]. *BRCA* genes are a part of the homologous repair (HR) pathway that assists in repairing DNA strand breaks. Mutations in *BRCA* or other members of the HR pathway lead to error-prone DNA

repair, predisposing the individual to genetic instability. The prevalence of these germline mutations may also vary by geography and ethnicity. For example, the Ashkenazi Jews have a substantially higher frequency of *BRCA1/2* founder mutations[11]. Reports demonstrate that women from a few European countries (France, Poland, Iceland) also harbor certain founder mutations in *BRCA1/2* genes that are region-specific and account for majority of familial ovarian cancer cases in their region[12].

ii. Incessant Ovulation Theory

In 1971, Fathalla and colleagues were the first group of investigators to suggest that the frequency of ovulations is directly proportional to the increased risk of developing malignant ovarian cancer from the ovarian epithelium[13]. Although the exact mechanism of ovarian cancer formation due to ovulation is not well understood, several investigators have demonstrated a plausible relationship between the "tear-and-repair" function of the ovarian surface epithelium in response to ovulation. It is fairly well established that ovulation is a highly inflammatory process that results in the release of inflammatory molecules and leads to accumulation of DNA mutations[13]. This constant process of damage and repair is believed to promote transformation of the OSE. Therefore, factors that increase lifetime ovulations, such as early menarche, late menopause, nulliparity and infertility are risk factors of ovarian cancer. The use of fertility treatments, such as hormone replacement therapy, has been reported to increase the risk of ovarian cancer. Events such as pregnancy, early menopause, and use of oral contraceptives that reduce the number of lifetime ovulations are associated with decreasing a lifetime risk of developing this disease[14-17].

Although the OSE was considered to be the source of origin for HGSC, substantial evidence now supports the fallopian tube epithelium (FTE) to be the primary source for most serous ovarian cancers. Unlike in the OSE, ovulation did not affect FTE cells proliferation as measured by bromodeoxyuridine incorporation in superovulated animals as compared to unstimulated animals[18]. However, ovulation did increase phospho-$_{\gamma}H_2AX$ staining indicating that these fallopian tube epithelial cells are susceptible to DNA damage[18]. Hypothetically, the close proximity of the fimbriated end of the fallopian tube to the ovulation site might possibly increase the ability of FTE cells to be transformed by inflammatory molecules that are released during the process of ovulation. A study has shown that these FTE cells exfoliate to the ovary, which consists of chemotactic factors that possess the ability to attract pre-malignant and malignant FTE cells. These data might explain how ovulation can influence the FTE cells to migrate to a habitable microenvironment that is conducive to form serous cancer[19]. Further investigation is warranted to determine the influence of ovulatory factors on the FTE cells and their putative role in serous cancer formation.

iii. Inflammation-Induced Oxidative Stress Theory

Ovulation is a highly inflammatory process that generates molecules like bradykinin, prostaglandins, and leukotrienes through the process of repairing the wound on the OSE as well as through the recruitment of macrophages to the site of ovulation[18, 20]. The cells of the OSE are prone to repeated tear and repair process during ovulation. These cells are often compromised by exposure to oxyradicals that may lead to initiation of malignant transformation. Reactive oxygen species generated by the inflammatory process results in potentially mutagenic lesions.

Studies have demonstrated that inflammatory molecules induce transformative changes in both, the OSE and the FTE[18]. These data further indicate that inflammatory molecules play a crucial role in promoting tumorigenic events irrespective of the tissue of origin. Perhaps, the close proximity of the fallopian tube fimbriae to the ovulatory site, possibly explains ovulation-induced DNA damage in the FTE. Further studies are warranted to better understand the role of prostaglandins and cytokines in promoting cancer initiation and progression.

iv. Gonadotropins Theory

A strong body of evidence exists that links high circulating levels of gonadotropin hormones to increased risk of ovarian cancer. Several epidemiological studies reconcile with research observations[21]. Gonadotropin hormone levels undergo a significant increase at the onset of menopause, when the negative feedback loop fails to keep them under check. As a result, there is a striking rise in follicle stimulating hormone (FSH) and luteinizing hormone (LH) levels that occurs at menopause, which averages at about 51 years. The incidence of ovarian cancer considerably increases at menopausal age. About two years after menopause, FSH and LH levels shoot up by 10-20 times (50-100 mIU/ml) and 3-4 times (20-50 mIU/ml), respectively compared to the menstrual phase[22]. Reports indicate that 85-90% cases of ovarian cancer are detected in peri- or postmenopausal women, with only 10-15% being detected at early stages. Investigators have shown that high circulating levels of FSH and LH increase tumorigenic properties of OSE cells as well as activate downstream signaling pathways commonly associated with ovarian cancer[23]. Our lab has shown that menopausal levels of FSH and LH activate the same pathways as serous cancer such as Birc5, Cdk2, Cdk4, and Cdkn2a in

addition to epidermal growth factor receptor (EGFR) and AKT in the OSE[23]. Interestingly, AKT and EGFR inhibitors blocked gonadotropin-induced cell proliferation in 3D organ and 2D cell culture of the murine OSE[23]. Several animal studies have supported the relationship between high gonadotropin induction and increased proliferation of the OSE[24-26]. The direct link between increased gonadotropin levels and EOC initiation is yet to be established. In light of the FTE being a potential source of origin of serous ovarian cancer, it is valuable to study the effect of FSH and LH on the FTE cells.

Apart from factors listed above, a variety of environmental factors have demonstrated a weak link between ovarian cancer and use of talc[27], obesity[28], tobacco smoke[29] and caffeine[30]. Also, prior incidence of PCOS[31], pelvic inflammatory disease[32] or endometriosis[33] has been associated with increased risk of ovarian cancer. Emerging literature strongly supports the distal end of the fallopian tube as the primary source for most high-grade serous carcinomas. Therefore, in search of a reliable precursor lesion for serous cancer, efforts are focused towards identifying key factors and signaling mechanisms that influence transformation of the fallopian tube epithelial cells.

D. Fallopian Tube and Ovary: Function

The main function of the fallopian tube is to capture the mature oocyte that is released from the ovary during the process of ovulation and make it available for fertilization. A distinct layer of epithelial cells lines the ovary and the fallopian tube. The epithelial cells lining the ovary (OSE) are derived from the coelomic epithelium that can switch between cuboidal and squamous epithelial subtypes and are incompletely committed. In contrast, the epithelial cells lining the fallopian tube

(FTE) are completely differentiated and comprised of ciliated and secretory subtype[34]. It is becoming apparent that the secretory subtype of the FTE may be the progenitor of HGSC[35].

E. Fallopian Tube Epithelium: Source of Serous Ovarian Cancer

The origin and molecular pathogenesis of high-grade serous ovarian carcinoma (HGSC) has perplexed the medical community for decades. HGSC was conventionally thought to originate from the single layer of epithelial cells surrounding the ovarian surface (OSE). Historically, investigators accumulated evidence to lend support to the ovarian surface epithelium as the primary source of origin for serous carcinoma. Investigators assumed that the OSE is the primary site of tumor origin because during surgical debulking, a major tumor mass was typically identified in close proximity to the ovary. However, in 2001, a team of Dutch investigators proposed a new paradigm shift[36]. They reported that the fallopian tubes from women with a genetic predisposition to HGSC harbored precursor lesions that resembled those observed in serous cancer tumors[36]. These data provided researchers with evidence of an alternative source of serous cancer origin – the fallopian tube epithelium (FTE). Retrospectively, the failure to detect these lesions previously, was attributed to the fact that they did not exist in the ovaries and that the fallopian tubes were not extensively examined as compared to the ovaries. Subsequent studies used Sectioning and Extensively Examining the FIMbriated End (SEE-FIM) protocol to section the fallopian tubes in order to look for putative precursors and malignant lesions[37]. A few studies also hypothesized that malignant cell populations from the fimbriated end of the fallopian tube colonized the ovary, which provided a unique microenvironment for the tumor mass to grow and

eventually metastasize in the peritoneal cavity[38, 39]. Several investigators carefully examined the fallopian tubes from women with BRCA1/2 germline mutations and those with sporadic ovarian cancer to reveal that these early lesions were always confined to the distal end of the fallopian tube[37, 40-47].

F. Serous Cancer Precursor Lesions from the Fallopian Tube Epithelium

The fallopian tube hypothesis has developed and been expanded over time. It has started to define a series of precursor lesions that form in the fallopian tube prior to development of serous ovarian cancer. These lesions have specific genetic alterations and are primarily identified in the secretory epithelial cells located at distal end of the fallopian tube. Putative progression of these lesions is outlined in **Fig. 1**. Clinically, the three precursor lesions identified were the "secretory cell outgrowths (SCOUTs)", "p53 signatures" and "serous tubal intraepithelial carcinomas (STICs)". Because pathologists have discovered these lesions in women predisposed to getting HGSC and in serous tumor samples, there lacks conclusive evidence whether they occur in a stepwise manner. Aligning the order of these lesions is critical to understanding disease progression and pathogenesis. Further details about each precursor is described below:

i. SCOUT: Secretory Cell Outgrowths (SCOUTs) are benign precursors that occur with significantly higher frequency in the fallopian tubes of women with serous cancer (~30%) versus only ~5% in normal cycling women[48]. Development of SCOUTs may be a natural phenomenon because of their detection in the fallopian tubes of women without the malignancy. Pathological studies have shown that the prevalence of SCOUTs is highest in the oviducts of women with serous cancer. The

fallopian tubes of women with benign hysterectomies had lower frequency of SCOUTs as compared to those of serous cancer patients. SCOUTs are rarely identified in the fallopian tubes of patients with post partum sterilization and in pediatric autopsies. Investigators also showed that the frequency of SCOUTs increased as a function of age but were independently associated with serous tumor[49]. SCOUTs are fairly equally distributed between the proximal and distal end of the fallopian tube[49]. It remains to be determined whether formation of SCOUTs results in functional and genetic alterations that influence serous cancer progression in the fallopian tube. It is important to point out that SCOUTs are seen in the oviduct of women with and without the malignancy, which begs the question whether it is a true precursor lesion. Nevertheless, SCOUTs do harbor genetic aberrations like loss of PAX2, which is linked to pelvic serous cancer. Chapter IV will address this question by developing a murine oviductal cell model that mimics SCOUTs, revealing the molecular abnormalities associated with SCOUT formation and how these changes may be associated with initiation of high-grade serous cancer.

ii. **p53 signature**: Based on the TCGA, mutation in *TP53* is the most common genetic alteration seen in 96-100% HGSC cases[50]. Experimental evidence suggests focal accumulation of p53 protein in cortical inclusion cysts (CICs), in the fallopian tubes of women with serous cancer and those that were genetically at a high risk to get ovarian cancer. These positive patches were noted to be non-proliferative, with low Ki-67 index and were confined to the distal end of the fallopian tube[51]. Lee *et al*[52], designated this phenomenon as a "p53 signature". A recent study[51] evaluated 75 ovaries and fallopian tubes from a population cohort with *BRCA*1/2 mutation and revealed that clusters of secretory epithelial cells from 29 patients stained positive for

p53 protein and in some cases, stained positive for the DNA damage marker, $_{Y}H_2AX$. However, only one p53 signature was detected in the OSE and none in CICs. These data further strengthen the argument that p53 signatures preferentially arise in the fallopian tube. However, these reports were not sufficient to establish p53 signatures as a definitive precursor to HGSC. Although, p53 signatures were tightly associated with serous cancer, two independent groups showed that frequencies of p53 signatures were 11 and 19%[47] and 24 and 33%[52] in women with *BRCA* mutation and in control population respectively. These reports suggest that the prevalence of p53 signatures is equally common in women with and without *BRCA* mutation. However, p53 signatures were often detected in association with malignant lesions in the fallopian tubes where both the cell populations were shown to share a common mutation in *TP53*[52]. This paradoxical observation makes it difficult to assign the p53 signature as a confirmed precursor to serous cancer. However, it is logical to assume that the mutation of *TP53* is essential but not sufficient to drive tumorigenesis and requires additional genetic and molecular alterations to progress to malignant precursor lesion – STICs.

iii. STIC: Serous tubal intraepithelial carcinomas (STICs) are established malignant precursors to high-grade serous ovarian cancer in the fallopian tube. STICs are hypothesized to progress from p53 signatures when sufficient molecular changes accumulate and are identified by high proliferative index, high nuclear atypia, abnormal chromatin pattern and high expression of $_{Y}H_2AX$, indicating extensive DNA damage[37, 40, 43, 44, 53]. Immunohistochemically, they demonstrate intense staining for p53 and Ki-67[54]. Expression levels of several oncogenes and tumor suppressors are comparable between STICs and serous tumor samples[50]. Some of them include

overexpression of Cyclin E[55], p16, upregulation of the PI3K pathway[56], loss of retinoblastoma protein and amplification of hTERT[57]. Kindelberger and colleagues followed the SEE-FIM protocol to extensively section and evaluate fallopian tubes from 55 cases of serous carcinoma without germline *BRCA* mutation. They showed that more than 70% of the cases involved the endosalpinx and about half harbored STICs[44]. This study also confirmed that the serous tumors and STICs shared the same *TP53* mutations, further implying the fallopian tube as the source for HGSC. A few more studies identified STICs in 47% of primary peritoneal serous carcinomas[58] and about 35% of high-grade fimbrial ovarian carcinomas[59]. Extensive molecular and genetic characterization of STICs is necessary to understand disease progression. The molecular events that precede formation of STICs are still unclear and are termed serous tubal intraepithelial lesions (STILs). STILs are not well defined and are essentially p53 signatures with a high proliferative index. Further studies are warranted to establish the focal points that lead up to development of STICs.

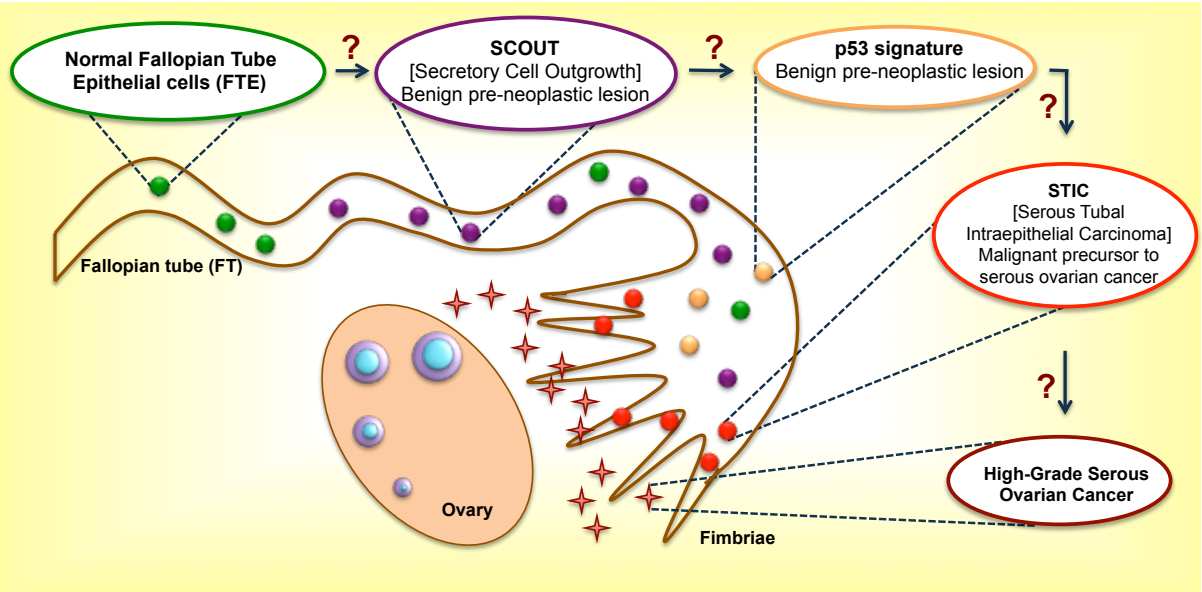

Figure 1: Proposed Progression of High-Grade Serous Cancer from the Fallopian Tube Epithelium.

G. Clinical Implication of Defining Precursor Lesions

A complete genetic profile of SCOUTs, p53 signatures and STICs is essential to draw comparisons with serous cancer samples. Teasing apart the molecular events that influence progression of benign lesions to malignant counterparts is essential to develop preventive therapies and to detect the disease at an early stage. These lesions are identified in fixed tissues making it difficult to confirm the molecular signaling and regulation of protein expression that occurs in lesion development. To address these questions, researchers have developed several animal and cell-based models as valuable resources to support the fallopian tube as a source of serous cancer as well as understand the molecular basis of lesion development.

H. Animal Models of FTE-Derived Serous Cancer

Investigators have developed murine and human FTE-cell derived serous cancer models with a variety of oncogenes to validate that transformation of the fallopian tube epithelium can indeed result in tumor formation that mimics human disease[35, 60-62].

A study used PAX8-TetON-Cre promoter to drive deletion of PTEN, BRCA1/2, and mutation of *TP53* in combination as well as deletion of *TP53* together with PTEN in murine oviductal FTE cells. These genetic manipulations formed invasive carcinomas that metastasized to the peritoneal cavity and immunohistochemical analysis revealed high similarity with human high-grade serous markers[63]. Because 70-80% HGSC cases are sporadic and do not harbor mutation in BRCA1/2[50], Eddie *et al.* investigated the tumorigenic potential of oviductal cells harboring *TP53* mutation and PTEN loss in the absence of *BRCA* mutation and showed that these

cells are capable of forming high-grade carcinoma *in vivo*[60]. This was the first study to show that knockdown of PTEN alone is sufficient to drive tumorigenesis from FTE cells whereas the combination of PTEN loss with mutation of *TP53* reduced the extent of tumor spread[60]. Another study conditionally silenced Dicer and PTEN using the MISRII promoter driving Cre-recombinase expression to demonstrate that high-grade carcinomas develop in the FTE, with the primary epithelial tumors arising in the fallopian tube stroma[64]. Unfortunately, MISRII-Cre is not efficient in specifically infecting the oviduct without affecting surrounding cell types, such as the ovary and uterus, resulting in uncertainty of the cell types involved in tumor formation. STIC lesions reported from OVGP1-SV40 mice are a result of the viral oncoprotein, which renders Rb inactive, sequesters p53 and stabilizes expression of wild-type p53[65]. Recently, our lab serially passaged murine oviductal epithelial (MOE) cells (MOE^{HIGH}) from CD1 mice[61]. Subcutaneous injection of MOE^{HIGH} cells in mice resulted in undifferentiated high-grade carcinoma, but failed to metastasize and form peritoneal tumors. This represents the first cellular spontaneous mouse model of cancer derived from the oviductal cells[61]. Quartuccio *et al.,* demonstrated that although *TP53* is mutated in almost 100% HGSC cases, murine oviductal cells that harbor *TP53* mutation alone are not sufficient to drive tumorigenesis[66], unless combined with secondary genetic alteration, such as overexpression of $KRAS^{G12V}$ or knockdown of PTEN[66]. Several studies have demonstrated the formation of serous and mucinous tumors derived from human FTE cells harboring overexpression of KRAS mutant and c-Myc, however, these cells are often immortalized using SV-40 T antigen, which sequesters p53 protein[35, 62, 67]. This makes it impossible to evaluate the impact of p53 mutation, which represents the majority of serous tumors.

Although these models mimic human disease and affirm fallopian tube as the source of origin, they have yet to address the multistep carcinogenesis pathway and the events leading to serous cancer formation. Recently, several interesting reports have emerged that show the downregulation of PAX2, a member of the Paired Box gene family, in endometrial and serous carcinomas. Interestingly, pathologists observed lack of PAX2 protein in SCOUTs and p53 signatures as well. These led researchers to believe that sudden loss of PAX2 might be one of the earliest changes occurring in the FTE prior to formation of p53 signatures. Therefore, determining the regulation and function of PAX2 in the fallopian tube epithelium is critical to improve our understanding about early serous carcinogenesis.

I. PAX genes

The name PAX stands for Paired Box family of transcription factors that play a critical role in embryonic development and organogenesis. PAX genes were first identified based on their sequence homology with *Drosophila* segmentation genes[68]. All PAX proteins possess a 128-amino acid DNA binding domain, called "Paired Domain (PD), that is conserved across several mammalian species. For all PAX proteins, the C-terminal amino acid contains the transactivation domain (TD). As demonstrated in **Fig. 2**, the PAX family consists of nine members (PAX1-9) that are divided into four groups based on the genomic and the structural properties, presence or absence of an octapeptide domain (OD), and either a homeodomain (HD) or a partial homeodomain[69]. Unlike several PAXs, PAX 3,4,6 and 7 possess the additional DNA binding domain - homeodomain (HD). The octapeptide motif is a highly conserved eight-amino-acid linker between PD and HD that exists in all PAX genes except PAX4 and 6[70]. Deletion of OD in some PAXs is associated with

inhibitory transcriptional activity[71]. Protein-protein interactions with PAXs affect transcriptional activation and repression and epigenetic regulation. The complexity of structural and functional characteristics suggests multiple overlapping roles of PAX proteins during early stages of development and in disease states.

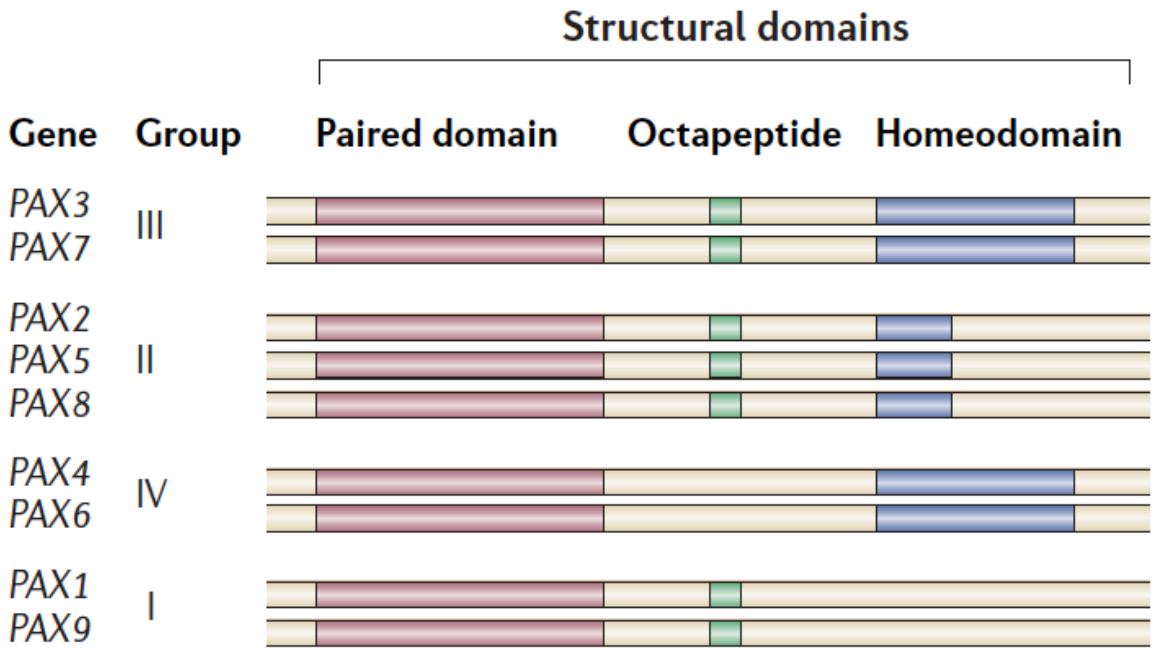

Figure 2: PAX family subgroups based on presence or absence of structural domains. Figure adapted from Robson *et al.*[70]

J. PAX2: Expression and Function in the Female Reproductive Tract

PAX2 is the earliest expressed PAX gene during human embryonic development, at day 7.5. PAX2 is expressed in a spatial and temporal fashion during early developmental stages in the Müllerian duct, eye, brain, inner ear, kidney and thyroid. In structures derived from the Müllerian duct - the fallopian tubes, uterus, cervix and upper vagina, PAX2 expression continues throughout development and persists at adult stages. In these tissues, the timely expression of PAX2 is essential for efficient cell growth and migration. In contrast, the ovarian surface epithelial (OSE) cells do not express PAX2 at any stage of development.

Immunohistochemical studies showed positive PAX2 staining in the secretory epithelial cells of the fallopian tube, endometrial and cervical glands. Intense PAX2 staining was observed in normal proliferative endometrium. Although PAX2 went undetected in the OSE, it was present in the glands of endometriosis, endosalpingiosis, and rete ovarii in the ovary. Interestingly, compared to what is already known about PAX2 in renal development, the clinical significance and function of PAX2 in the fallopian tube and uterus is relatively unexplored.

Analysis of PAX2 knockout mice revealed the importance of PAX2 in the fallopian tube, eye, ear, midbrain and kidney[72, 73]. Homozygous PAX2 deletion results in the lack of Müllerian structures and kidneys, and the mice die perinatally. Researchers have shown that heterozygous PAX2 deletion leads to underdeveloped ureters, kidneys and these mice lack fallopian tubes[72, 74].

K. PAX2 Expression in Ovarian Tumors: Pathological Evidence

Unlike the kidney, thyroid and prostate tissues, where PAX2 expression is turned off after embryonic development, PAX2 persists even at adult stages in the uterus and the fallopian tube epithelium, where it is essential to maintain cell proliferation and growth. Several investigators have recently noted consistent loss of the PAX2 protein in serous tumors that are thought to originate from tissues derived from the Müllerian duct. Some groups have reported histotype-specific PAX2 expression profiles in ovarian tumors. PAX2 protein was detected in mucinous and clear cell tumors but was absent in most endometrioid and serous tumors. A study reported that PAX2 is highly expressed in 59% of low malignant potential tumors, 63% of low-grade serous cancer and cortical inclusion cysts[75]. In contrast,

pathologists have extensively reported that serous tumor tissues consistently lack PAX2 expression when analyzed by immunohistochemistry[49, 58, 74-76].

The use of PAX2 as a diagnostic marker is context dependent. PAX2 is widely expressed in endometrial tissues. Similar to serous cancer, PAX2 loss is associated with endometrial malignancy and endometrial intraepithelial neoplasia (EIN)[77]. Several groups have consistently reported inactivation of PTEN in endometrial cancers. Analysis of normal proliferative endometria, premalignant EIN and endometrial cancer tissues revealed that PAX2 and PTEN were jointly lost in an increasing order of malignancy. Combined loss of PAX2 and PTEN was noted to increase from 21% in normal endometrial tissue to 31% in premalignant to 55% in endometrial carcinoma. Loss of PAX2 protein and mRNA was observed in about 77% of endometrial adenocarcinomas as compared to its abundant expression in normal endometria[77, 78]. Based on a recent analysis, the PTEN pathway is altered in approximately 30% of serous cancer cases[79]. Therefore, it will be interesting to evaluate the association between PTEN and PAX2 in HGSC samples and determine whether loss of PTEN influences PAX2 expression in fallopian tube epithelial cells. However, exhaustive studies are required to determine the molecular genesis of PTEN and PAX2 loss, their influence on downstream signaling pathways and define the early events of serous cancer transformation.

A group of researchers revealed that downregulation of PAX2 might occur much earlier in the serous carcinogenesis pathway. SCOUTs are proposed to be the earliest precursors in progression of HGSC that are identified in the FTE that lack PAX2 expression. A study reported that the frequency of SCOUTs was highest, (~83%) in women with serous cancer, followed by women that are genetically predisposed to getting HGSC (~18%) and was the lowest in control fallopian tube

tissue (~12%)[48]. These data strongly suggest that aberration in the PAX2 protein occurs at an early stage in serous carcinogenesis and that there are additional alterations (such as mutation of *TP53*) necessary to promote tumorigenesis. Experimental cell models of the FTE have recently emerged. Details about existing and novel models, their utility in research and pitfalls will be explored in chapter IV.

L. PAX2 Expression in Ovarian Cancer Cell Models

A comprehensive panel of twenty-six ovarian cancer cell lines was screened for PAX2 expression by qPCR. PAX2 presence is highly tumor specific and differs between the different histotypes. Pathological evidence convincingly demonstrates that PAX2 overexpression is absent in serous tumor tissues. A lack of PAX2 protein in serous cancer cell lines corroborated existing clinical data[76]. A study evaluated the functional significance of overexpressing PAX2 in HGSC cell line (OVCAR3) and reported significant reduction in cell viability. These data (including data from Chapter IV) supports the role of PAX2 as a tumor suppressor in HGSC. In a murine model of high-grade serous cancer derived from serially passaging murine OSE cells, the effect of overexpressing PAX2 conferred protective properties[80]. In contrast, PAX2 expression was detected in cell lines that represent clear cell (RMUGL) and mucinous (TOV21G) histotypes[76]. Knockdown of PAX2 in RMUGL and TOV21G cell lines resulted in reduced proliferation and downregulation of cell motility. Downregulation of PAX2 in these cell lines also enhanced apoptotic signaling compared to those with intact PAX2 expression, suggesting that PAX2 might be oncogenic and crucial for these cancer cells to survive[76].

The contrasting roles of PAX2 in serous versus non-serous histotypes of epithelial ovarian cancer points to a dualistic regulation of PAX2 in this tumor type.

There is a vast gap between pathological observations and experimental models outlining the mechanistic regulation of PAX2 in each of these tumors. It is essential to tease apart the role of PAX2 in serous cancer, not only because it is the most common and the most lethal histotype of EOC, but because it could serve as a novel target for therapeutic intervention. Further, these divergent roles could be explained by different histotypes arising in the ovarian surface or the fallopian tube.

M. Role of PAX2 in Non-Ovarian Tumors

PAX2 is crucial at developmental stages in the kidney, thyroid, eye, inner ear and CNS. Unlike in the Müllerian duct-derived tissues, PAX2 expression is switched off in the kidney, thyroid, inner ear, eye and CNS at adult stages. Therefore, aberrant expression of PAX2 in these tissues, at adult stages is often associated with severe abnormalities. A immunohistochemical study by Muratovska and colleagues demonstrated that 90% of 54 cancer cell lines and 25% of 406 tumors were PAX2 positive[81]. PAX2 expression was observed in 90% of clear cell renal cell carcinoma (RCC), which is the most common type of renal neoplasm[82, 83]. Studies have shown that PAX2 inactivation promotes cisplatin-induced cell death in renal carcinoma cells[83, 84]. Knockdown of PAX2 in prostate cancer cells resulted in reduced cell invasion and proliferation suggesting the tumorigenic properties conferred by PAX2[85, 86]. In Kaposi's sarcoma cells, PAX2 expression is associated with increased resistance to apoptosis[87]. Mutations in one copy of PAX2 are identified in at least 50% of the patients associated with diseases such as renal hypoplasia, optic nerve coloboma and kidney agenesis[88].

N. Differential PAX2 Expression in Serous Ovarian Cancer vs. Other Tumors

Deregulation of PAX2 gene is linked to multiple cancer types; however, the precise physiological role of PAX2 gene in initiation and progression of tumorigenic events is not well characterized and is highly tissue specific. It is crucial to note that PAX2 is expressed in all adult tissues derived from the Müllerian duct – the fallopian tube, uterus, cervix and upper vagina. However, PAX2 expression is attenuated at adult stages in all the remaining tissue types (example - prostate, breast, renal, colon cancer). Because PAX2 is otherwise not expressed in these tissues, acquisition of PAX2 is associated with tumorigenesis. Although significant progress is made in understanding the role of PAX2 in renal and thyroid tumors, the tumorigenic regulation of PAX2 is fundamentally opposite to serous ovarian tumors. In HGSC, aberrant loss of PAX2 in the fallopian tube epithelium, which normally expresses PAX2, is associated with cancer formation. Therefore, what is already known about PAX2 regulation in other tumor types provides very little information about pathogenesis of serous ovarian cancer. Although PAX2 has been extensively studied in renal and thyroid carcinogenesis, information about its clinical significance and regulation in the fallopian tube and serous ovarian cancer is very sparse. The purpose of this project was to investigate the regulation and function of PAX2 in normal fallopian tube tissue and in addition, determine the mechanism of PAX2 loss in order to define the pathway of serous cancer progression.

Although there are several unanswered questions about PAX2 biology and aberrant expression in serous ovarian cancers, it is clear that PAX2 is essential during early developmental stages as well as in adult tissues and mounting evidence supports its potential as a therapeutic target. Investigating the downstream targets

of PAX2 genes in specific tissue types will reveal important information on signaling molecules that can serve as targeted therapies.

O. Treating Serous Ovarian Cancer – Delivery Platforms and Challenges

Treating serous ovarian cancer is a challenge due to multiple factors – difficulty in early diagnosis, a lack of symptoms that can detect the disease before metastatic spread to the peritoneal cavity, a lack of biomarkers and efficient imaging technologies. The traditional route of combating serous cancer is cytoreductive surgery to remove the bulk of the tumor cells followed by chemotherapy. Unfortunately, there fails to be any major breakthroughs in discovering novel chemotherapeutic agents. Cytoreductive surgery and intraperitoneal administration of carboplatin and paclitaxel are currently the standard of care. Although the majority of serous cancers respond well to this combination, the relapse rate is almost 70%. Unfortunately, the recurrent disease is often resistant to these drugs. Several new drugs that can be combined with existing treatment are currently under clinical trials.

A variety of these novel treatments include drugs that are designed to alter specific pathways in serous cancer cells. One such example is the development of PARP inhibitors. In December 2014, the U.S. FDA approved the first PARP inhibitor, Olaparib (Lynparza®), marketed by Astra Zeneca. DNA is highly susceptible to replication errors during increased stress, toxic metabolite buildup or a genetic insult, which results in single stranded breaks (SSBs) that are recognized and repaired by PARP enzymes. When a compound such as Olaparib inhibits PARP activity, the SSBs convert to double stranded breaks (DSBs), which are repaired by the homologous repair (HR) or the non-homologous end-joining (NHEJ) pathway.

However, inability to repair the DSBs due to defects in the HR (example: *BRCA*1/2 mutation or methylation) or the NHEJ pathway results in cell death due to synthetic lethality. More than 50% of serous tumors demonstrate aberration in the HR DNA repair pathway. Therefore, PARP inhibitors, in combination with DNA alkylating agents, are designed to inflict permanent damage to cancer cells by resulting in cell cycle arrest.

The ability to specifically target tumor cells may provide a new way to improve the treatment of ovarian cancers. Dose dense chemotherapy trials in Japan and IP therapy both suggest that a higher concentration of local delivery is more effective than traditional routes of administration. Serous ovarian cancer is unique in one aspect that the metastatic spread is confined to the peritoneal spaces and does not typically involve distant organs. Recent advances in drug delivery combines chemistry with nanotechnology platforms. Some of these include self-assembling multi-molecular complexes from lipids, conjugation of drugs with carrier molecules like peptides, aptamers or antibodies and drugs absorbed onto or encapsulated within the complex nanomaterials such as quantum dots or dendrimers. A variety of factors determine successful biological effect of these novel targeted carriers – ease of administration, bioavailability and clearance, mode of degradation. Chapter V describes the biological validation of a dendrimer nanocarrier in effectively targeting ovarian cancer cells expressing the follicle stimulating hormone receptor (FSHR). The uniqueness about the model described in Chapter V is that it has the potential to be used not only as a therapy, but also as a prophylactic treatment for high-risk ovarian cancer patients who wish to preserve the option of fertility, and FSHR is expressed in both the OSE and the FTE.

Overall, this thesis seeks to define the significance of ovulation on the ovarian surface epithelium versus the fallopian tube epithelium, both of which are putative precursors of serous cancer. A significant portion of this project is focused on investigating the molecular pathways that are associated with precursor lesion development and pathogenesis of HGSC from the fallopian tube. The objective is to develop *in vitro* models of early lesions of serous cancer because they will serve as an important resource that could be utilized to better understand the underlying mechanism of disease progression. The goal of these projects is to identify drugs that can halt cancer progression or reduce tumor burden and also to develop a novel delivery system that can transport these drugs to specific cell types while sparing the healthy cells of off-target effects.

P. Specific Aims

Aim 1: To investigate the influence of gonadotropins on the ovarian surface epithelium (OSE). Ovulation has been established as a potential contributor to ovarian cancer through multiple mechanisms including stimulation from gonadotropin hormones. It is unclear how these hormonal factors physiologically regulate the OSE. We utilized the 3D ovarian organ culture and 2D murine OSE culture systems to investigate the effects of follicle stimulating hormone (FSH) and luteinizing hormone (LH). Effects of FSH and LH as single agents and as combination will be evaluated at cycling and postmenopausal concentrations in 3D and 2D OSE culture systems. The ability of the gonadotropin hormones to promote proliferation and colony formation via the AKT and EGFR pathways will be investigated as a mechanism for transformation.

Aim 2: To elucidate the regulators of PAX2 and functional significance of PAX2

loss in the fallopian tube epithelium and high-grade serous ovarian cancer. PAX2, a transcription factor regulated by p53, and expressed by normal FTE, is completely lost in HGSC and putative precursor lesions of serous cancer in the tube. Pathologists have identified sporadic occurrences of SCOUTs and p53 signatures in FTE of women that are genetically predisposed to getting ovarian cancer. Murine oviductal epithelium (MOE) cells stably expressing knockdown of PAX2 alone, mutation in *TP53* alone, and a combination of PAX2 loss and *TP53* mutation will be generated. Functional assays will determine the significance of PAX2 loss and *TP53* mutation. PTEN loss is sufficient to drive fallopian-derived tumorigenesis in a murine model created in our lab. We will determine whether reduced levels of PTEN negatively regulate PAX2 expression in FTE cells and whether re-expression of PAX2 reduces the pro-proliferative and pro-migratory effects from PTEN silencing. We will determine if re-expression of PAX2 can block PTEN-mediated tumor formation and metastatic colonization. Re-expressing PAX2 might present a novel therapeutic strategy to reverse or stop cancer progression. However, mutation of *TP53*, which occurs in 100% of HGSC, may repress the PAX2 promoter. We will use ChIP and luciferase reporter assays to define this regulation. To provide additional means of enhancing PAX2 expression, we will screen a library of FDA approved drugs to determine if any of them can activate the PAX2-promoter in a novel high-throughput assay developed in our lab. We will monitor mRNA and protein expression as well as the ability of these compounds to activate PAX2 in normal fallopian tube cells.

Aim 3: To develop a targeted nanocarrier system that delivers a therapeutic drug to selectively kill cells expressing the follicle stimulating hormone receptor (FSHR). FSHR is overexpressed in ovarian cancer cells and expressed by

the OSE as well as the FTE cells. We will conjugate dendrimers to FITC imaging agent and targeting molecules (amino acids 33-53 of the FSH β chain (FSH33)) that allow a highly localized density of ligands to achieve the strong binding effect. The targeting efficacy of the nanocarriers will be validated using 3D *in vitro* organ cultures and 2D OSE cells. We will also perform an *in vivo* study to validate the preferential uptake of targeted nanocarriers by the ovary and oviduct tissues.

II. MATERIALS AND METHODS

(Manufacturer's details can be found in **TABLE III**).

A. Animals

Day 16 female CD1 mice were used for all organ culture experiments. The Animal Care Committee approved the protocol A14-180. All xenograft experiments in Chapter IV were performed as described previously[60, 66]. Animals were sacrificed at humane endpoints and tissues were collected and analyzed as shown previously[60]. "Animals were not primed with eCG (Chapter III)"[23]. "Female BALB/c mice (6-8 week old) were used for the in vivo efficacy experiment (Chapter V)"[89]. "All mice were acquired through in-house breeding, and all breeders were purchased from Harlan laboratories. Animals were treated in accordance with the National Institutes of Health Guide for the Care and Use of Laboratory Animals and the established Institutional Animal Care and Use protocol at the University of Illinois at Chicago. Animals were housed in a temperature and light-controlled environment (12 h light: 12 h darkness) and were provided food and water ad libitum[90, 91]."[23, 89, 92]

B. Cell Culture

In all chapters, Murine Oviductal Epithelium (MOE) cells and high-grade serous cancer cell lines – OVCAR3, OVCAR4, KURAMOCHI and OVSAHO were cultured as previously described[93, 94]. Cell lines were stably or transiently transfected using Mirus TransIT LT1^{TM} according to manufacturer's protocol with antibiotic resistant plasmids containing the gene of interest **(Table I)** as described previously[60]. In Chapter III, "mouse ovarian surface epithelium cells (MOSE; Barbara Vanderhyden, University of Ottawa, Ottawa, ON Canada) were grown in alpha-MEM (Mediatech, INC), 1% L-glutamine, 10% fetal bovine serum (FBS; Gibco), epidermal

growth factor (2 µg/mL; Roche), insulin/transferrin/selenium (insulin 5 µg/mL; transferrin 5 µg/mL; selenite 5 ng/mL; Roche), gentamycin (1 µg/mL; Mediatech), and penicillin-streptomycin (0.5 µL/mL). MOSE cells from passage numbers 7–13 were used for all experiments in this paper. MK-2206 (Selleck Bio) or AG1478 (Cell Signaling) were added to cultures to inhibit Akt or EGFR activation, respectively"[23]. In Chapter V, "SKOV-3 ovarian cancer cells were grown in McCoy's 5A (Sigma Aldrich) with 10% fetal bovine serum, and 1% penicillin-streptomycin and was purchased from American Type Culture Collection and incubated at 37˚C, 5% CO2."[89]

TABLE I

PLASMIDS UTILIZED FOR STABLE AND TRANSIENT TRANSFECTIONS

Target	Vector	Manufacturer
Scrambled shRNA	pMLP-GFP	transOMIC
PAX2 shRNA-1	pMLP-GFP	transOMIC
PAX2 shRNA-2	pMLP-GFP	transOMIC
p53 R273H	pCMV-Neo-Bam	Addgene
NEO	pCMV6	Origene*
PAX2	pCMV6-Myc	Origene*
PAX2 Luciferase	pGL3-Basic	Promega*

* Indicates the plasmid was a gift

- NEO and PAX2 – Dr. Kwong Wong, M.D. Anderson Cancer Center, Houston, TX
- PAX2 Luciferase construct – Dr. Gregory Dressler, University of Michigan, Ann Arbor, MI

C. Organ Culture

"Ovaries from pre-ovulatory day 16 mice were dissected as previously described[93, 95]. Briefly, ovaries were dissected in dissection media composed of Liebovitz media with L-glutamine, 100 U penicillin (Gibco), and 100 µg/mL streptomycin. The bursa was removed with forceps and ovaries were cut with a scalpel into two pieces, termed organoids. The organoid was then placed in growth media that consisted of alpha-MEM (Invitrogen), 100 U penicillin (Gibco) and 100 µg/mL streptomycin. In chapter V, to validate the targeting efficacy of the dendrimers to ovarian cells expressing FSHR, the organoids were treated with 500 nM of G5-Ac-FITC-FSH and G5-Ac-FITC in serum-free media for 5 h. Another set of organoids was pre-treated with100 µM FSH33 for 2 h, followed by 5 h incubation with the dendrimer conjugates. Unlike previously described[18, 95], the organoids were directly treated with the nanocarriers prior to alginate encapsulation to ensure effective peptide and nanocarrier penetration to the ovarian tissue. At the end of the incubation period, each organoid was placed into a 0.5% w/v alginate/PBS droplet formed on mesh fiber. The alginate-encapsulated organoid was placed into 50 mM $CaCl_2$ for 2 min to cross-link the alginate, forming a gel around the organoid"[89]. In Appendix A, "the alginate-encapsulated organoid was cultured for 7 d in basal medium composed of αMEM (Gibco), 100 U penicillin (Gibco), and 100 µg/ml streptomycin. DMSO was added at a final concentration of 0.01% (v/v) as a solvent-only negative control. Bovine insulin (Sigma-Aldrich, St. Louis, MO) or recombinant human IGF-I (Ipsen Biopharmaceuticals Inc.) was added to cultures at a concentration of 5 µg/ml. AG1024 (Calbiochem) was dissolved in DMSO and added at a final concentration of 10 µM. LY294002 (Cell Signaling) was dissolved in DMSO

and added at a final concentration of 25 μM. U0126 (Cell Signaling) was dissolved in DMSO and added at a final concentration of 10 μM."[92]

D. Western Blot

(Antibody dilutions are listed in **Table II**)

In Chapter III, MOSE cells were cultured in basal media, serum starved overnight and treated with the gonadotropins for specified periods of time. In Chapter V, "For FSHR expression, OVCAR-3 cells were treated for 24 h with FSH (10 mIU/mL), G5-Ac-FITC-FSH (500 nM), or FSH in the presence of G5-Ac-FITC-FSH (500 nM) before washing." [89] In all western blot experiments, cells and organoids were washed with ice cold PBS and lysed in RIPA buffer (25 mM Tris-HCl pH 7.6, 150 mM NaCl, 1% (v/v) Triton-X, 1% (v/v) sodium deoxycholate, 0.1% SDS), 1X Complete Mini Protease Inhibitor Cocktail tablets (Roche), and 1X Phosphatase Inhibitor Cocktail III (Sigma). The bicinchonic acid assay (Pierce) was used to determine protein concentration. Cell lysate (30 μg) was run on varying percentages of SDS-PAGE gel under reducing conditions and transferred to a nitrocellulose membrane. Membranes were blocked for 1 h at RT in blocking buffer. Primary antibodies were incubated on blots overnight at 4 °C. After washing in TBS-Tween, membranes were incubated with goat anti-rabbit or goat anti-mouse horseradish peroxidase secondary antibody (Cell Signaling) at 1:1000 in blocking buffer for 1 h. Membranes were washed and visualized using SuperSignal West Femto substrate (Thermo Scientific) on a Protein Simple gel documentation system. All gels were run in three individual experiments with the representative image shown[23, 89].

E. Immunohistochemistry (IHC)

(Antibody dilutions are listed in **Table II**)

Organoids were removed from culture media and fixed as previously described[95] using reagents from Vector Labs Inc. unless otherwise noted. Immunohistochemistry was performed as previously described[18, 24, 95]. Section thickness for the all tissues was 5 microns. Sections were mounted on Superfrost®Plus Microscope slides (Fisher scientific). Briefly, heat-induced antigen retrieval was performed using 10 mM sodium citrate. Tissues being stained for BrdU were treated with 4 M hydrochloric acid for 10 min followed by 10 min incubation with 0.1 M sodium tetraborate. Tissues were blocked with 3% H_2O_2, avidin and biotin for 15 min each. Control slides received serum block instead of primary antibody. The primary anti-bodies against PAX2, BrdU, cytokeratin 8 (CK8), FITC, WT-1, PAX8 and Fut8 were incubated overnight at 4 °C. Slides were washed and incubated with biotinylated secondary antibody in 3%-BSA-TBS. Following three washes in TBS-Tween, slides were incubated for 30 min in avidin/biotin complex (ABC). The antigen-antibody-HRP complex was visualized using diaminobenzidine reagent for 3–5 min and counterstained with hematoxylin. All conditions that had a minimum of 5 organoids (Chapter III) or 3 organoids (Chapter V) and the experiments were performed in triplicates[23, 89]. "IHC images were acquired on a Nikon E600 microscope using a DS-Ri1 digital camera and NIS Elements software (Nikon Instruments). At least three random fields from at least two independent experiments were imaged."[89] In Chapter IV, tissues were prepared for hematoxylin and eosin stain as described in past publications[60]. In Chapter III and Appendix A, "The percentage of proliferating OSE relative to the total number of OSE was quantified using Image J software (NIH)."[92]

TABLE II

PRIMARY ANTIBODY CONCENTRATIONS FOR WESTERN BLOTTING AND IMMUNOHISTOCHEMISTRY (IHC)

Antibody	Western Blot Dilution	IHC Dilution	Company	Catalog Number
Actin	1:1000	-	Sigma Aldrich	A2066
Fut8	1:1000	1:40	Proteintech	12560-1-AP
PAX2	1:500	1:50	Life Technologies	71-6000
Mme	1:500	-	Proteintech	18008-1-AP
p53	1:500	-	Santa Cruz Biotechnology	sc-6243
Stathmin	1:500	-	Cell Signaling	3352
WT-1	-	1:50	Abcam	ab89901
PAX8	-	1:100	Proteintech	10336-1-AP
Survivin	1:500	-	Cell Signaling	2808
FSHR	1:1000	-	Epitomics	S0522
p-Akt	1:1000	-	Cell Signaling	4060
p-ERK	1:1000	-	Cell Signaling	4370
p-PTEN	1:1000	-	Cell Signaling	9551
PTEN	1:1000	-	Cell Signaling	9188
Akt (pan)	1:1000	-	Cell Signaling	4691
Cdk2	1:500	-	Cell Signaling	2546
Cdk4	1:1000	-	Cell Signaling	2906
BrdU	-	1:200	Abcam	ab6326
TROMA-1 (CK8)	-	1:100	Developmental Studies Hybridoma Bank	
FITC	-	1:400	SIGMA	B0287
Müllerian inhibiting substance (MIS)	-	1:50	Santa Cruz Biotechnology	sc-6886
pGSK3β^{Ser9}	-	1:400	Cell Signaling	9323
total GSK3β	-	1:100	Cell Signaling	9315
collagen IV	-	1:100	EMD Millipore	AB756P
Cdkn2a	1:500	-	Abcam	ab80

F. Cell Viability Assay

Cells were seeded into 96 well plates at 1 × 10^4 cells/100 µL (Chapter III)[23] or 1.0 x 10^3 cells per well of media with serum (Chapter IV). "The next day cells were treated with FSH, LH, or a combination of FSH and LH at 1, 10 and 100 mIU/mL. The cells were allowed to grow for 8 days."[23] Proliferation was measured using sulforhodamine B (SRB) colorimetric assay as described previously[66]. Media was aspirated and cellular proteins were fixed to the plate with 20% trichloroacetic acid for 1 h. Cells were washed with water and stained for 30 min with sulforhodamine B. Excess dye was washed with 1% (*v*/*v*) acetic acid. The protein-bound dye was re-suspended in 10 mM Tris buffer. Spectrophotometric analysis was completed using a Biotek Synergy 2 multi-mode microplate reader (Biotek). All conditions were tested in three replicates in triplicate experiments.

G. Wound Healing (Scratch) Assay

In Chapter IV, cells were seeded at 1.0 X 10^5 cells/ well and assay was performed as described previously[23, 66]. Pictures were taken at 0 and 8 or 12 or 24 hours after scratching using an AmScope MU900 with Toupview software (AmScope).

H. Soft Agar Transformation Assay

Soft agar colony formation assay was performed as previously described[66]. "OSE were collected from organoids cultured for 3 days in media containing FSH, LH, or FSH+LH, followed by analysis of anchorage-independent growth as measured by growth in soft agar. The base layer of the agar consisted of DMEM (Gibco), and

0.5% agarose (Sigma). The top layer consisted of DMEM, 0.35% agarose and 15 × 10^3 cells/well in a 24 well plate. The agar was overlaid with DMEM, 4% FBS, and penicillin-streptomycin. After 14 days, colonies were imaged on a Nikon Eclipse TS100 using a DS-Ri1 digital camera and counted using NIS Elements software. All conditions were tested in three replicates in triplicate experiments."[23]

I. RNA isolation, cDNA synthesis and RT-qPCR

In Chapter IV, RNA extraction was performed using Trizol and chloroform with isopropanol precipitation followed by ethanol washes and DNAse step as described in[66]. iScript™ cDNA synthesis kit (BioRad) and SYBR green (Roche) were used according to manufacturer's instructions to synthesize cDNA and quantify DNA, respectively. All qPCR runs were performed on the ABI ViiA7 (Life Technologies). In Appendix A, "organoids were cultured 3d in basal media, 5 μM insulin, or 5 μM IGF-I[18, 95]. OSE were collected by treatment with collagenase[18], mRNA was extracted, RNA (0.5 μg) was reverse transcribed using the RT^2 First Strand kit (Qiagen), and cDNA was added to RT^2 Profiler PCR Cancer Pathway Finder Arrays (Qiagen) according to manufacturer's recommendations. Gene expression changes were analyzed on an iCycler real-time PCR detection system and normalized relative to the average expression of β-actin, Gusb, Hprt, Hsp90ab1, and Gapdh according to manufacturer's instructions (Bio-Rad)."[92]

J. Flow Cytometry

In Chapter IV, OVCAR4 cells were transiently transfected with NEO (Control) or PAX2 overexpression plasmid in a 6-well plate. After 48 hours, cells were harvested using trypsin. Cell suspension was centrifuged at 800 g for 5 minutes at

4°C. Pellet was re-suspended in Annexin V binding buffer (10 mM HEPES, 140 mm NaCl, 2.5 mM CaCl2, pH 7.4). 200 µl from the “control” treated cells was divided into two new centrifuge tubes. One served as “unstained” control and the second tube was treated with, propidium iodide (PI) and Annexin V as described below. 300 µl from PAX2 treated cells was divided into three tubes. First tube was treated with PI alone and second tube with Annexin V alone. Third tube was treated with both, PI and Annexin V. PI (stock concentration: 1 mg/ml) was diluted 1:10 in Annexin V binding buffer. 2 µl of 1:10 diluted PI, was added per tube (final PI concentration – 2 µg/ml). Annexin V/APC conjugate (Life technologies) was diluted 1:60 in Annexin V binding buffer. 1 µl was added per tube. Cells were incubated in dark for 15 minutes. 400 µl Annexin V binding buffer was added to each tube. Cell suspension was allowed to pass through 5 ml polystyrene round-bottom tube with cell strainer cap (Fisher). Tubes were placed on ice and transported to the Flow Cytometry Core Facility at UIC. Samples were run on the Beckman Gallios 3 laser/10 color cytometer. Quantitative analysis was performed using Summit 3.0 software.

In Chapter V, “OVCAR-3 cells were seeded in 12-well plates at a density of 1 × 105 cells/well and incubated in supplemented MEM media for 24 h. Cells were treated with G5-Ac-FITC-FSH (500 nM) for 5 h, with or without pre-treatment with FSH33 (100 µM) for 2 h, and G5-Ac-FITC (500 nM). Cells were then washed with PBS and suspended with trypsin. Cell suspensions were centrifuged at 1000 rpm for 5 min. The pellet was resuspended in 500 µL of 1% paraformaldehyde, and transferred to flow cytometry sample tubes. Fluorescence signal intensities from the samples were measured using a Becton Dickinson Fortessa cell sorter (BD) and data analysis was performed using FlowJo vX. The experiment was performed in triplicates.”[89]

K. Statistical Analysis

Statistical analysis was carried out using GraphPad Prism software (GraphPad). All conditions were tested in three replicates in at least triplicate experiments. Statistical significance between two groups was determined by Student's t -test, and one-way ANOVA followed by Dunnett's post-hoc test was used in case of more than two groups. * indicates $p \leq 0.05$, which was considered significant.

L. Methods unique to Chapter IV

i. Chromatin Immunoprecipitation (ChIP)

Chromatin immunoprecipitation was performed as described previously[96]. Briefly, for each pulldown, 30 µl Dynabeads protein G (Life technologies) were incubated with control and test antibodies overnight at 4°C. Antibodies: Normal rabbit IgG (Cell signaling, 1:100) and p53 (Santa Cruz, 1:100). Pulldowns were re-suspended in 100 µl ChIP dilution buffer. Cell lysis and Cross-linking: Murine Oviductal Epithelium (MOE) cells (10cm dish) were treated with 10 µM proteasome inhibitor MG132 (Sigma) for 4 hours. Cells were fixed with 270 µl of 37% formaldehyde (Sigma) for 15 minutes at room temperature. Reaction was quenched by adding 1.28 ml of 1 M glycine (final concentration was 125 mM) for 5 minutes at room temperature. Cells were washed twice with 2 ml of ice cold PBS + Pi (protease inhibitor - 1 cOmplete^{TM}, Mini, EDTA-free tablet in 10 ml PBS, Roche). 1 ml of PBS+Pi was added to each plate. Cells were scraped and centrifuged at 3000 rpm for 5 minutes at 4°C. Pellet was re-suspended in 750 µl ChIP lysis buffer. Sonication was carried out on ice using a Sonic Dismembrator (Branson, Model 500) as described previously[97]. Sonicated lysate was cleared by centrifuging at 14,000 rpm

for 10 minutes at 4°C. 250 µl supernatant was saved as “input sample” at -20°C. Cross-linking was done by combining 250 µl supernatant with 100ul of Protein G bead slurry attached to IgG and p53 antibodies and incubated overnight at 4°C. De-crosslinking: Beads were washed with following buffers, in the order listed: Low salt buffer, High salt buffer, Lithium Chloride Complex and 1X TE buffer. 400-µl of elution buffer was added to sample tubes and incubated for 15 minutes by 360° rotation at room temperature. Eluate was collected and made up to 400 µl with elution buffer. 16uL of 5 M NaCl was added to each pull-down and input. Tubes were sealed with parafilm and allowed to de-crosslink overnight at 65°C. DNA purification: 8 µl of 500 mM EDTA (pH 8.0), 16 µl of 1 M Tris-HCl (pH 6.5) and 0.1ug/mL RNAse A were added to sample and input tubes followed by 1 hour incubation at 37°C. 1 ul of 20 mg/ml proteinase K was added and tubes were incubated at 45°C for 1 hour. Lysates were carried forward for phenol chloroform extraction using UltraPure™ Phenol:Chloroform:Isoamyl Alcohol (25:24:1, v/v) as described by manufacturer’s protocol (Thermo Fisher Scientific). PCR Quantification and data analysis: Input sample was diluted 1:100 prior to PCR setup. SYBR green master mix PCR was carried out at final concentration of 10 µl (3.6 µl dH_2O, 10 µM primer pair, 5 µl SYBR green mix) in 96-well plates on ABI ViiA7 (default three-step method, 40 cycles). The relative occupancy of the immunoprecipitated protein at a target gene promoter was estimated using the following equation: $2^{\wedge}(Ct^{IgG} – Ct^{p53})$, where Ct^{IgG} and Ct^{p53} are mean threshold cycles of PCR done in replicate on DNA samples precipitated from IgG and p53 subtracted from the input mean Ct.

ii. High Throughput Screen (HTS)

The UIC HTS core facility provided a library (Prestwick) of 1200 FDA approved drugs for high throughput screen. Drugs that increased PAX2 promoter activity more than 170% compared to DMSO control were selected for future analysis. Primary HTS assay: MOE cells were transiently transfected with PAX2 promoter driving luciferase expression (PAX2-Luc, 100 ng/well) and β-Galactosidase (β-Gal, 100 ng/well) for 18 hours. Cells were seeded in 96-well plates at 7.5 X 10^3 cells/well. Drugs were added to the cells after 3 hours. 50 µM drug stock solutions were prepared in MOE culture media and 20 µl was dispensed in each well (final drug concentration was 10 µM). Cells were incubated for 10 hours at 37°C in a 5% CO_2 incubator. To measure luciferase production, cells were lysed in 110 µl GME buffer (25 mM glycylglycine (pH 7.8), 15 mM $MgSO_4$, 4 mM EGTA, 1 mM dithiothreitol, 1% Triton X-100), and 50 µl lysates were added to assay buffer (GME buffer, 16.5 mM KPO_4, 2.2 mM ATP, 1.1 mM dithiothreitol). Luciferase activity was measured for 30 seconds on a Biotek Synergy 2 multi-mode plate reader (Biotek). LacZ activity (remaining 50 µl lysate) was measured by cleavage of ONPG. The sample results were normalized to β-galactosidase (internal control) to account for transfection efficiency by dividing the luciferase activity by the β-galactosidase activity. Fold change was calculated by taking the luciferase value, dividing by the β-galactosidase activity, and then dividing by the solvent (DMSO) control, which was set equal to one [98]. Each 96-well plate contained 16 wells treated with DMSO and remaining 80 wells with drugs from PRESTWICK library. Top 2% drugs that increased PAX2 promoter activity (more than 170% compared to DMSO) were re-tested to confirm consistent activity and three drugs (hits) were selected for future analysis. Secondary biological screen: MOE cells were treated with 10 µM of "hits"

from the primary screen (incubation time was 10 hours). Cells were lysed either with TRIZOL or RIPA lysis buffer to extract RNA or protein respectively. Amount of PAX2 mRNA (by qPCR) and protein (western blot analyses) was quantified and compared between cells treated with "hits" and DMSO. Determination of z-factor: MOE cells were transfected with PAX2-Luc, β-Gal and either GATA4 or mutant $p53^{R273H}$ plasmids. GATA4 significantly upregulates (positive control) whereas mutation in *TP53* reduces (negative control) PAX2 promoter activity as measured by luciferase assay. Calculated z-factor for this assay was 0.6.

M. Methods unique to Chapter V

i. Materials

"G5 PAMAM dendrimer, acetic anhydride, triethanolamine (TEA), FITC, dimethylsulfoxide (DMSO), methanol, and deuterium oxide (D2O) were obtained from Sigma-Aldrich. Sulfo-SMCC was obtained from Thermo Fisher Scientific. FSH33 peptide with the sequence YTRDLVYKDPARPKIQKTCTF was synthesized at the University of Illinois at Chicago Research Resources Center (UIC RRC, Chicago, IL). All other chemicals used in this study were obtained from Sigma-Aldrich unless stated otherwise."[89]

ii. Preparation of partially acetylated FITC- and Cy5.5-labeled G5 PAMAM dendrimers (G5-Ac-FITC-NH2 and G5-Ac-Cy5.5-NH2)

"G5 PAMAM dendrimer was partially acetylated as previously described[99-102]. Briefly, G5 PAMAM (20 mg, 7.0 × 10-4 mmol) was dissolved in 4 mL methanol, to which acetic anhydride (6.4 μL, 6.8 × 10-2 mmol, 75% the number of primary amines on G5) and TEA (11.4 μL, 8.2 × 10-2 mmol) was added under vigorous stirring at RT for 24 h. The product was purified by ultrafiltration using an Amicon Ultra-15

Centrifugal Filter Unit (MWCO 3000, Millipore) at 4000 rpm and 4 °C for 20 min, with repeated washing with deionized distilled water (ddH_2O) ten times. The product was then re-dissolved in ddH2O and lyophilized, resulting in partially acetylated G5 (G5-Ac-NH2). G5-Ac-NH2 was labeled by reaction with FITC and Cy5.5 as previously described.[100-102]. Briefly, G5-Ac-NH2 (10 mg, 3.5 × 10-4 mmol) was dissolved in ddH2O, to which either FITC (0.7 mg, 1.7 × 10-3 mmol) or Cy5.5 (0.9 mg, 0.8 × 10-3 mmol) dissolved in 100 µL DMSO was added under vigorous stirring at RT for 24 h. Excess FITC was removed by ultrafiltration as described above. The product was finally re-dissolved in ddH_2O and lyophilized, resulting in G5-Ac-FITC-NH2. The number of FITC molecules attached to the dendrimer was determined using UV/Vis (DU800 UV/Vis Spectrophotometer, Beckman Coulter) based on a standard curve of FITC in ddH_2O at 499 nm absorbance wavelength"[89].

iii. Preparation of FSH33-targeted dendrimers (G5-Ac-FITC-FSH-NH2 and G5-Ac-Cy5.5-FSH-NH2)

"G5-Ac-FITC-NH2 and G5-Ac-Cy5.5-NH2 (5 mg, 1.7 × 10-4 mmol) was dissolved in 2 mL of conjugation buffer, pH 7.8. Sulfo-SMCC (3.8 mg, 8.7 × 10-3 mmol) was dissolved in 100 µL of DMSO and 400 µL ddH2O, and then added to the dendrimer solution under vigorous stirring at RT for 2 h. Excess sulfo-SMCC was removed by ultrafiltration (MWCO 3000, 4000 rpm, 20 min) and washing with ddH2O three times. The product was re-dissolved in 2 mL conjugation buffer, pH 7.2, and FSH33 peptide (2.2 mg, 8.7 × 10-4 mmol, 5 molar equivalents to G5) dissolved in 500 µL ddH2O was added under vigorous stirring at RT for 24 h. Excess FSH33 was removed by dialysis against ddH2O using a 12000-14000 MWCO dialysis membrane for two days with frequent changing of the water. The resulting G5-Ac-

FITC-FSH-NH2 and G5-Ac-Cy5.5-FSH-NH2 was then lyophilized. The number of FSH33 molecules attached to the dendrimer was determined using UV/Vis based on a standard curve of FSH33 in ddH2O at 273 nm absorbance wavelength.

In order to minimize nonspecific interactions with biological membranes[103, 104], the remaining primary amines on all the conjugates prepared were capped by full acetylation. Five milligrams of each conjugate (1.7 × 10-4 mmol) was dissolved in 1 mL methanol, to which excess acetic anhydride (3.9 μL, 4.1 × 10-2 mmol) and TEA (6.8 μL, 4.9 × 10-2 mmol) was added under vigorous stirring at RT for 24 h. Each product was diluted with ddH2O, purified by ultrafiltration as described above, re-dissolved in ddH2O and lyophilized, resulting in the fully acetylated conjugates G5-Ac-FITC, G5-Ac-FITC-FSH, G5-Ac-Cy5.5 and G5-Ac-Cy5.5-FSH. G5-Ac-Cy5.5 and G5-Ac-Cy5.5-FSH were also characterized by 1H NMR as described in our earlier publications[90, 91]".[89]

iv. Cytotoxicity of G5 PAMAM Dendrimers

"OVCAR-3 cells (n = 4) were seeded into 96-well plates at 1 × 104 cells/well. The next day, cells were treated with 0.5, 1 and 5 μM G5-Ac-FITC and G5-Ac-FITC-FSH. The cells were allowed to grow for 24 h. Cell viability was measured using sulforhodamine B (SRB) colorimetric assay. Media was aspirated and cellular proteins were fixed to the plate with 20% trichloroacetic acid for 1 h. Cells were washed with water and stained for 30 min with SRB. Excess dye was washed with 1% (v/v) acetic acid. The protein-bound dye was re-suspended in 10 mM Tris buffer. Spectrophotometric analysis was completed using a Biotek Synergy 2 multi-mode microplate reader (Biotek)."[89]

v. Cellular Uptake Studies in 2D Cell Culture

"OVCAR-3 and SKOV-3 cells were plated in 8-well chamber slides (Millipore) at a density of 2 × 104 cells/well for 24 h. OVCAR-3 cells were then treated with 250 nM and 500 nM of G5-Ac-FITC-FSH for 5 h. Another set of OVCAR-3 cells was pre-treated with 100 μM FSH33 for 2 h, before adding the different concentrations of G5-Ac-FITC-FSH as above. OVCAR-3 cells were also treated with 250 nM and 500 nM of G5-Ac-FITC for 5 h. SKOV-3 cells were treated with 500 nM of G5-Ac-FITC-FSH for 5 h. At the end of each incubation period, cells were washed with PBS, fixed in 4% paraformaldehyde for 5 min, washed with PBS, and mounted with Vectashield Mounting Medium with DAPI (Vector Laboratories)."[89]

vi. Confocal Microscopy Observation

"Cells were visualized using a Zeiss LSM 510 Meta confocal laser-scanning microscope (CLSM, Carl Zeiss). A 25 mW diode UV 405 nm laser was used for excitation of DAPI, and the 488 nm line of a 30 mW tunable Ar laser was used for the excitation of FITC. Emission was filtered at 420 nm and 505-530 nm for DAPI and FITC, respectively. Images were captured using a 63x/1.2 Water DIC C-Apochromat objective."[89]

vii. In Vivo Efficacy Study and Tissue Analysis

"Six- to eight-week-old female BALB/c mice (6 animals per group) were injected i.p. with 15 mg/kg targeted (G5-Ac-Cy5.5-FSH) or nontargeted (G5-Ac-Cy5.5) dendrimer conjugates in ~100 μL saline. At 6 h post-injection, animals were euthanized using CO2, followed by cervical dislocation to ensure death. Organs (ovary, oviduct, uterus, and kidney) were harvested for analysis. Each organ was

weighed and transferred to a microcentrifuge tube containing 225 µL of ddH2O. The samples were homogenized on ice using a manual homogenizer. Tissue homogenates were centrifuged at 13,200 rpm at 4 °C for 30 minutes. Supernatants were collected in a fresh tube, and the fluorescence from the supernatants was measured at 675 nm excitation and 694 nm emission wavelengths using a BioTek Synergy 4 microplate spectrofluorometer. The fluorescence counts were normalized to the weight of the tissue."[89]

TABLE III

MANUFACTURER'S INFORMATION

Company	City	State
Harlan Laboratories	Indianapolis	IN
Mirus	Madison	WI
Mediatech, Inc.	Manassas	VA
Gibco	Carlsbad	CA
Roche	Indianapolis	IN
Selleck Bio	Houston	TX
Abcam	Cambridge	MA
Cell Signaling	Beverly	MA
Developmental Studies Hybridoma Bank	Iowa City	IA
Sigma Aldrich	St. Louis	MO
American Type Culture Collection	Manassas	VA
Invitrogen	Grand Island	NY
Life Technologies	San Diego	CA
Ipsen Biopharmaceuticals, Inc.	Basking Ridge	NJ
Calbiochem	Billerica	MA
Pierce	Rockford	IL
Thermo Fisher Scientific	Waltham	MA
Protein Simple	Santa Clara	CA
Vector Labs, Inc.	Burlingame	CA
Fisher Scientific	Pittsburgh	PA
Nikon Instruments	Melville	NY
NIH	Bethesda	MD
EMD Millipore		
ProteinTech Group, Inc.	Chicago	IL
Santa Cruz Biotechnology	Santa Cruz	CA
Biotek	Winooski	VT
AmScope	Irvine	CA
BioRad	Hercules	CA
Qiagen	Valencia	CA
Becton Dickinson (BD)	Franklin Lakes	NJ
GraphPad	La Jolla	CA
Millipore	Billerica	MA
Vector Laboratories	Burlington	CA
Carl Zeiss	Germany	
transOMIC	Huntsville	AL
Origene	Rockville	MD
Promega	Madison	WI

III. GONADOTROPINS ACTIVATE ONCOGENIC PATHWAYS TO ENHANCE PROLIFERATION IN NORMAL MOUSE OVARIAN SURFACE EPITHELIUM

(Reprinted with permission from *Int J Mol Sci, 14*(3), 4762-4782, doi:10.3390/ijms14034762)

A. INTRODUCTION

While the etiology of ovarian cancer is poorly understood, there are a number of proposed hypotheses, all of which incorporate ovulation as a component in ovarian cancer initiation and promotion. The gonadotropins, follicle stimulating hormone (FSH) and luteinizing hormone (LH), are implicated in the etiology of ovarian cancer primarily because the median age of onset of ovarian cancer typically intersects with menopause and physiologically elevated levels of FSH and LH[22, 105]. High levels of gonadotropins during ovulation, loss of gonadal negative feedback during menopause, and premature ovarian failure are all thought to play a role in ovarian cancer[18, 22]. The gonadotropin hypothesis is supported by the decreased risk of ovarian cancer from a reduction of exposure to FSH and LH by the use of oral contraceptives, multiparity, and breast-feeding[22], and an increased risk of the disease with early menarche, late menopause, nulliparity, and the use of fertility drugs[105, 106]. However, the effects of gonadotropins on completely normal OSE cultured in the ovarian microenvironment are not fully characterized.

The gonadotropins, FSH and LH, are glycoprotein hormones synthesized in the anterior pituitary[22, 107]. Both FSH and LH share a common α-subunit, but each has a distinctive β-subunit, which confers the specificity of the two hormones[108]. FSH is responsible for the maturation of immature follicles to Graafian follicles[109]. LH triggers ovulation and development of the corpus luteum. The effects of FSH and LH on granulosa and theca cells[110, 111] have been published, but the role of these gonadotropins on normal OSE is less well characterized. FSH receptors (FSHR)

and LH receptors (LHR) are expressed in normal OSE, normal fallopian tube epithelium, and ovarian tumor samples[22, 112, 113]. Several investigators have attempted to address the possible role of the gonadotropins in OSE using tumorigenic models as it pertains to EOC. *In vivo* studies demonstrate that FSH and LH increase OSE proliferation[24-26]. *In vitro* studies have reported that FSH or LH alone increases[105, 112], decreases[114, 115], or has no effect on cellular proliferation of OSE cells[22, 116, 117]. Tubal epithelial cells express FSH and LH receptors, but normal TECs do not proliferate in response to gonadotropins[18]. FSH and LH signal together *in vivo* in post-menopausal women and during ovulation these hormones are almost always found at the same time. However, very little has been published regarding the combined effects of gonadotropins on signaling in OSE or ovarian cancer.

The purpose of this study was to identify the pathways downstream of the gonadotropins in normal OSE and their contribution towards proliferation and oncogenesis. Many *in vitro* studies using SV40T immortalized OSE cells or *in vivo* studies using animal models have been reported to evaluate the role of FSH and LH, but these systems fail to separate ovulation and the effects of gonadotropins, do not use completely normal cells, or separate the cells from their microenvironment[20, 22, 107]. This study used two different model systems to evaluate the actions of gonadotropins on normal OSE function. A three-dimensional (3D) organ culture system was employed to study the role of gonadotropins in normal cells grown within their microenvironment in the absence of ovulation[95]. Simultaneously, the effects of gonadotropins on the OSE alone were studied using a normal mouse OSE cell line. FSH, LH and the combination of FSH and LH (FSH+LH) enhanced cellular proliferation by activating Akt signaling and upregulating pro-proliferative cyclin dependent kinases and anti-apoptotic Birc5.

B. RESULTS

Gonadotropins enhance proliferation of normal OSE

Gonadotropins have been reported to have widely variable growth stimulatory properties on OSE *in vitro*[118-120], but *in vivo* they seem to enhance proliferation[24, 26]. Therefore, to further characterize the contribution of the gonadotropins to OSE proliferation, a 3D organ culture system that propagates normal OSE in an alginate hydrogel was employed. Ovarian organoids were cultured for 8 days with FSH, LH and the FSH+LH at a dose of 1, 10 or 100 mIU/ml, representing a range of physiologically relevant concentrations. To determine the percentage of proliferating cells, BrdU was incorporated into the culture media 24h prior to fixation. FSH at all three doses in 3D significantly increased proliferation of OSE as compared to basal media, while LH and the combination of FSH and LH only significantly increased proliferation at 10 and 100 mIU/ml **(Fig. 3A)**. In order to compare the effects of FSH, LH and FSH+LH on OSE proliferation *in vitro*, 2D mouse ovarian surface epithelial cells (MOSE) were analyzed for proliferation after stimulation with gonadotropins for 8 days[121]. FSH at 1, 10 and 100 mIU/ml increased proliferation above basal levels, LH increased proliferation at 1 and 10 mIU/ml, and FSH+LH increased proliferation at 10 and 100 mIU/ml **(Fig. 3B)**.

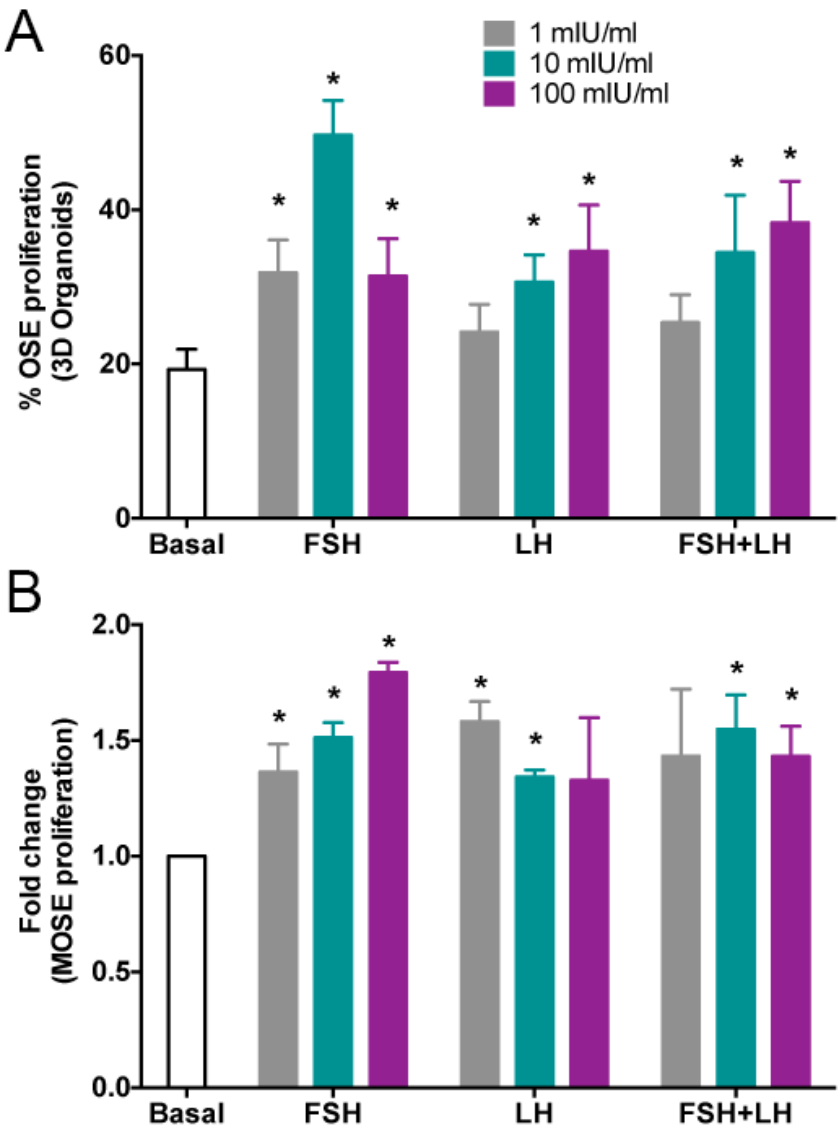

Figure 3: Gonadotropins increase OSE proliferation in 3D organoids and MOSE cell line. A) Using BrdU as a marker of DNA synthesis, the gonadotropins increased proliferation of OSE in organoids after 8 days. **B)** Proliferation of MOSE cells in response to gonadotropin stimulation was measured by SRB assay after 8 days. [(*) different than basal $p<0.05$].

Gonadotropins regulate oncogenic signal transduction pathways in normal mouse OSE cultured in 3D

To investigate the signal transduction pathways altered in normal mouse OSE cultured in 3D that may be involved in the proliferative response observed following culture with the gonadotropins, organoids were cultured for 3 days in basal media followed by 24h incubation with 10 mIU/ml FSH, LH or FSH+LH. The organoids were incubated with collagenase to collect an enriched OSE cell preparation and the mRNA was subjected to a Cancer Pathway Finder qPCR array. The array identified several signal transduction pathways in OSE that were altered in response to FSH, LH and FSH+LH as compared to OSE from organoids cultured in basal media. The gonadotropins increased gene expression of some pro-proliferative factors, including Akt. Although both FSH and LH significantly amplified the Akt pathway, LH and FSH+LH amplified both Akt1 and Akt2 isoforms, while FSH only amplified the Akt2 isoform. The pro-proliferative epidermal growth factor receptor (EGFR) was upregulated more by FSH and FSH+LH than LH alone. FSH and FSH+LH treated OSE amplified cyclin-dependent kinase 2 (Cdk2) as well as Cdk4 mRNA expression when compared to basal cultured OSE. The anti-apoptotic factor, Birc5, was amplified more when treated with FSH and FSH+LH than LH alone **(Table IV).** The gonadotropins alone and combined also upregulated expression of angiopoietin 1, which is involved in vascularization, and reduced the expression of pro-apoptotic caspase 8. Expression of mRNA for cyclin-dependent kinase inhibitor 2A (Cdkn2a), which slows progression through the cell cycle, was increased in response to FSH, LH and FSH+LH.

TABLE IV

ONCOGENIC PATHWAYS MODULATED BY GONADOTROPINS

Proliferation/ Cell Cycle Control			
Gene	**FSH**	**LH**	**FSH+LH**
Akt1	3.5	61	55
Akt2	58	58	37
Cdk2	3.7	1.0	2.6
Cdk4	22	0.9	175
Cdkn2a	38	25	17
Chek 2	1.6	0.7	1.0
Cyclin D1	1.4	0.6	1.3
EGFR	5.8	1.8	5.3
Mdm2	3.0	1.0	2.1
Myc	1.7	0.7	1.4
Trp53	2.5	1.0	2.0
Angiogenesis/ Metastasis/ Adhesion			
Angpt1	32	16	4.9
Mcam	3.0	1.2	2.0
c-Met	2.1	0.70	2.4
S100a4	3.2	0.6	2.2
Vegfc	3.5	1.1	2.4
Apoptosis			
Birc5	2.2	1.2	2.6
Casp8	0.92	0.1	0.45

The OSE from FSH, LH or FSH+LH treated organoids was removed using collagenase and mRNA was isolated. cDNA was reverse transcribed and added to a RT^2 Profiler PCR Mouse Cancer Pathway Finder Array. Numbers represent fold change compared to basal cultured organoids of pathways regulated by the gonadotropins.

Gonadotropins enhance Akt expression in normal OSE

In order to evaluate the effects of gonadotropins on Akt expression in the OSE, MOSE cells were employed[121]. MOSE cells were treated with FSH, LH or FSH+LH at 100 mIU/ml each for 5min, 15min, 1h, and 24h. A significant increase in the expression of phosphorylated Akt (p-Akt) was noted after 5 minutes when stimulated with FSH or LH **(Fig. 4)**. FSH and FSH+LH also enhanced p-Akt expression after 24h. Gonadotropin treatment did not affect the expression of total Akt in any of the treatment groups. The phosphatase PTEN inactivates Akt, and loss of homozygosity or mutation of this gene has been noted in ovarian cancer and endometrioid ovarian cancer, respectively[122, 123]. Therefore, PTEN expression was analyzed to determine if its loss contributed to the activation of Akt. Levels of PTEN and p-PTEN were not altered upon stimulation with FSH, LH or FSH+LH **(Fig. 4)**. Because p-ERK expression has previously been noted downstream of FSH and LH in human immortalized OSE and in human ovarian cancer cells, the activation of p-ERK was investigated[118]. Expression of p-ERK in all three groups was elevated after 5 minutes, but did not persist after 24h **(Fig. 4)**.

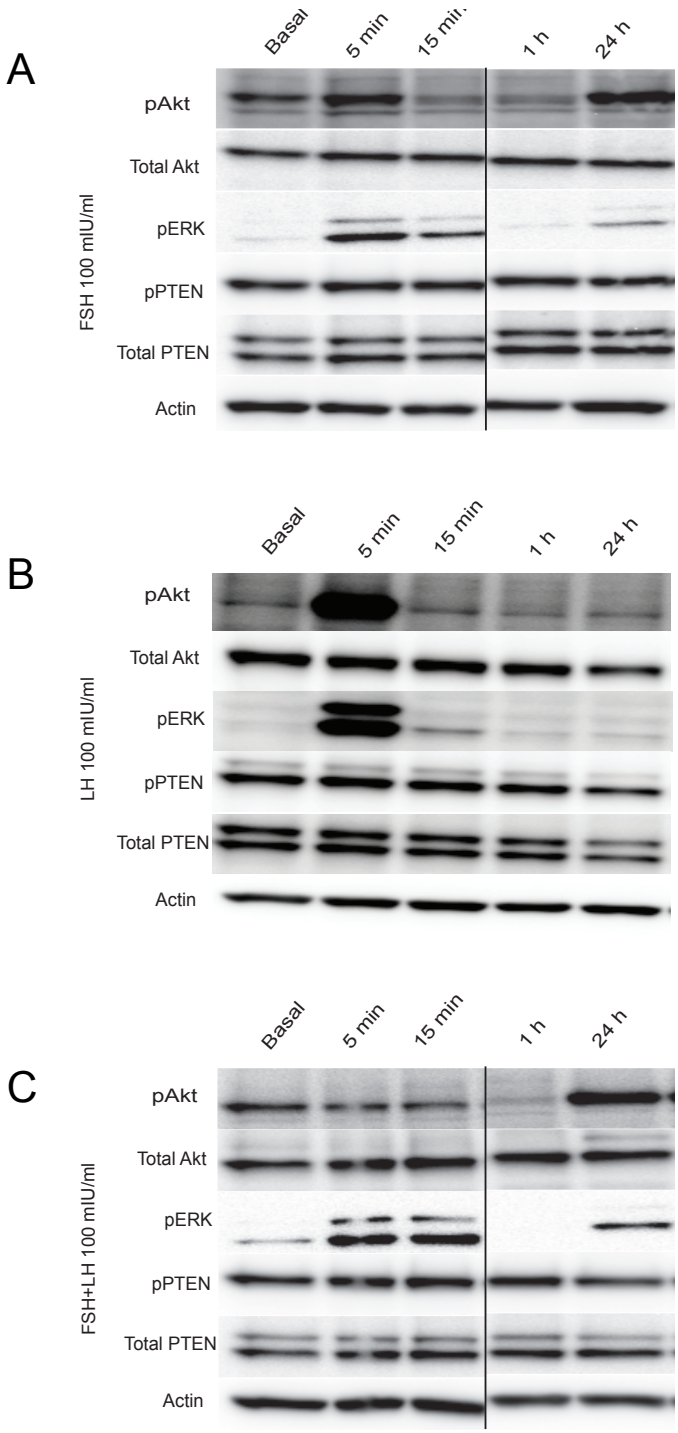

Figure 4: Gonadotropins upregulate pAkt and pERK expression in MOSE cells. Activated pAkt and pERK expression was observed in MOSE after treatment with 100 mIU/ml of **A)** FSH, **B)** LH or **C)** FSH+LH. Activated p-PTEN and total PTEN levels were similarly probed. Protein was normalized to actin.

The gonadotropins increased proliferation of the OSE in 3D organ culture (**Fig. 3**). To determine if proliferation of the OSE induced by the gonadotropins could be blocked by inhibiting the Akt pathway, organoids or MOSE cells were cultured with gonadotropins in the presence of MK-2206, a chemical inhibitor of Akt phosphorylation. First, 5 μM MK-2206 was added to the MOSE culture media for 5min in the presence of 100 mIU/ml of FSH or LH to validate that MK-2206 decreased p-Akt expression **(Fig. 5)**. Next, proliferation of OSE in 3D organ culture and 2D MOSE cells was monitored in the presence of gonadotropins combined with MK-2206. MK-2206 significantly decreased 3D OSE proliferation induced by FSH, LH or FSH+LH **(Fig. 6A)**. MOSE cells treated with the gonadotropins in the presence of MK-2206 exhibited a decreased rate of proliferation as compared to MOSE cells treated with the gonadotropins alone **(Fig. 6B)**. Inhibition of Akt also blocked basal levels of proliferation.

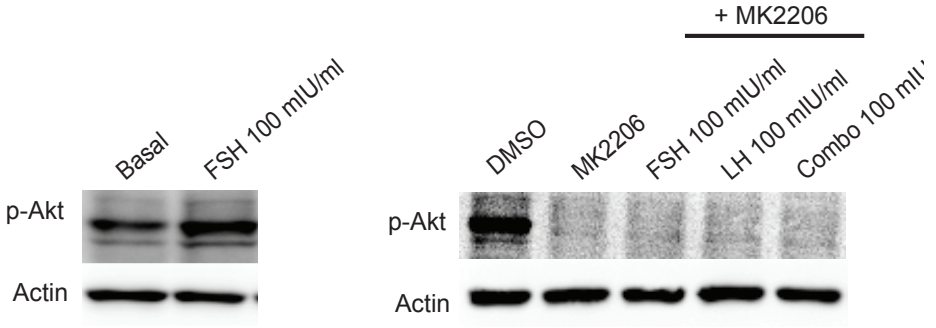

Figure 5: Gonadotropin induced p-Akt protein expression in MOSE cells was blocked in presence of an Akt inhibitor, MK-2206 at 5 min

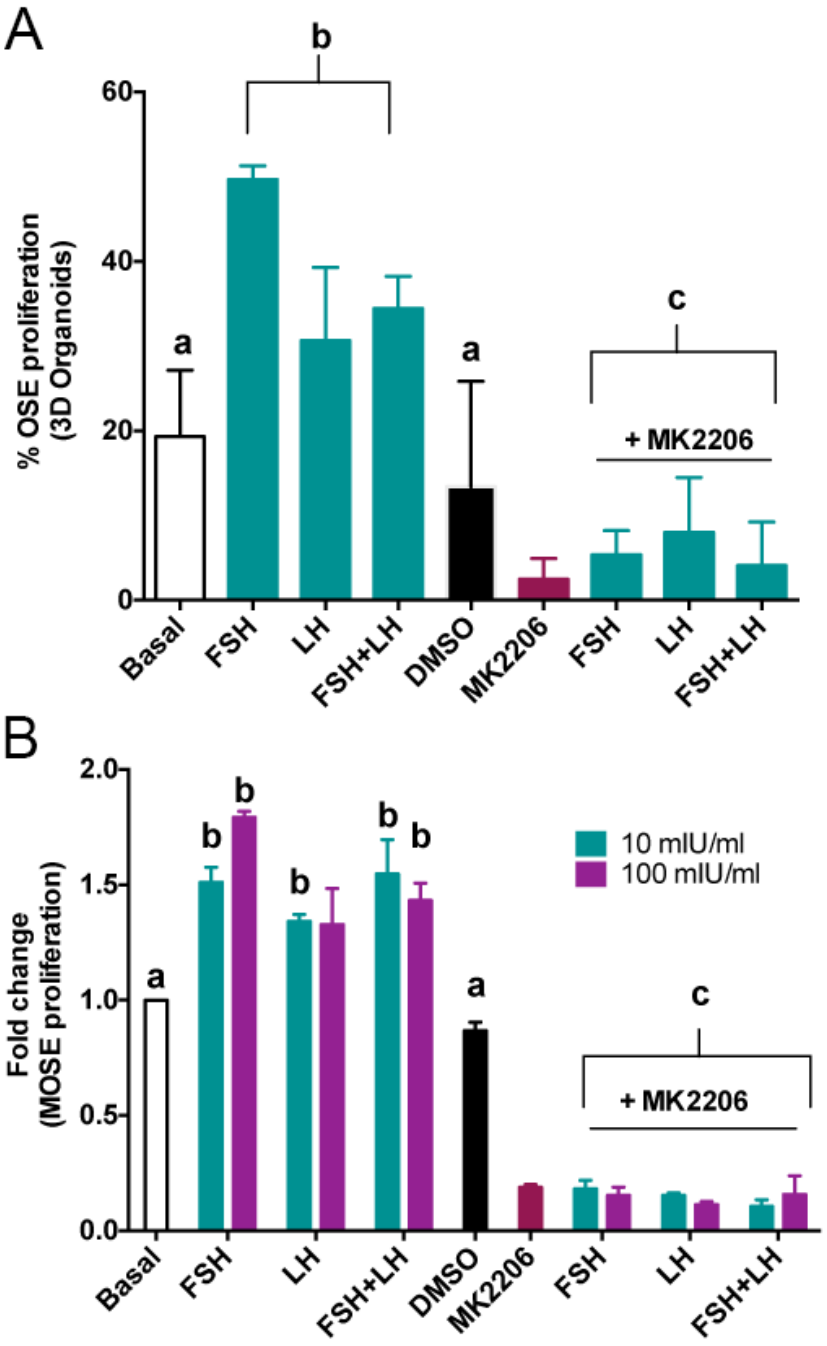

Figure 6: Inhibition of Akt signaling decreases gonadotropin regulated OSE proliferation. An Akt specific inhibitor MK-2206 significantly decreased gonadotropin induced OSE proliferation in **A)** 3D organoids (10 μM) and **B)** a MOSE cell line (2 μM). ['a' is different than 'b'; $p<0.05$, 'c' is different than groups treated with gonadotropins in absence of the inhibitor; $p < 0.05$].

The transcription pathway array indicated that EGFR mRNA was upregulated by gonadotropins, which has been observed in other studies using human ovarian cancer and normal OSE cells[118]. First, 100 nM AG1478 was added to the MOSE culture media for 5min in the presence of 100 mIU/ml of FSH or LH to validate that AG1478 decreased p-ERK expression, which is downstream of EGFR **(Fig. 7)**. To determine if inhibition of EGFR signaling blocked OSE proliferation, organoids were cultured for 8 days with FSH, LH or FSH+LH alone or with AG1478. AG1478 decreased OSE proliferation stimulated by FSH, LH, or FSH+LH in 3D organ cultures **(Fig. 8A)** and in MOSE cells treated with the gonadotropins **(Fig. 8B)**.

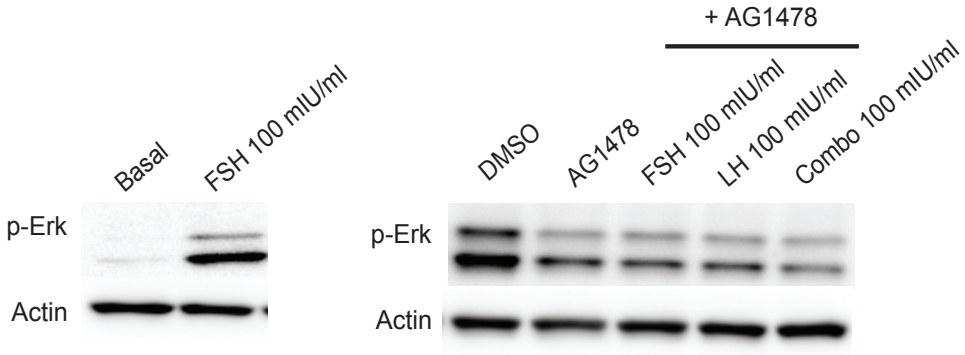

Figure 7: Gonadotropin induced p-Erk protein expression was suppressed in presence of EGFR inhibitor, AG1478 at 5 min.

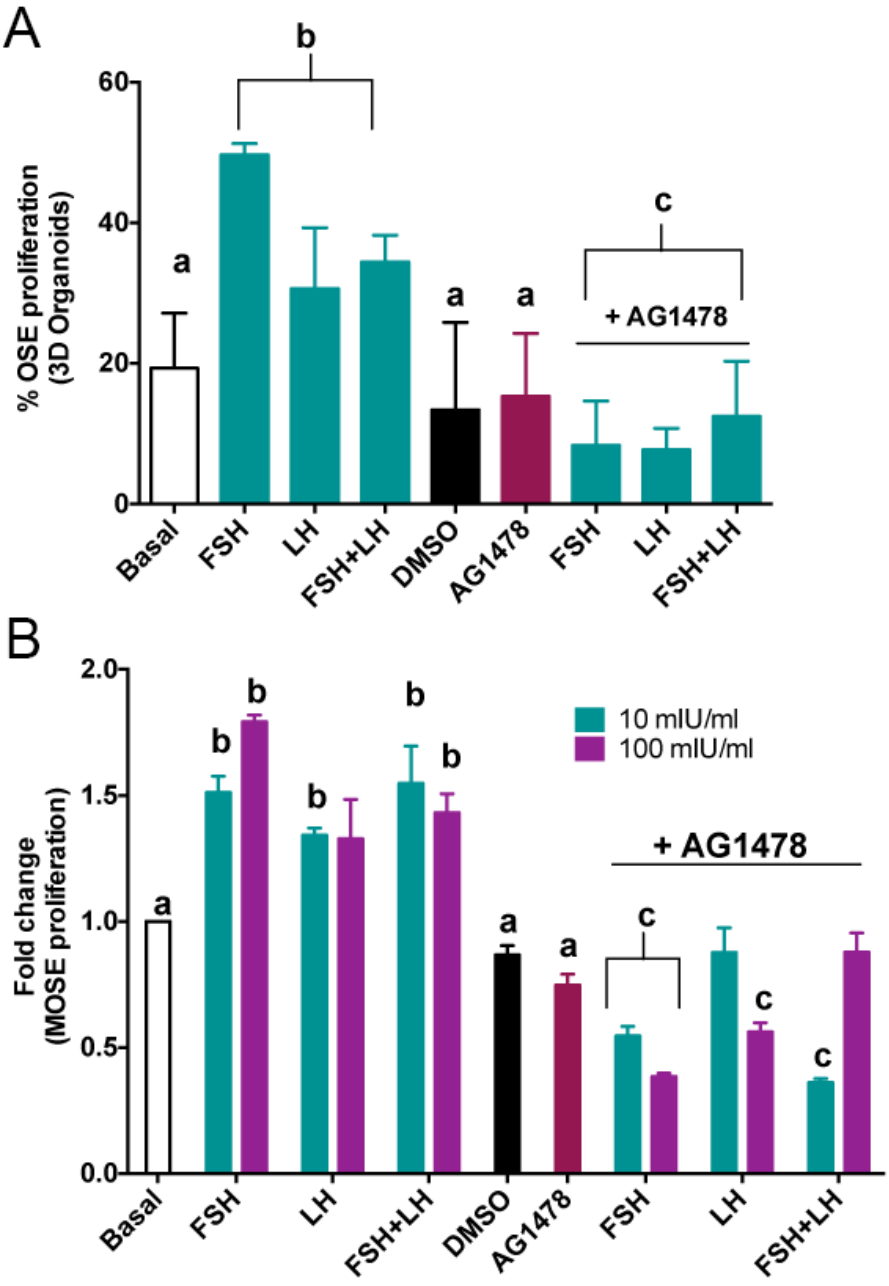

Figure 8: Inhibition of EGFR signaling repressed OSE proliferation in **A)** 3D and **B)** MOSE cells. Proliferation of the OSE caused by the gonadotropins is blocked after 8 days of culture in the presence of EGFR inhibitor AG1478 (100 nM) in both 3D cultured organoids and 2D cultured MOSE cells. [‘a’ is different than ‘b’; $p<0.05$, ‘c’ is different than groups treated with gonadotropins in absence of the inhibitor; $p < 0.05$].

Gonadotropins increase expression of proliferative and anti-apoptotic proteins in normal OSE

To determine if the mRNA expression levels identified from the transcription array correlated with protein expression, western blot analyses were performed for Birc5, Cdk2, Ckd4 and Cdkn2a. MOSE cells were treated with serum-free basal media or the gonadotropins for 15min, 1h and 24h. Birc5, also known as survivin, is an anti-apoptotic protein that could modulate the total number of cells as measured in the growth assays. Birc5 protein was upregulated by FSH, LH and FSH+LH at 24h when compared with basal conditions **(Fig. 9)**. Incubation with the Akt inhibitor MK-2206 was able to block Birc5 induction by FSH, LH and FSH+LH. The EGFR inhibitor AG1478 did not antagonize gonadotropin induction of Birc5, indicating that FSH and LH regulate Birc5 expression through an Akt-dependent pathway. Despite the fact that DMSO enhanced basal levels of protein expression, the Akt and EGFR inhibitors were able to block DMSO and gonadotropin induced expression of proteins[124].

Cdk2 protein was increased by FSH, LH and FSH+LH at 24h **(Fig. 9)**. Both the Akt inhibitor MK-2206 and the EGFR inhibitor AG1478 mitigated the induction of Cdk2 by FSH and FSH+LH. However, only MK-2206 reduced the expression of Cdk2 in LH treated MOSE cells. Cdk4 was induced by FSH, LH and FSH+LH **(Fig. 9)**. MK-2206 and AG1478 mitigated the gonadotropin induced Cdk4 expression suggesting that Cdk4 is located downstream of Akt and EGFR. Protein expression for cyclin-dependent kinase inhibitor 2A (Cdkn2a) was elevated at shorter time points, but was repressed after 24h when treated with FSH and LH, despite the increase in mRNA expression identified by the transcription array. In the presence of

FSH and LH alone, MK-2206 and AG1478 failed to relieve this repression of Cdkn2a at 24h. FSH+LH failed to repress Cdkn2a expression at 24h.

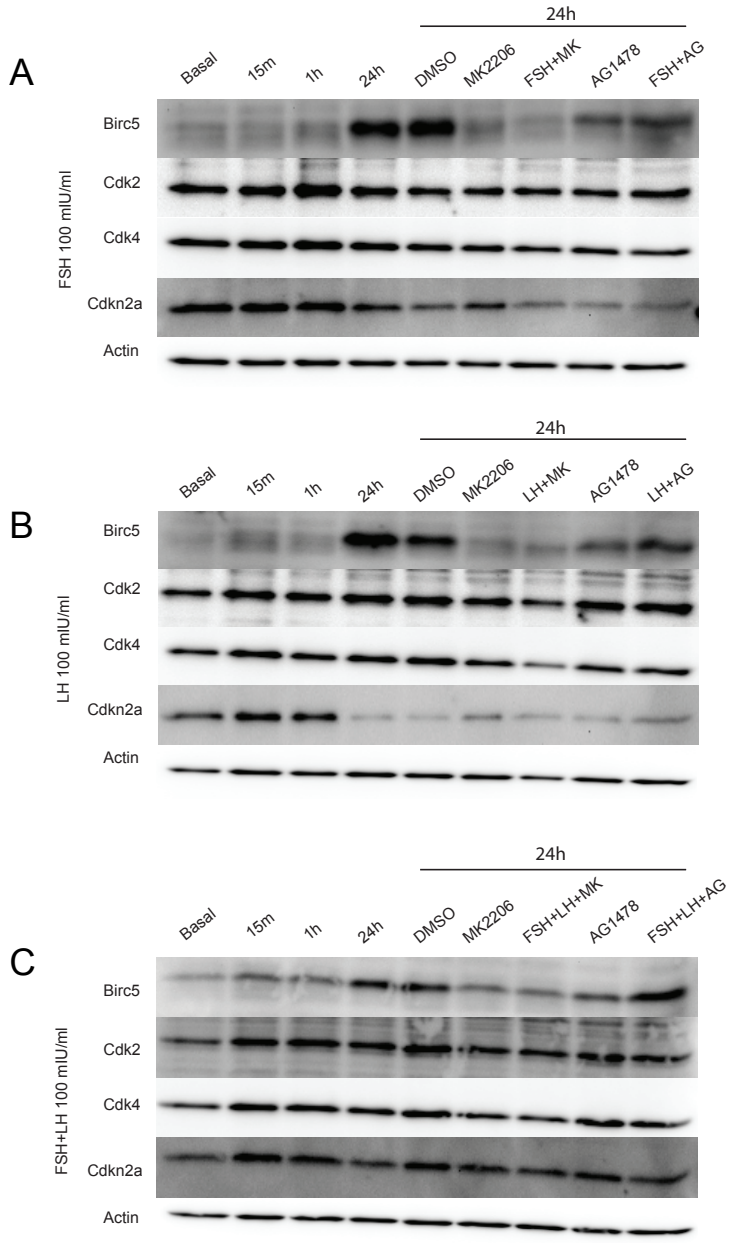

Figure 9: Gonadotropins regulate proliferative and anti-apoptotic signaling pathways in normal OSE downstream of Akt and EGFR. MOSE cells treated for 15min, 1h and 24h with **A)** FSH 100 mIU/mL, **B)** LH 100 mIU/mL and **C)** FSH+LH 100 mIU/mL and protein was analyzed for Birc5, cdk2, cdk4, and Cdkn2a. MOSE cells were treated for 24h with gonadotropins supplemented with the Akt inhibitor MK-2206 5 μM and AG1478 100 nM.

Gonadotropins enhance soft agar colony formation

To determine if the gonadotropins enhanced growth of colonies in soft agar, OSE from 3D organoids were cultured in 10 and 100 mIU/ml FSH, LH or FSH+LH for 3 days. Following stimulation with gonadotropins, the OSE from the organoids was collected using collagenase as previously described[93]. Only OSE from the organoids cultured in 100 mIU/ml LH demonstrated a significant increase in the number of colonies compared to those cultured in basal medium **(Fig. 10A)**. FSH and the combination of FSH+LH did not enhance colony formation. In order to investigate if the LH-induced increase in colony formation was dependent on Akt and EGFR signaling pathways, MK-2206 and AG1478 were added to 3D organoids cultured with LH. Both the inhibitors significantly reduced the number of colonies compared to those cultured without the inhibitors. To determine if gonadotropins promoted colony formation, organoids were cultured in 1mM H_2O_2 for 3 days, a condition that previously supported soft agar colony formation[93] followed by addition of OSE to soft agar overlaid with FSH, LH or FSH+LH medium. H_2O_2-induced OSE colonies in soft agar overlaid with 100 mIU/ml FSH showed a significant increase in number of colonies compared to those cultured in basal overlay media **(Fig. 10B)**. MK-2206 and AG1478 in presence of FSH in the media overlay significantly reduced the number of colonies formed compared to those formed by the OSE cultured with FSH alone.

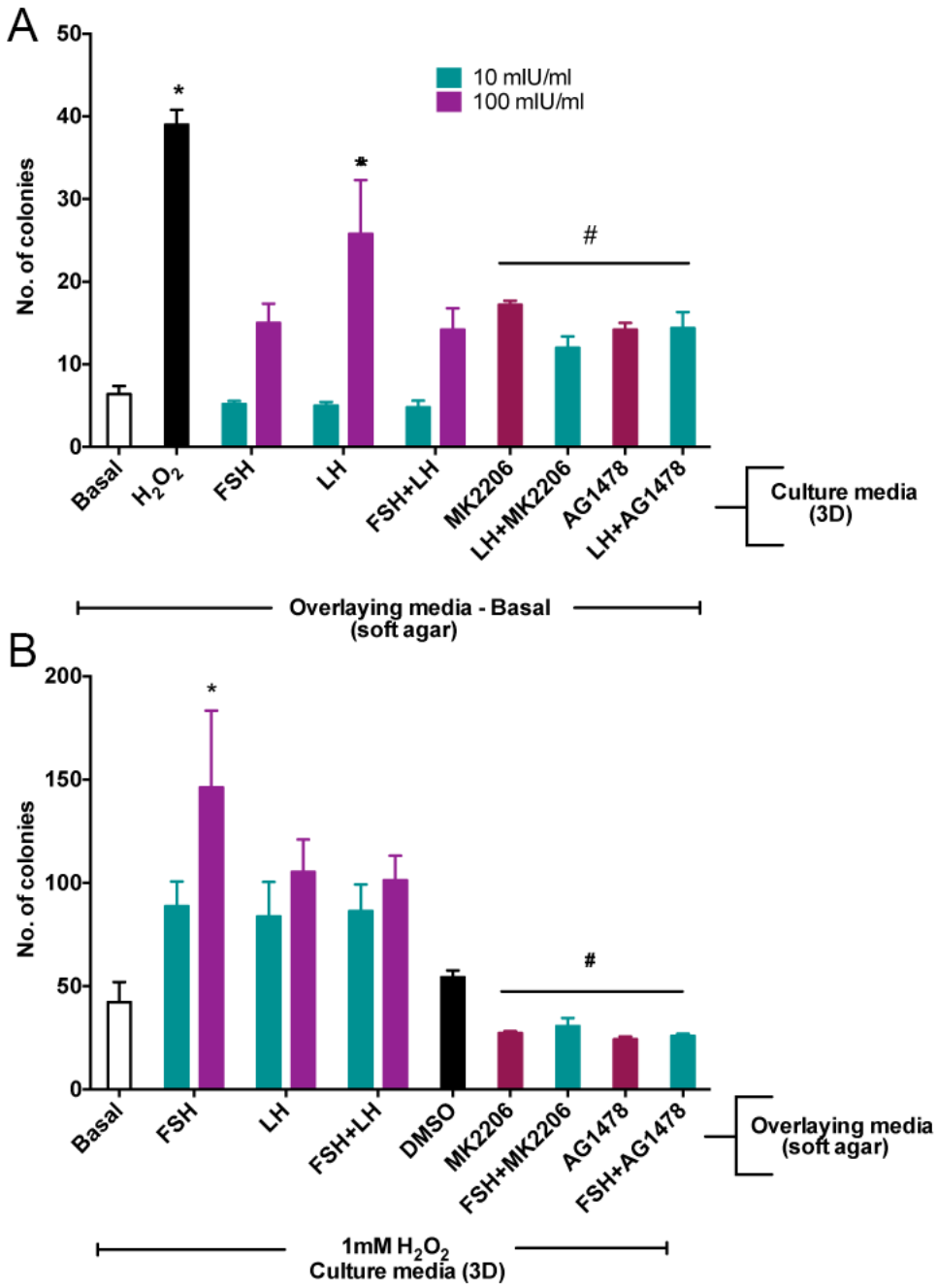

Figure 10: LH treated OSE increased anchorage independent growth. **A)** OSE from 3D organoids cultured in 100 mIU/ml LH demonstrated an increase in colony formation when compared to basal cultured organoids that could be blocked with MK-2206 and AG1478 whereas **B)** OSE cultured in 1mM H_2O_2 and overlaid with FSH showed an increase in colony formation compared to OSE overlaid with basal medium that could be blocked with MK-2206 and AG1478. [(*) different than basal; $p < 0.05$, '#' is different than (*); $p < 0.05$]

C. DISCUSSION

Ovarian cancer is commonly diagnosed in post-menopausal women, when the levels of FSH and LH are elevated[107]. The intersection between high levels of gonadotropins and the average age of incidence of ovarian cancer is the basis of a hypothesis suggesting a relationship between gonadotropins and an increased risk and incidence of ovarian cancer. Gonadotropins induced OSE proliferation in an *in vitro* 3D mouse model of primary OSE cells and in a normal mouse OSE cell line. Elevated levels of cell cycle regulatory and anti-apoptotic proteins that regulate proliferation were observed in MOSE cells treated with gonadotropins. LH stimulated colony formation of 3D cultured OSE in soft agar. FSH+LH was not able to completely mimic either hormone alone and reduced colony formation as compared to LH. Proliferation and colony formation could be blocked with both Akt and EGFR inhibitors indicating that these are important regulators of growth in normal OSE. FSH, LH, and the combination of FSH+LH induced Birc5, which was blocked when Akt was inhibited. FSH and FSH+LH induced Cdk2, which was reduced by Akt and EGFR inhibition. Overall these data indicate that the gonadotropins individually and in combination regulate proliferation, but the mechanisms of regulation by each hormone are different.

Proliferation of the OSE and its association with ovulation has been suggested to play a role in OSE transformation and cancer progression[24]. The results from this study are similar to *in vivo* findings of increased OSE proliferation in response to the gonadotropins in different animal models[24-26, 125]. When comparing the 2D and 3D systems, OSE grown in 2D, stimulated with gonadotropins, began to proliferate much faster (day 2-data not shown) than in 3D (day 8). However, both 2D and 3D systems displayed enhanced proliferation after 8 days. The discrepancy between

model systems implies that the architecture of the ovarian microenvironment likely impacts the proliferation of normal OSE. This report did not evaluate estrogen receptor (ER) signaling in the ovarian surface, which potentially could occur if the gonadotropins are stimulating the follicles to secrete estrogen in the organoid[105, 126]. Further, the 2D proliferation assay and the CK8/BrdU labeled immunohistochemistry on 3D organ culture did not account for the ERα induced OSE signaling that could have occurred in addition to proliferation.

Investigating pathways involved in carcinogenesis allowed for the detection of a series of specific genes regulated in the OSE by FSH, LH and FSH+LH. Akt is a serine/threonine kinase that is activated in roughly 68% of ovarian cancers[122]. Akt1 is activated in ovarian cancer, Akt2 is overexpressed in primary tumors as well as human ovarian carcinoma cell lines[127-130], and Akt3 expression is elevated in 20% of ovarian cancers[131]. The qPCR array identified transcriptional upregulation of Akt1 and Akt2 by LH and FSH+LH, while FSH increased expression of only Akt2. The transcription array data indicated that total Akt expression was enhanced but it did not correlate with the 2D MOSE cell line data likely because the mRNA was from an enriched OSE preparation that contained some underlying stromal cells. In addition to stromal cells, the OSE preparation is likely to be contaminated with a small percentage of theca and granulosa cells that express gonadotropin and EGF receptors[110, 132]. FSH and LH signaling via these receptors could account for the discrepancy in the fold change observed in Akt1 and Cdk4 in response to FSH, LH and FSH+LH. Immunohistochemistry indicated that the stroma had abundant expression of Akt after stimulation with gonadotropins (data not shown). However, the 2D cell line data does support that Akt is phosphorylated by the gonadotropins. The Cancer Genome Atlas Network did not identify mutation of Akt as the primary

mechanism for its activation, suggesting that perhaps stimulation by gonadotropins, is one possible mechanism for the elevated p-Akt levels observed in ovarian cancer.

Epidermal growth factor receptor (EGFR) is a transmembrane glycoprotein that contains an external binding domain and an intracellular tyrosine kinase domain[133, 134]. EGFR has been implicated in growth and progression of ovarian cancer, and may represent a prognostic indicator or potential therapeutic target[134]. EGFR overexpression has been shown to correlate with poor survival outcomes in women that have advanced ovarian cancer and have undergone cytoreductive surgery and combined therapy[133, 135, 136]. Inhibition of EGFR signaling by AG1478 in organ culture and MOSE cells significantly decreased OSE proliferation likely due to reduced expression of Cdk2 and Cdk4.

A soft agar assay demonstrated that post-menopausal concentrations of LH induced growth of OSE in soft agar. Initiation of anchorage–independent growth was recently demonstrated in non-tumorigenic ovarian epithelial cells that overexpressed β-hCG, which is a ligand that also activates LHR[137]. Overexpression of the hormone specific β-subunit of hCG induced cell cycle progression through elevated cyclin D1 expression and Cdk2 and Cdk4, similar to the results reported by this study[137]. Interestingly, when LH was combined with FSH it was no longer capable of inducing transformation, suggesting that FSH may somehow block LH induced transformation. Furthermore, when colony formation was initiated by exposure to oxidative stress, LH did not further enhance colony growth. However, FSH increased the formation of colonies that were derived from oxidative stress. We have recently demonstrated that oxidative stress transforms OSE by activating Akt, damaging DNA, and stimulating secretion of an ovarian stromal factor[93]. An interesting future direction will be to determine if FSH functions similarly to the

stromal factor to enhance colony formation downstream of DNA damage and Akt activation.

While the gonadotropins are typically studied as individual hormones, the current study attempted to monitor OSE proliferation when exposed to both hormones simultaneously. In postmenopausal women as well as during ovulation, FSH and LH are almost always circulating at the same time. Since the circulating levels of FSH and LH fluctuate periodically during the month, it is challenging to recapitulate the exact ratio of FSH and LH experimentally. Western blot analysis revealed that FSH+LH regulated the expression of proliferative proteins differently than the individual treatments of FSH or LH. FSH, LH, and FSH+LH were all able to stimulate the anti-apoptotic protein Birc5, which possibly accounts for the overall increase in survival at day 8. Birc5 was blocked by MK-2206, but not AG1478, indicating that Birc5 is more heavily regulated by Akt compared to EGFR. Intriguingly, average proliferation of OSE cultured in both 2D and 3D was lower when the gonadotropins were given simultaneously as compared to FSH alone. Furthermore, the combination of FSH and LH led to growth of fewer colonies in soft agar than LH alone. This may be reflective of the observation that the combination of gonadotropins reduced p-Akt expression after 5 minutes as compared to FSH alone. Interestingly, FSH and LH alone repressed the cell cycle inhibitor Cdkn2a expression at 24h, which was not seen with the combination of FSH+LH. Taken together, these findings support the hypothesis that gonadotropins affect specific oncogenic signaling pathways that enhance proliferation in normal mouse OSE.

D. CONCLUSION

Our study supports that gonadotropins induce proliferation in normal OSE cells of ovarian organ culture as well as MOSE cells. Gonadotropins regulate proliferation, cell cycle progression, apoptosis, and growth in soft agar. An improved understanding of molecular signaling mechanisms in normal OSE may help to identify novel targeted therapeutic approaches to slowing the growth of ovarian cancers derived from this cell type.

IV. INVESTIGATING PAX2 AS A NOVEL TARGET IN FALLOPIAN TUBE-DERIVED HIGH GRADE SEROUS OVARIAN CANCER

A. INTRODUCTION

Increasing evidence from high-risk population demonstrates that specific changes might represent a step-wise progression of serous cancer from the distal end of the fallopian tube[36, 37, 44]. Pathologists have suggested that a SCOUT (secretory cell outgrowth) may be one of the earliest changes observed in the fallopian tube epithelium in the progression to serous cancer. SCOUTs are clusters of ≥ 30 secretory cells that lack expression of the PAX2 protein[48]. SCOUTs are thought to progress into "p53 signatures" after the *TP53* gene is mutated, which often stabilizes expression of the p53 protein. SCOUTs and p53 signatures are benign, but p53 signatures are hypothesized to progress into serous tubal intraepithelial carcinomas (STICs), which are malignant precursors to serous carcinoma[138]. These lesions are identified in fixed tissues making it difficult to confirm the molecular signaling and regulation of protein expression that occurs in lesion development. In order to accurately model pelvic serous carcinogenesis, it is critical to determine the mechanism of precursor formation, and the signals that are downstream of key protein loss and gene mutation.

Several *in vitro* and *in vivo* animal models have been developed that further validate that neoplastic transformation from the FTE can result in tumor formation resembling human disease[60-63]. Several FTE-derived cellular models of murine and human origin have been engineered with a variety of oncogenes to form tumors in mice[35, 60, 62]. A study using PAX8-TetON-Cre promoter to drive deletion of BRCA1 and 2, PTEN and mutation of *TP53* in combination as well as deletion of *TP53* together with PTEN in murine oviductal FTE cells formed invasive carcinomas that

metastasized to the peritoneal cavity and immunohistochemical analysis revealed high similarity with human disease markers[63]. Another study conditionally silenced Dicer and PTEN using *Amhr2-Cre* to demonstrate that high-grade carcinomas develop in the FTE, with the primary epithelial tumors arising in the fallopian tube stroma[64]. STIC lesions reported from OVGP1-SV40 mice are a result of the viral oncoprotein, which sequesters p53 and inhibits the activity of wild-type p53[65]. Most of these *in vitro* human models do not accurately recapitulate the important changes that occur with *TP53* mutations since p53 is either silenced or sequestered by SV40. Therefore, a recently published murine oviductal epithelium (MOE) cell line that harbors mutation in *TP53* and is not immortalized by SV40, will serve as a valuable resource in evaluating early transformative events associated with HGSC[66]. Although these models mimic human disease and affirm fallopian tube as the source of origin, they fail to recapitulate the early transformative events and molecular pathways influencing precursor lesion development, such as loss of PAX2.

PAX2 belongs to the paired homeobox domain family and plays an important role during embryonic development[139]. PAX2 is critical for the development of the urogenital tract, thyroid, kidney, inner ear, eye and central nervous system[140]. PAX2 is also reported to interact with a nuclear protein containing BRCT domains, called PTIP (Pax transactivation-domain interacting protein)[141]. Studies have shown that PTIP is responsible for methylation of histone H3 at lysine 4 (H3K4)[142] and also plays a critical role in DNA damage repair[143]. Recruitment of co-repressor Grg4 displaced PTIP and H3K4Me complex in HEK293 cells[144]. Interestingly, studies have shown that wild-type p53 directly binds to multiple sites on the PAX2 promoter and stimulates PAX2 transcriptional activity in embryonic kidney cells[145]. PAX2 is expressed in Müllerian derived tissues such as the fallopian tube epithelium, but it is

not expressed in the OSE. Multiple studies have reported that PAX2 is absent in human HGSC cell lines as well as in serous tumor samples[49, 76, 138, 146]. Forced PAX2 expression in some HGSC cells reduced proliferation[76, 80]. Recent study reported that forced PAX2 expression induced tumorigenicity in murine OSE whereas in a murine model of high-grade serous ovarian cancer, PAX2 expression improved survival[80]. Therefore, understanding regulation of PAX2 and the mechanism of its loss in the fallopian tube epithelium might assist in clinical diagnosis of HGSC at an earlier stage.

The goal of this study was to determine functional significance of PAX2 loss in the fallopian tube cells, alone and in combination with a mutation in *TP53*. In addition, this study sought to determine whether re-expression of PAX2 was able to reduce serous tumor formation and growth. In order to develop a strategy for increasing PAX2, a small molecule screen was performed to look for molecules that activated a PAX2 promoter driving luciferase. PAX2 expression holds potential use for both prevention and therapy of fallopian tube derived serous tumors.

B. RESULTS

PAX2 expression in human serous tumor samples is associated with increased overall survival

Currently, several tools are available to perform prognostic analysis from publicly accessible databases. Microarray data from a Gene Expression Omnibus (GEO) database, with the accession number GSE69429 was retrospectively analyzed for comparing PAX2 expression between samples that represented normal fallopian tubes, STICs and serous cancer (n=6 per group)[147, 148]. PAX2 expression progressively declined from STICs to HGSC when compared to normal FTE **(Fig. 11A)**. A Kaplan-Meier survival analysis software (www.kmplot.com) allows for meta-analysis of several published ovarian cancer microarray datasets to identify biomarkers associated with survival[149]. When the patient population was stratified to include data only from stage III or IV serous tumor samples (n=956), high PAX2 expression significantly correlated with increased overall survival **(Fig. 11B)**. Similarly, the TCGA dataset demonstrated that a small subset of patients whose tumors had amplification in the PAX2 gene, survived longer than those without any alteration in PAX2 **(Fig. 11C)**. The TCGA also reports that the locus is not methylated or mutated, but rather the reduction is due to loss of mRNA.

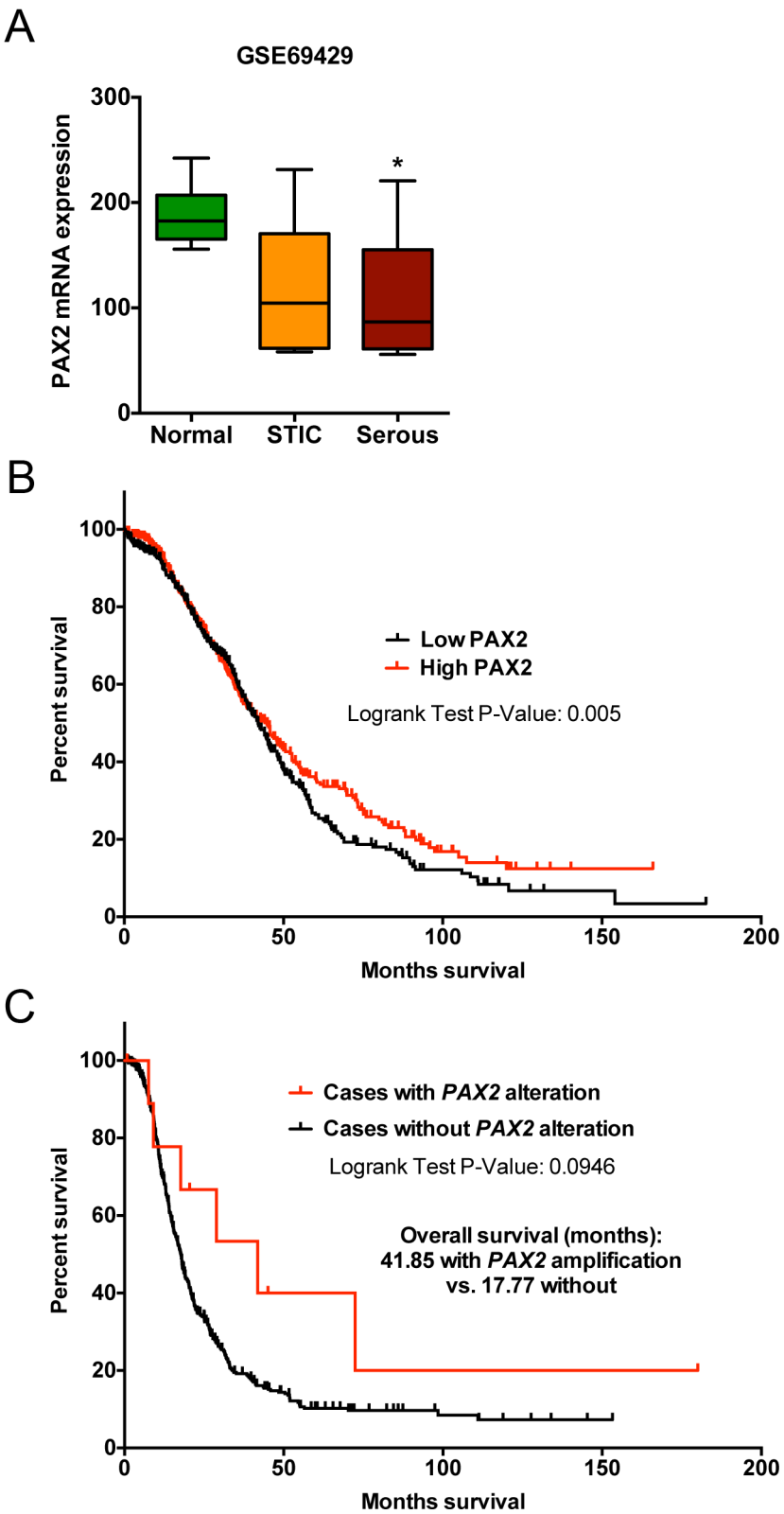

Figure 11: PAX2 expression in serous tumors is associated with increased survival. A) PAX2 mRNA expression in normal FTE, STIC and HGSC (n=6) samples, analyzed using the GSE69429 microarray data. Human HGSC data mined from **B)** the kmplot.com and **C)** the TCGA, indicate tumors with high PAX2 (red line) are associated with improved survival compared to other HGSC (black line).

Silencing PAX2 does not alter functional characteristics of murine fallopian tube epithelial cells

The earliest precursor of fallopian-derived high grade serous tumors is termed as a SCOUT, which is marked by a series of 30 or more secretory fallopian tube epithelial cells that lack the PAX2 protein. PAX2 is expressed by the human fallopian tube epithelial cells but not by the ovarian surface epithelium[76]. Murine fallopian tube or oviductal epithelial (MOE) and murine ovarian surface epithelial (MOSE) cells were tested for PAX2 mRNA and protein expression by qPCR and western blot analysis. PAX2 was abundantly expressed in the MOE cells; however, both mRNA and protein were absent in the MOSE cells (**Fig. 12A, 12B)**. In order to mimic SCOUTs, MOE cells were stably transfected with two unique sequences of shRNA directed against PAX2 ($PAX2^{shRNA-1}$, $PAX2^{shRNA-2}$) and a scrambled control shRNA (SCR^{shRNA}). The cells were validated to express less transcript and PAX2 protein (61% and 78% protein reduction in $PAX2^{shRNA-1}$ and $PAX2^{shRNA-2}$ respectively) **(Fig. 12C, 12D)**. MOE: $PAX2^{shRNA-1}$ and MOE: $PAX2^{shRNA-2}$ proliferation was compared to the MOE: SCR^{shRNA} and was not statistically different after 1, 2, 3, 4 or 5 days **(Fig. 14A)**. PAX2 knockdown had no significant effect on migration of MOE cells compared to MOE: SCR^{shRNA} when analyzed by scratch assay over 8 hours **(Fig. 14B)**. At 14 days, there was no significant increase in colony formation observed in MOE: $PAX2^{shRNA-1}$ and MOE: $PAX2^{shRNA-2}$ cells compared to control shRNA **(Fig. 14C)**. Therefore, proliferation, migration, and anchorage independent assays determined that loss of PAX2 by itself did not alter functional characteristics *in vitro* of MOE cells, which is consistent with their classification as benign lesions and suggests that additional molecular aberrations are necessary to drive tumorigenesis.

DNA binding mutation of *TP53* combined with loss of PAX2 in fallopian tube cells results in increased proliferation, migration and colony formation

SCOUTs are suggested to progress to p53 signatures when *TP53* is mutated. In order to mimic p53 signatures, MOE: PAX2$^{shRNA-1}$ cells were stably transfected with human mutant *TP53* (p53^{mut}) harboring a R273H mutation. This is the most frequently identified mutation in serous cancers and is located in the DNA binding domain. We previously reported that MOE cells stably expressing mutant *TP53* display enhanced migration but did not enhance proliferation or soft agar colony formation[150]. Overexpression of mutant *TP53* and consistent knockdown of PAX2 in MOE: PAX2$^{shRNA-1}$+p53^{mut} was validated by qPCR and western blot **(Fig. 13A, 13B)**. MOE: PAX2$^{shRNA-1}$+p53^{mut} cells proliferated more than the control (SCR^{shRNA}) over a period of 5 days **(Fig. 14A)**. The addition of p53^{mut} to MOE: PAX2$^{shRNA-1}$ cells increased migration compared to control (SCR^{shRNA}) over 8 hours **(Fig. 14B)**. However, this increase was comparable to the previously observed effect in MOE cells harboring the mutant *TP53* alone, suggesting that PAX2 was not contributing to this change[66]. Anchorage independence was measured by soft agar colony formation. MOE: PAX2$^{shRNA-1}$+p53^{mut} cells formed significantly more colonies compared to scrambled shRNA control MOE cells **(Fig. 14C)**. These results suggested that mutation of *TP53* when combined with loss of PAX2 enhanced tumor like behavior such as proliferation and anchorage independence, while changes in motility are largely related to only mutant *TP53*.

A

Cell line	18s (C_t)	PAX2 (C_t)
MOE	6.74	25.6
MOSE	8.34	Undetermined

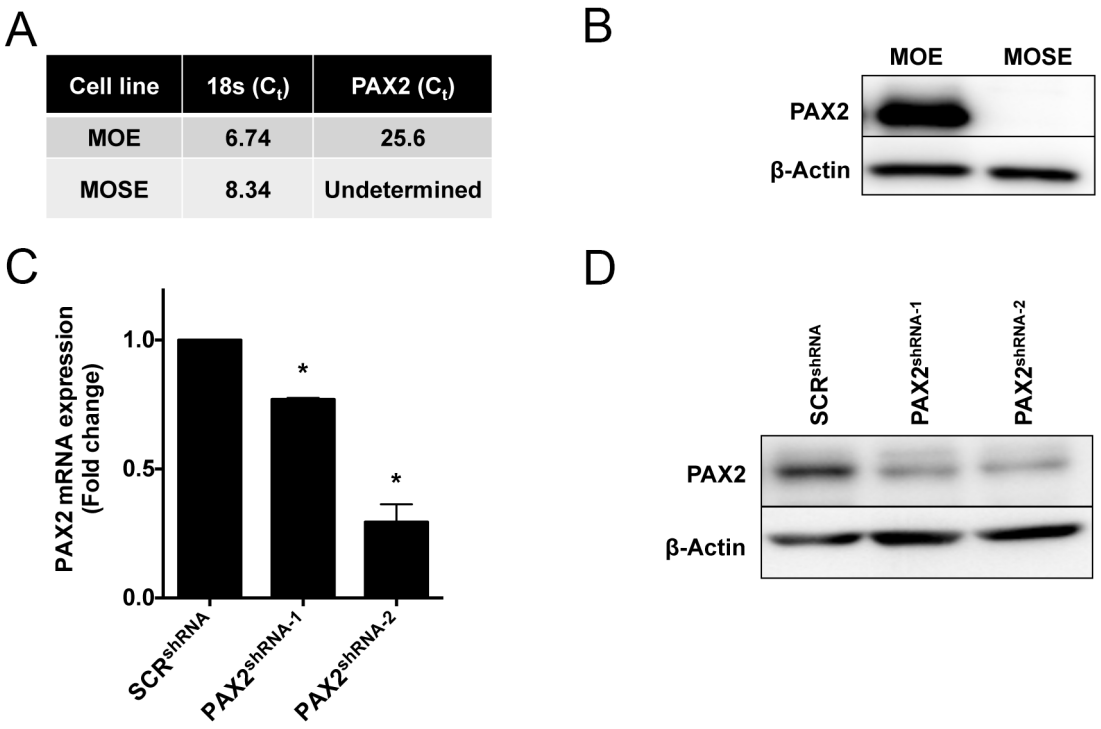

Figure 12: Validation of PAX2 knockdown in MOE cells. PAX2 is expressed in oviductal cells (MOE) but not in the ovarian surface epithelial (MOSE) cells based on **A)** mRNA and **B)** protein. Validation of PAX2 knockdown in MOE cells by **C)** qPCR and **D)** western blot.

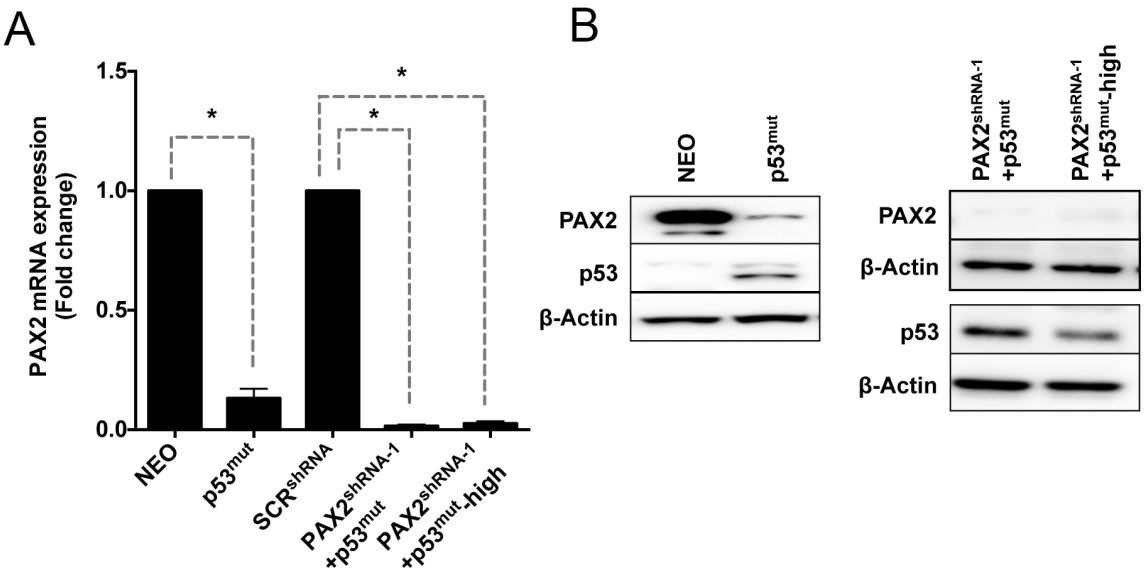

Figure 13: Validation of *TP53* overexpression in MOE cells with PAX2 knockdown. Reduced PAX2 protein and stabilized p53 expression in MOE: PAX2$^{shRNA-1}$+p53^{mut} and MOE: PAX2$^{shRNA-1}$+p53^{mut}-high cell lines were confirmed by **A)** qPCR (PAX2 mRNA) and **B)** western blot.

Serial passaging of MOE cells harboring mutation of *TP53* and loss of PAX2 enhance *in vitro* growth and migration but was insufficient to drive tumorigenesis *in vivo*

Not all p53 signatures progress to malignant lesions, suggesting that a series of events occur that stimulates the benign lesions to progress into malignant ones. The events that define these changes are unknown. To determine the molecular changes necessary to drive MOE cells to form malignant serous tubal intraepithelial carcinomas (STIC) from p53 signatures, MOE: $PAX2^{shRNA\text{-}1}$+$p53^{mut}$ cells (passages 18-30) were serially passaged to generate an "aged" model called MOE: $PAX2^{shRNA\text{-}1}$+$p53^{mut}$-high (passages 80-120). These "aged" cells showed significantly increased proliferation **(Fig. 14D)**, migration **(Fig. 14E)** and colony formation **(Fig. 14F)** compared to MOE: $PAX2^{shRNA\text{-}1}$+$p53^{mut}$ cells. To investigate the tumorigenic potential *in vivo,* these genetically engineered MOE lines were xenografted subcutaneously (s.c.) and intraperitoneally (i.p.) into athymic mice and tumor formation was monitored over a period of six months (n=5). Mice xenografted with MOE: $PAX2^{shRNA\text{-}1}$, MOE: $PAX2^{shRNA\text{-}1}$+$p53^{mut}$ and MOE: SCR^{shRNA} did not display any evidence of tumor formation after six months **(Fig. 14G)**. Mice grafted with MOE: $PAX2^{shRNA\text{-}1}$+$p53^{mut}$-high cells did not form peritoneal disease, however, these animals developed hyperplastic glands in the uteri (data not shown). H&E staining revealed extensive tumor necrosis that was not epithelial in origin. These data strongly suggest that multiple additional molecular events are critical for benign early lesions to progress to malignant STICs. These models recapitulate the benign characteristics of these lesions that are currently known to form in the fallopian tube epithelium prior to progressing to serous cancer.

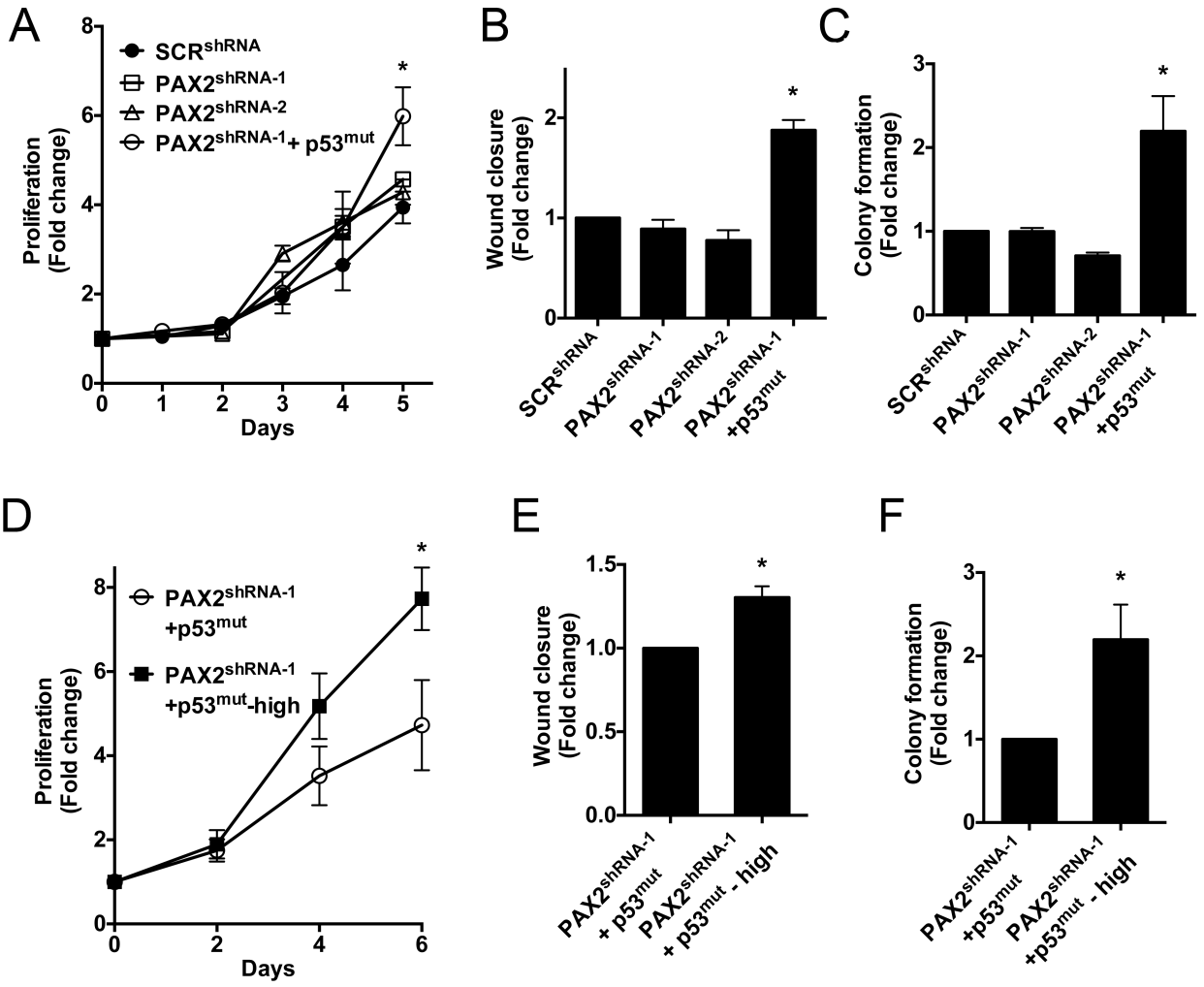

G

MOE cell line	Incidence of tumor formation	Survival (days)
PAX2$^{shRNA-1}$	0/5	No mortality
PAX2$^{shRNA-1}$+p53^{mut}	0/5	No mortality
PAX2$^{shRNA-1}$+p53^{mut} -high	0/5	No mortality

Figure 14: Combination of PAX2 loss and *TP53* mutation alters functional characteristics of MOE cells *in vitro* but is insufficient to drive tumorigenesis *in vivo*. A-C) Proliferation (day 5), migration (8 hours) and anchorage independent growth (day 14) (respectively) of MOE: SCR^{shRNA}, MOE: PAX2$^{shRNA-1}$ and MOE: PAX2$^{shRNA-1}$+p53^{mut}. **D-F)** Proliferation (day 6), migration (8 hours) and anchorage independent growth (day 14) (respectively) of MOE: PAX2$^{shRNA-1}$+p53^{mut} and MOE: PAX2$^{shRNA-1}$+p53^{mut}-high. **G)** Athymic nude mice injected with MOE: PAX2$^{shRNA-1}$, MOE: PAX2$^{shRNA-1}$+p53^{mut} and MOE: PAX2$^{shRNA-1}$+p53^{mut}-high cells demonstrated no tumorigenic growth *in vivo* at 6 months (n=5 mice per group).

Serially passaged MOE: PAX2$^{shRNA-1}$+p53^{mut} and human Type II SCOUTs share similar gene expression

A recent study compared human SCOUTs to HGSC using cDNA microarrays and validated that a subset of SCOUTS (termed Type II) had similar expression profiles to serous tumors[146]. MOE cells harboring mutation of *TP53* or PAX2$^{shRNA-1}$ or both, including the "aged" model represent a system with much less heterogeneity compared to human tissue samples for studying regulation of downstream targets of PAX2 and p53 that may contribute to tumor promotion. Gene expression profiles in cell line models was compared with expression data reported in the literature from human signatures[146]. A set of nine targets (*stmn1, fut8, mme, lef1, ezh2, runx2, rcn1, cox5a, ctnnb1*) was selected from the published cDNA microarray data that compared human FTE vs. Type II SCOUTs and tumor samples[146]. These targets were validated by qPCR in MOE: p53^{mut}, MOE: PAX2$^{shRNA-1}$, MOE: PAX2$^{shRNA-1}$+p53^{mut} and MOE: PAX2$^{shRNA-1}$+p53^{mut}-high cells **(Fig. 15)**. Based on the preliminary validation, three targets were chosen for further investigation – Stathmin, fut8 and mme. Stathmin protein expression was reduced from PAX2 silencing, upregulated by mutation of *TP53*, and highly upregulated by the combination as well as in the "aged" line **(Fig. 16B)**. Fut8 was upregulated by loss of PAX2, and was lost as the cells were serially passaged **(Fig. 16D)**. Mme was upregulated by PAX2 loss, and highly expressed in the cells that model p53 signatures and the cells that were "aged" **(Fig. 16F)**. Mme and fut8 are novel genes with very little information on their role in serous tumor progression or PAX2 regulation. Interestingly, a recently published undifferentiated high-grade carcinoma mouse model that expressed PAX2 and a p53 splice variant [61], failed to express fut8. In contrast, MOE cells harboring mutation of *TP53* and overexpression of KRAS^{G12V}, that formed poorly differentiated

carcinomas *in vivo* [66], did not express PAX2, but expressed fut8 **(Fig. 17A)**. These data further support that loss of PAX2 influences fut8 expression in fallopian tube cells. Several studies have reported the role of stathmin in high-grade serous carcinoma[56, 151]. To investigate the functional role of stathmin in the fallopian tube cells and its regulation by PAX2, stathmin was transiently knocked down in MOE cells harboring both, PAX2 loss and mutant *TP53* and the aged model **(Fig. 17B)**. Post 24-hour transfections with stathmin^{shRNA}, MOE cell models were subjected to scratch assays to measure wound closure over 12 hours. Downregulation of stathmin in MOE: PAX2$^{shRNA\text{-}1}$+p53^{mut}, including the aged model, demonstrated significant reduction in migration compared to cells transfected with control shRNA **(Fig. 17C)**. These results suggest that stathmin could be downstream of PAX2 and may contribute to migration of fallopian tube epithelial cells.

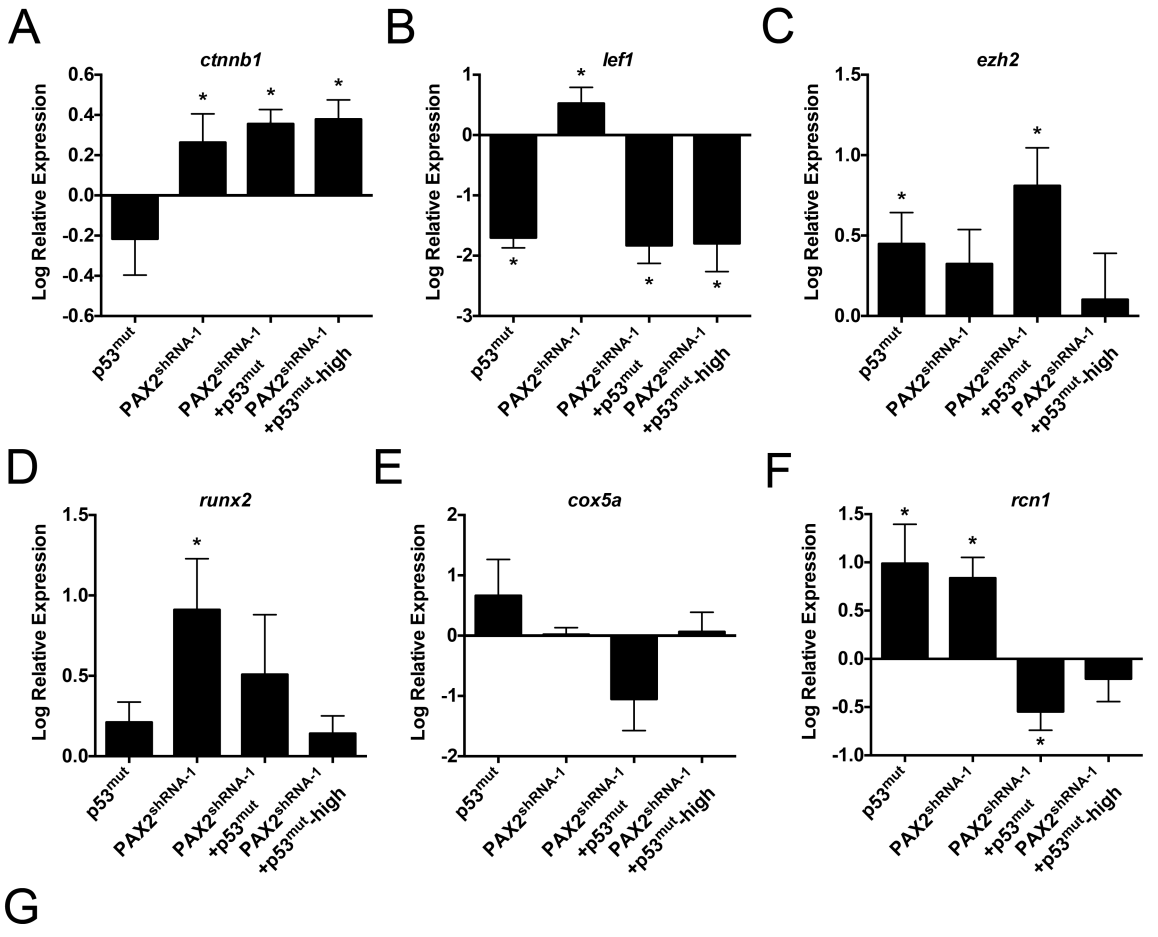

G

Gene	*ctnnb1*	*lef1*	*ezh2*	*runx2*	*cox5a*	*rcn1*	*stmn1*	*fut8*	*mme*
Type II SCOUT	Increased	Increased	Increased	Increased	Increased	Increased	Increased	Decreased	Increased

Figure 15: Loss of PAX2 and mutation of *TP53* in MOE cells alters candidate genes commonly affected in serous cancer. qPCR analysis comparing the expression of **A)** *ctnnb1* **B)** *lef1* **C)** *ezh2* **D)** *runx2* **E)** *cox5a* and **F)** *rcn1* in MOE: $p53^{mut}$, MOE: $PAX2^{shRNA-1}$, MOE: $PAX2^{shRNA-1}$+$p53^{mut}$ and MOE: $PAX2^{shRNA-1}$+$p53^{mut}$-high cells. **G) [Data extracted from Ning *et al.]*** Gene expression profile of human Type II SCOUTs compared to normal human FTE samples. "Increase" and "decrease" indicates change in gene expression in Type II SCOUTs when compared to human FTE[152].

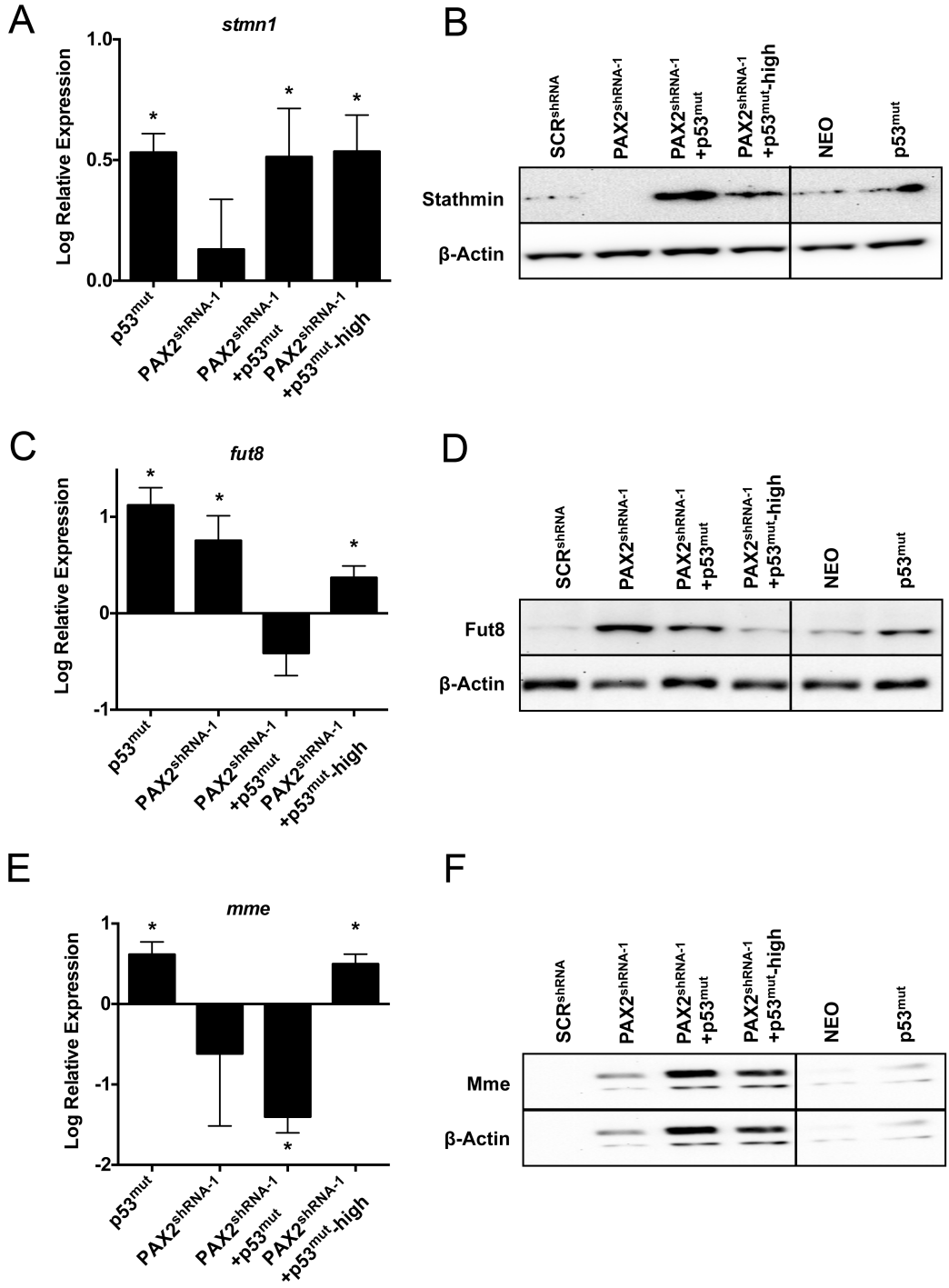

Figure 16: Comparison of gene signatures between human SCOUTs and MOE cells harboring PAX2 loss and mutant *TP53* suggests stathmin, fut8 and mme as downstream targets of PAX2 in the FTE. qPCR analysis of **A)** *stmn1*, **C)** *fut8* and **E)** *mme* mRNA expression and western blot analysis of **B)** stathmin, **D)** fut8 and **F)** mme protein expression in MOE: $p53^{mut}$, MOE: $PAX2^{shRNA-1}$, MOE: $PAX2^{shRNA-1}$+$p53^{mut}$ and MOE: $PAX2^{shRNA-1}$+$p53^{mut}$-high cells.

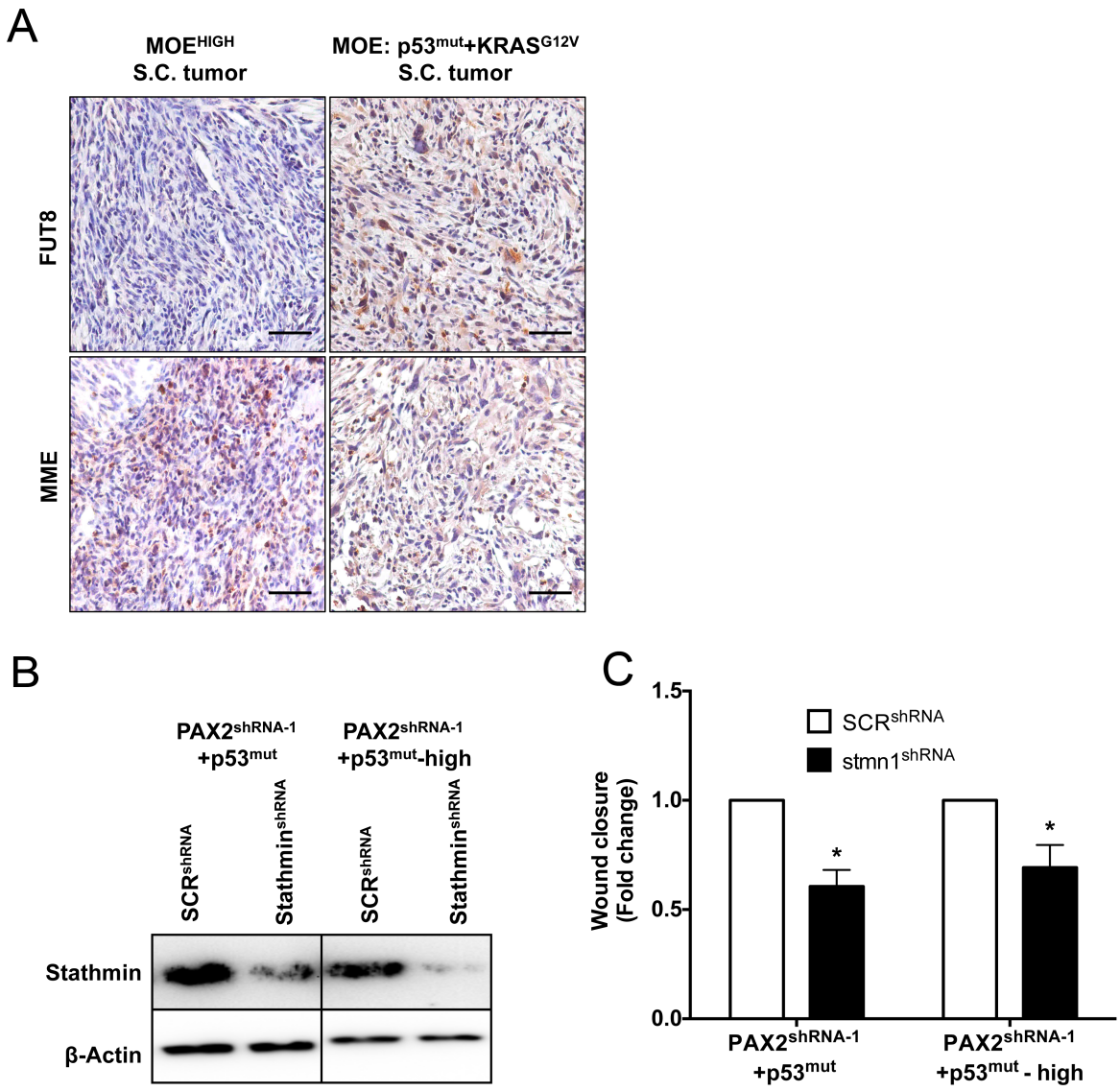

Figure 17: Fut8 and mme expression in tumors with differential PAX2 status and functional significance of stathmin knockdown in MOE cells. A) Immunohistochemical analysis of fut8 and mme expression in s.c. tumors derived from MOE^{HIGH} (CD1 mice) and MOE: p53^{mut}+KRAS^{G12V} xenografted cells. Scale bar equals 50 microns **B)** Western blot validating transient knockdown of stathmin in MOE: PAX2$^{shRNA-1}$+p53^{mut} and MOE: PAX2$^{shRNA-1}$+p53^{mut}-high cells. **C)** Migration assay (12 hours) comparing MOE: PAX2$^{shRNA-1}$+p53^{mut} and MOE: PAX2$^{shRNA-1}$+p53^{mut}-high cells transfected with SCR^{shRNA} and stathmin^{shRNA}.

Loss of PTEN regulates PAX2 and re-expression of PAX2 is sufficient to block tumorigenesis

Currently, there are no known mechanisms for how PAX2 would be lost in fallopian tube cells. Joint loss of PAX2 and PTEN has been reported in endometrial carcinomas[77]. PTEN silencing in MOE cells increases proliferation and migration *in vitro* without affecting anchorage independent growth in soft agar assay[60]. PTEN^{shRNA} cells formed high-grade Müllerian cancer in nude mice when xenografted i.p. indicating that loss of PTEN in fallopian tube cells is sufficient to drive tumorigenesis *in vivo*. Analysis of PAX2 expression in the fallopian tube cells with PTEN silencing revealed a significant reduction of PAX2 mRNA **(Fig. 18A)** and protein **(Fig. 18B)** compared to scrambled shRNA control. To investigate the functional significance of PAX2 re-expression in PTEN silenced fallopian tube cells, MOE: PTEN^{shRNA} were stably transfected with a PAX2 overexpression plasmid. Two clones (MOE: PTEN^{shRNA}+PAX2 (Clone 1) and MOE: PTEN^{shRNA}+PAX2 (Clone 2)) were generated and validated for PAX2 overexpression and PTEN knockdown **(Fig. 18C)**. Functional assays revealed that re-expression of PAX2 in PTEN silenced MOE cells significantly reduced PTEN^{shRNA}-induced proliferation **(Fig. 18D)** and migration **(Fig. 18E)**. MOE: PTEN^{shRNA}+PAX2 (Clone 1) and MOE: PTEN^{shRNA}+PAX2 (Clone 2) cells were i.p. xenografted into nude mice. Fallopian tube cells with PTEN silencing formed metastatic disease at 153 ± 24 days. One out of the three mice xenografted with MOE: PTEN^{shRNA}+PAX2 (Clone 1) cells developed metastatic disease on day 169 that had a similar presentation to PTEN^{shRNA}. The remaining mice xenografted with MOE: PTEN^{shRNA}+PAX2 (Clone 1) cells were disease free. All of the mice in the third group xenografted with MOE: PTEN^{shRNA}+PAX2 (Clone 2) cells appeared to be disease free with no tumor formation **(Fig. 19A)**.

Representative images of the gross tumor morphology of MOE: PTEN^{shRNA} grafted mice that formed disseminated peritoneal disease are shown in **Fig. 19B**. H&E staining determined the tumors to be histologically similar to the previous study[153]. Gross tumor morphology of one of the animals xenografted with MOE: PTEN^{shRNA}+PAX2 (Clone 1) was similar to MOE: PTEN^{shRNA} **(Fig. 19B)**. PAX2, PAX8 and WT-1 staining determined the PTEN^{shRNA}+PAX2 (Clone 1) tumors to be of a similar pathological grade as previously noted in MOE: PTEN^{shRNA} **(Fig. 19B)**. The remaining animals xenografted with PTEN^{shRNA}+PAX2 clones, presented with normal internal morphology **(Fig. 19C)**. Representative H&E staining of reproductive tracts from each clone expressing PAX2 in PTEN silenced MOE cells, demonstrated normal architecture of the uteri, oviduct and ovaries (data not shown). These results show that re-expressing PAX2 in PTEN silenced MOE cells attenuated and/or eliminated PTEN^{shRNA}-induced tumors and increased survival.

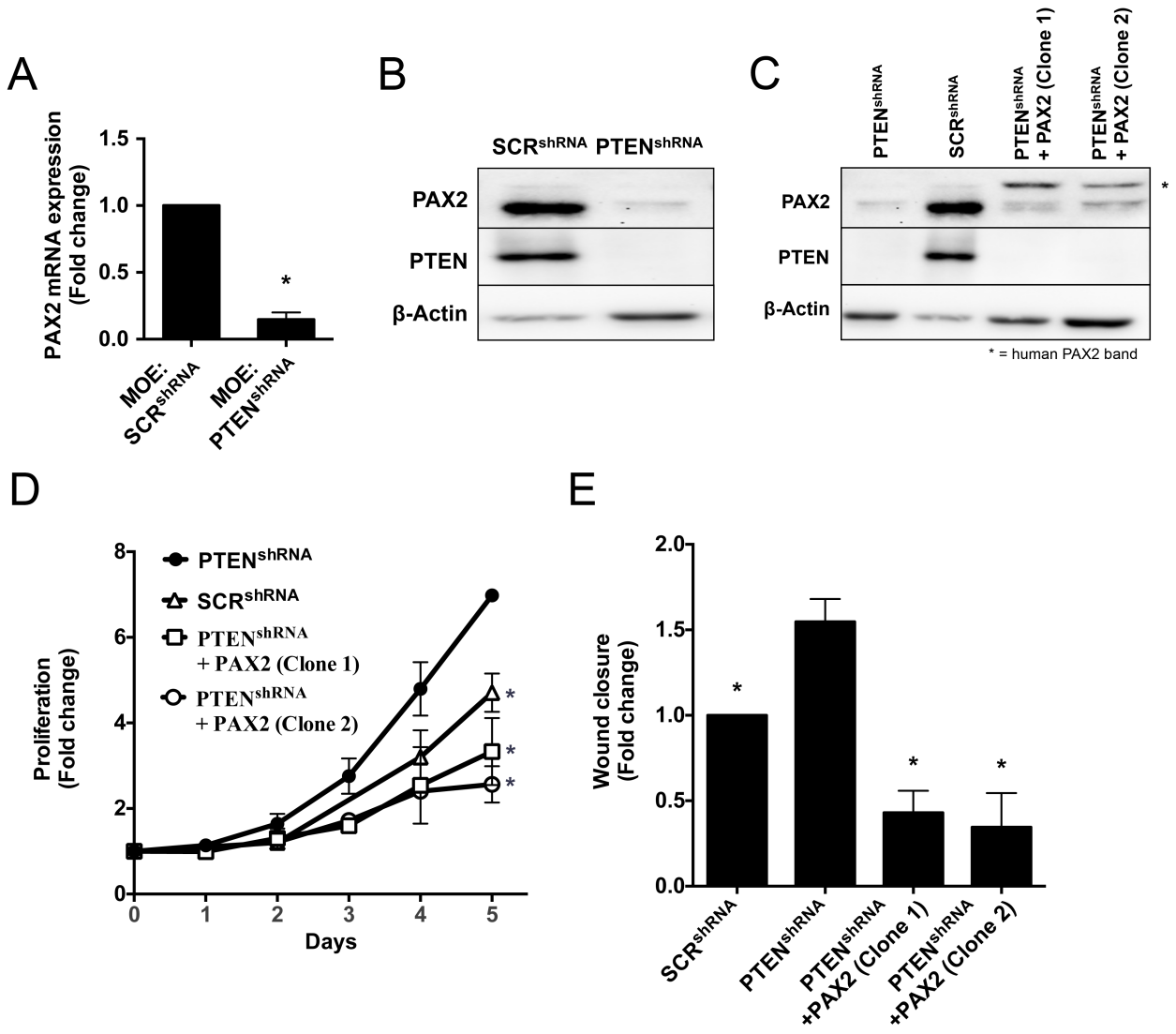

Figure 18: Loss of PTEN regulates PAX2 and re-expression of PAX2 is sufficient to reduce PTEN^{shRNA}-induced proliferation and migration. MOE: PTEN^{shRNA} cells expressed significantly lower PAX2 at the **A)** mRNA and **B)** protein level compared to MOE: SCR^{shRNA} control. **C)** Validation of stable PAX2 overexpression (Clone 1 and Clone 2) and consistent PTEN knockdown in MOE: PTEN^{shRNA} as compared to MOE: SCR^{shRNA} by western blot. MOE: PTEN^{shRNA}+PAX2 (Clone 1 and 2) reduced MOE: PTEN^{shRNA}-induced **D)** proliferation (day 5) and **E)** migration (hour 8).

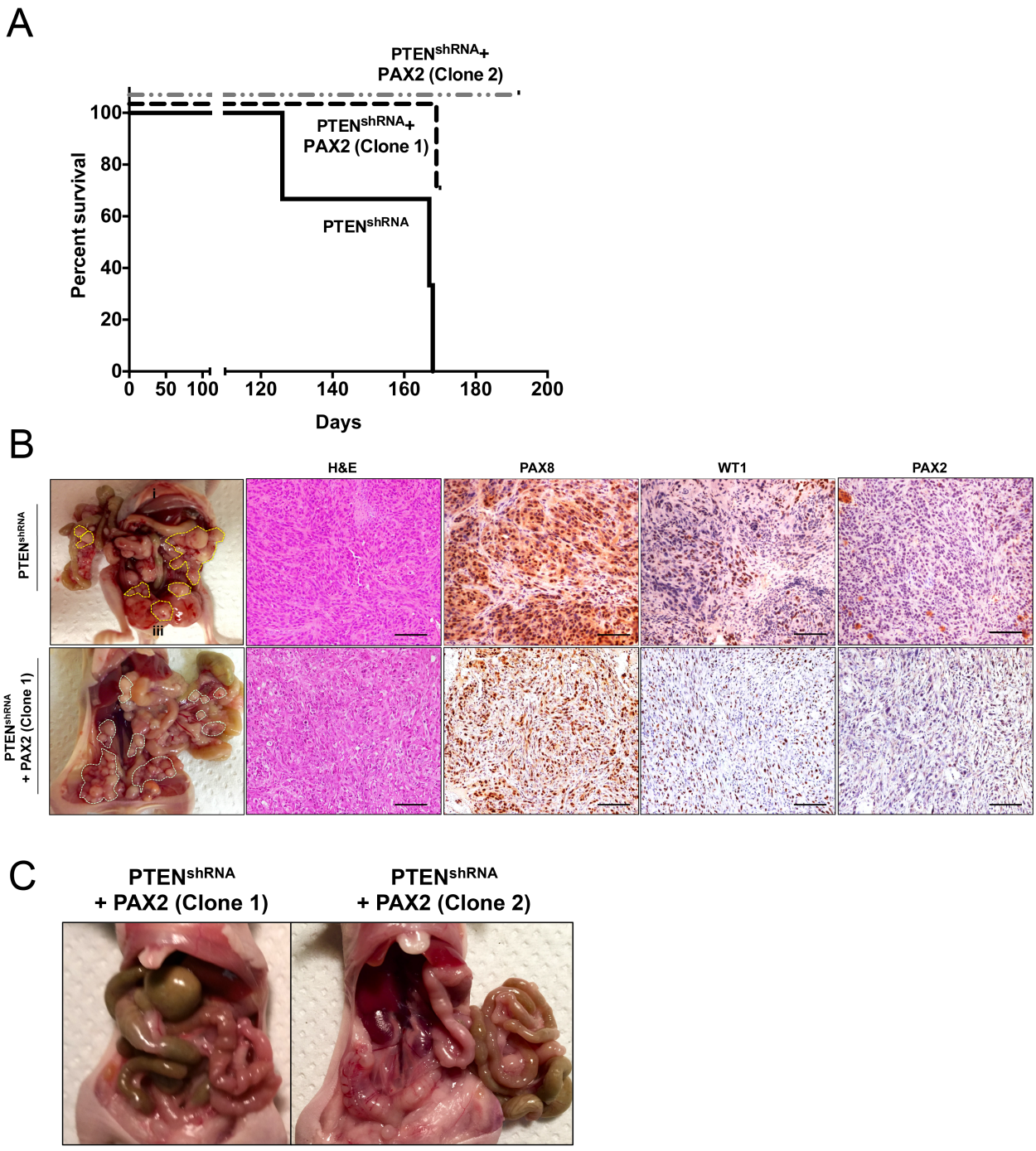

Figure 19: Re-expression of PAX2 is sufficient to block PTEN^{shRNA}-induced tumorigenesis in MOE cells. A) Kaplan-Meier survival plot showing that syngeneic PTEN^{shRNA}+PAX2 xenorafts survive longer. **B)** Tumors from a PTEN^{shRNA}+PAX2 (Clone 1) xenografted animal (n=1 out of 6) were similar in morphology to those of MOE: PTEN^{shRNA} as determined via H&E staining and expression of PAX8, WT1 and PAX2 staining. Scale bars equal 50 microns. **C)** Gross morphology of disease-free mice xenografted with MOE: PTEN^{shRNA}+PAX2 (Clone 1 and 2).

PAX2 overexpression in human high-grade serous cancer cell lines reduces proliferation and migration via apoptosis

PAX2 expression is absent in benign precursors such as SCOUTs, p53 signatures and malignant STICs as well as in HGSC tissues[138]. PAX2 is also absent in human serous cancer cell lines[76]. A panel of HGSC cell lines (OVCAR3, OVCAR4, KURAMOCHI and OVSAHO) failed to express PAX2 protein **(Fig. 20A)**. Attempts to stably express PAX2 in HGSC cells resulted in cell death. Therefore, to determine the impact of re-introducing PAX2, HGSC cells were transiently transfected with PAX2 or NEO (control) plasmid for 48 hours. PAX2 protein expression was confirmed by western blot **(Fig. 20B)**. Forced PAX2 expression in these HGSC cells resulted in significantly lower proliferation on day 3 **(Fig. 21A)** and reduced migration over 24 hours **(Fig. 21B)** compared to those transfected with NEO. To determine the effect of PAX2 on cell viability, apoptosis and necrosis in OVCAR4 cells, transiently transfected cells were subjected to Annexin V/APC and PI staining. Flow cytometry analyses revealed that PAX2 transfected cells had significantly more cells in early and late stages of apoptosis **(Fig. 21C)**. These data suggest that PAX2 re-expression in human cell lines may increase rate of apoptosis.

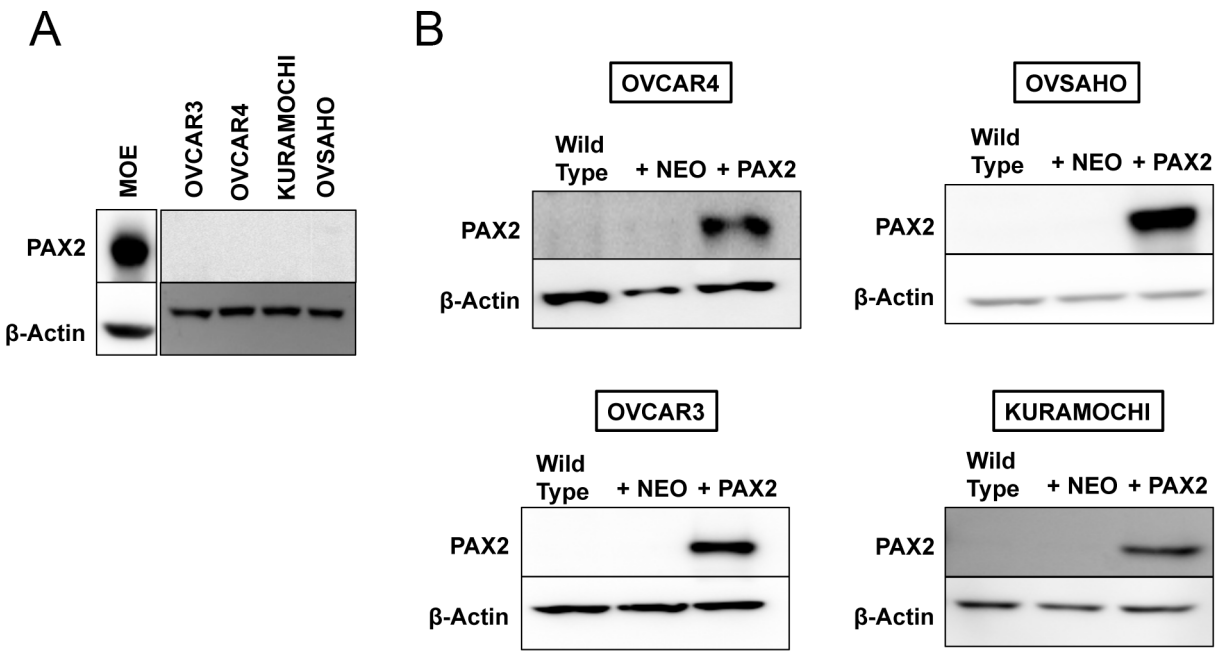

Figure 20: PAX2 expression in human high-grade serous cancer cell lines. A) Lack of PAX2 expression in human HGSC cells validated by western blot. **B)** Validation of transient PAX2 overexpression in OVCAR4, OVSAHO, OVCAR3 and KURAMOCHI cells by western blot. NEO serves as empty vector control.

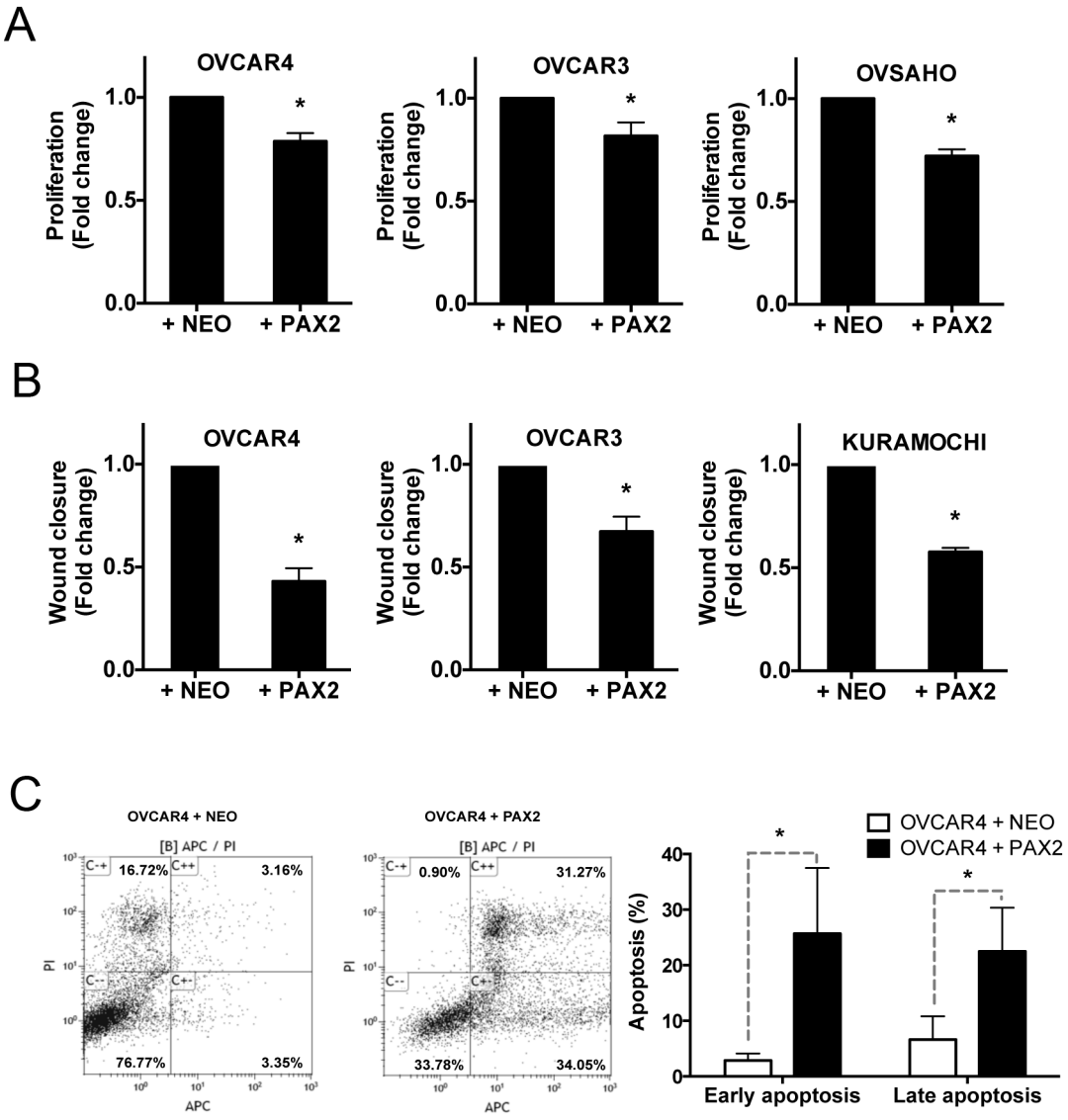

Figure 21: PAX2 re-expression in human HGSC cell lines reduced proliferation and migration via increased apoptosis. Forced PAX2 transient expression in PAX2-null serous cancer cell lines resulted in significant reduction in **A)** proliferation (day 3) and **B)** migration (hour 8). **C)** PAX2 expression in OVCAR4 cells significantly increased early and late apoptosis compared to OVCAR4 cells treated with NEO (measured by flow cytometry) at hour 48.

Identification of small molecules that can re-activate PAX2 expression in fallopian tube epithelial cells

Bioinformatics analysis of the TCGA data indicates that PAX2 is not methylated as a mechanism for repression in HGSC and that PAX2 is rarely mutated[50]. Therefore, transcriptional repression or lack of activation could be one mechanism responsible for the loss of PAX2. Identifying molecules that can re-activate PAX2 expression could provide therapeutic avenues to slow progression of pre-neoplastic lesions to malignant neoplasms. A high throughput-screening assay with the 4.1 kb murine PAX2 promoter driving luciferase construct was used to perform the screen. The murine and human PAX2 promoters share 80% sequence homology[154]. Prestwick library compounds (10 μM) were incubated for 10 hours to find molecules that stimulate PAX2 expression[155]. The primary assay revealed that the top 2% of the compounds increased PAX2 promoter activity by 193% ± 23% (Mean ± SD) compared to cells treated with DMSO control **(Fig. 22A)**. Upon re-testing, 12 out of the 24 compounds (top 2%) showed consistent activity (**Fig. 22B**). A secondary biological screen (endogenous PAX2 mRNA activation in MOE cells) identified the top 3 hits, luteolin, sulfasalazine and captopril **(Fig. 22C)**. In response to these data and published reports, future investigations focused on determining the effect of luteolin on FTE cells. Luteolin increased PAX2 protein and mRNA expression in MOE cells at 10 hours post incubation **(Fig. 23A, 23B)**. Luteolin significantly reduced proliferation **(Fig. 23C)** and migration in fallopian tube cells **(Fig. 23D)**. Future investigations will focus on evaluating the biological effect of luteolin in combination with existing treatments as well as in serous cancer cell lines.

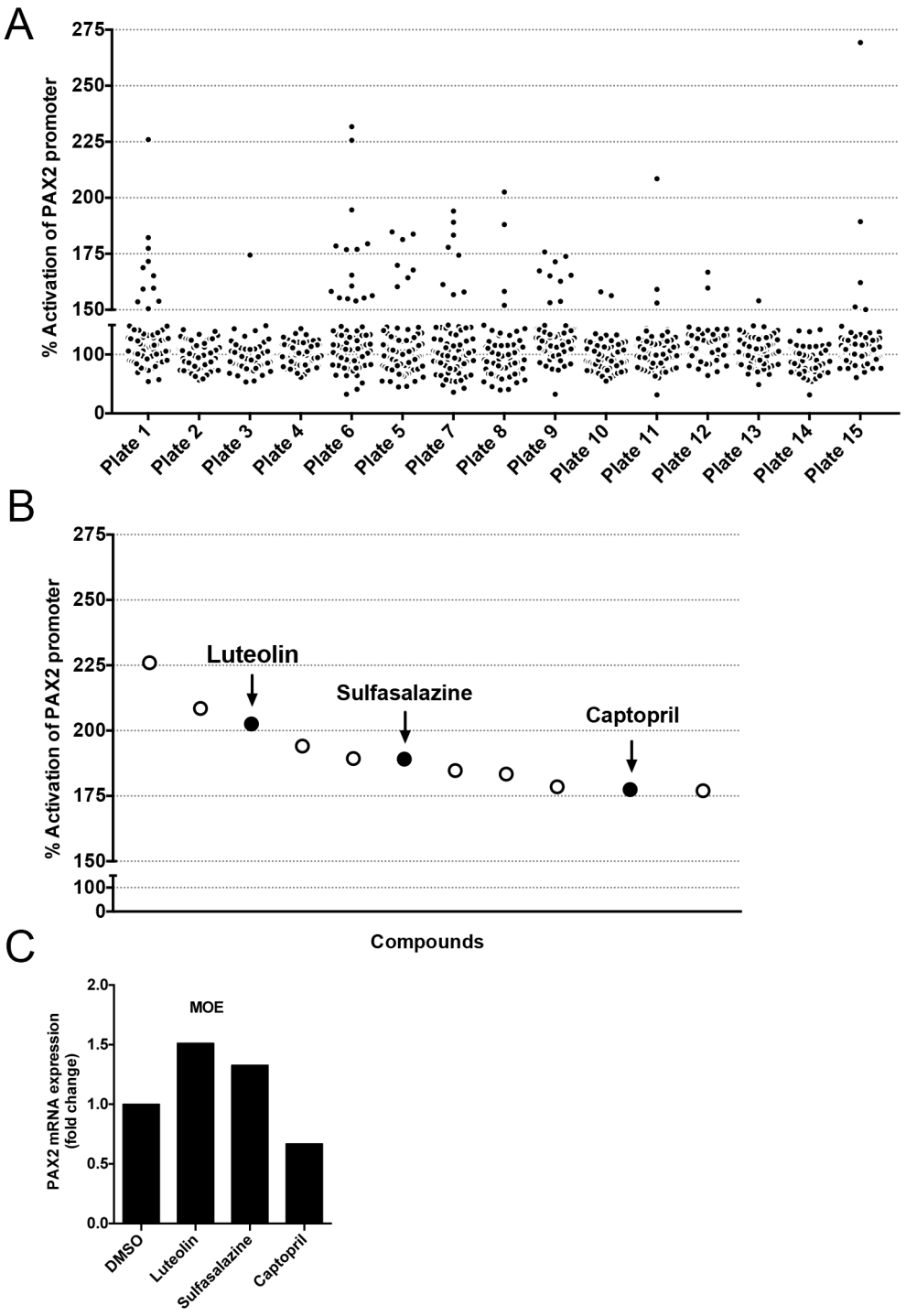

Figure 22: Biological screen to identify drug candidates that can increase PAX2 transcriptional activity in MOE cells. A) Primary biological screen investigating PAX2 promoter activation by 1200 compounds from the PRESTWICK library. **B)** Top 12 compounds that consistently activated PAX2 promoter activity upon re-testing. **C)** A secondary biological assay investigating endogenous PAX2 mRNA activation in MOE cells.

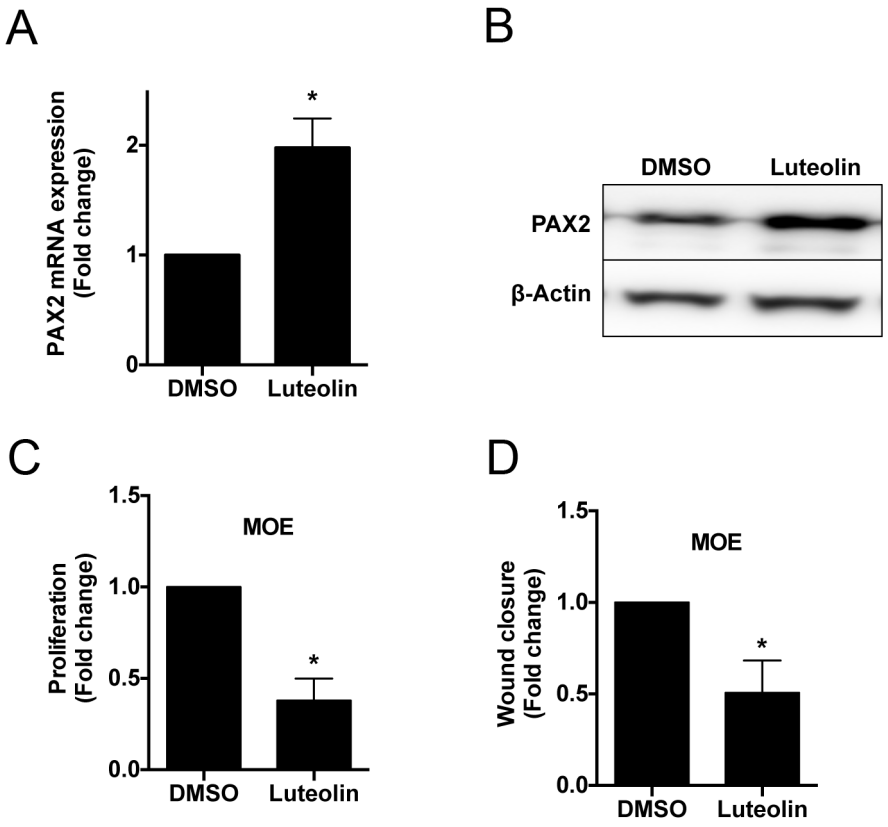

Figure 23: Biological effects of luteolin on MOE cells. Luteolin increased PAX2 **A)** mRNA and **B)** protein in MOE cells compared to DMSO. Functionally, luteolin significantly decreased **C)** proliferation (day 3) and **D)** migration (hour 24) in MOE cells.

Wild-type p53 directly binds to and activates PAX2 promoter whereas mutation in *TP53* significantly reduces p53 occupancy on PAX2 promoter in fallopian tube epithelial cells

Mutant p53 is a hallmark of HGSC, and mutant *TP53* may repress the PAX2 promoter **(Fig. 24A)**. Therefore, eliminating the p53 mutant protein may directly increase PAX2 or a combination of molecules that both refold p53 and enhance PAX2 expression may be required to fully activate PAX2 in HGSC. To investigate whether p53 regulates the PAX2 promoter in fallopian tube cells and whether mutation of *TP53* has any effect on promoter regulation, chromatin immunoprecipitation (ChIP) was performed in MOE cells. *In silico* analysis revealed two putative binding sites of p53 on the murine PAX2 promoter. Chromatin from MOE cells and MOE: $p53^{mut}$ cells were prepared for immunoprecipitation assays. Isolated chromatin was precipitated using IgG and p53 antibodies. PCR primer sets were designed against p53-PAX2 promoter binding region, a non-target region **(Fig. 24B),** MDM2 (positive control for p53 occupancy **(Fig. 24C)** and ATF (positive control for mutant p53 occupancy, **Fig. 24D**) and. The p53 occupancy on GAPDH promoter vs. PAX2 promoter was used to compare degree of enrichment relative to input. ChIP data demonstrated that wild-type p53 had a higher occupancy on the PAX2 promoter compared to IgG indicating that p53 can directly bind to and has the ability to regulate PAX2 transcriptional activity **(Fig. 24E)**. Mutation of *TP53* significantly abrogated occupancy on the PAX2 promoter as seen in **Fig. 24E.** These data suggest that mutant p53 represses whereas wild-type p53 activates PAX2 transcriptional activity by directly regulating the promoter. These results suggest, that combining molecules that inhibit *TP53* mutant along with molecules

such as luteolin, that activate PAX2 promoter might have the potential to stop tumor progression at early stages.

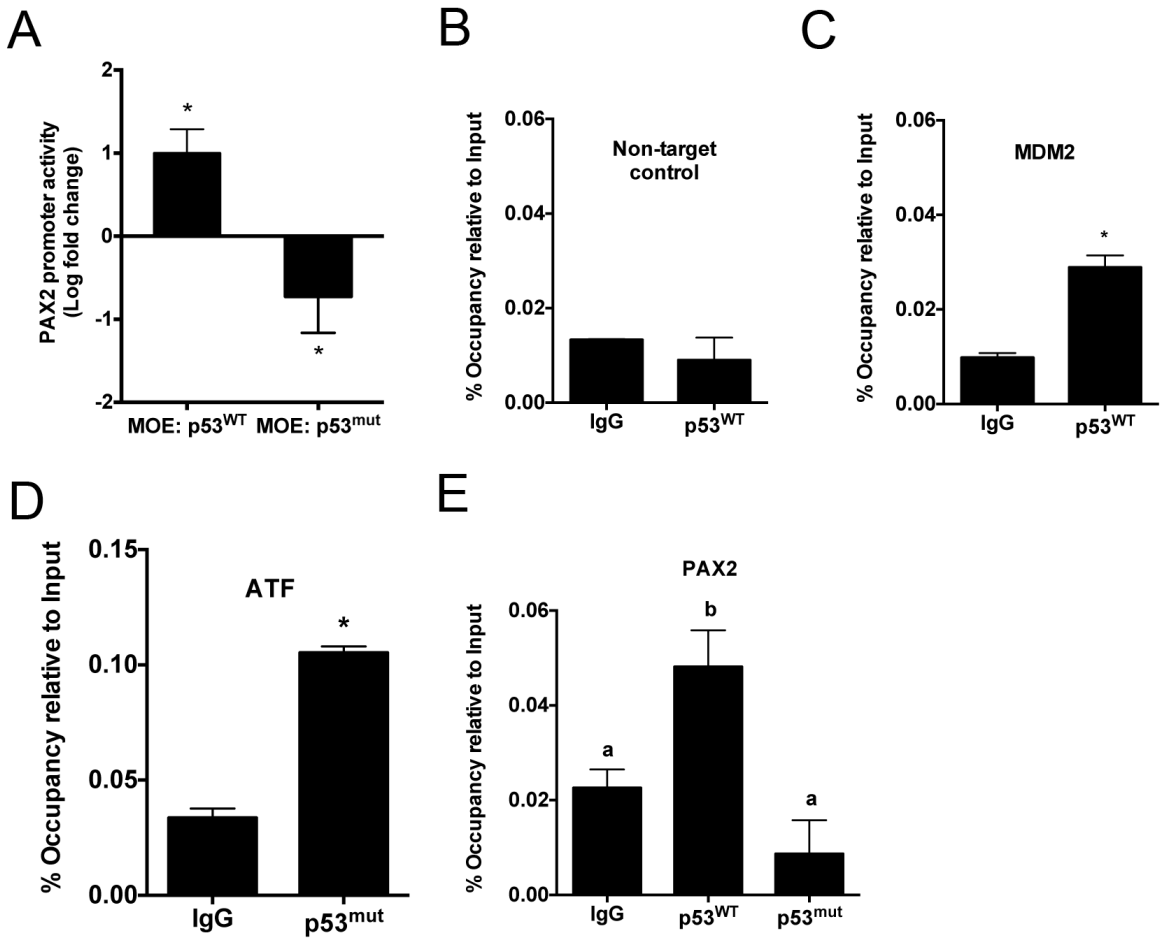

Figure 24: PAX2 is a direct transcriptional target of wild-type p53 and mutant p53 represses the p53-induced PAX2 transcription in MOE cells. A) Wild-type p53 activates whereas $p53^{mut}$ represses PAX2 transcriptional activity as measured by luciferase assay. Chromatin Immunoprecipitation (ChIP) analysis demonstrates wild-type p53 occupancy on **B)** Non-target control and **C)** MDM2, mutant p53 occupancy on the **D)** ATF promoter. **E)** ChIP analysis revealed that wild-type p53 enhanced whereas $p53^{mut}$ significantly reduced p53 occupancy on the PAX2 promoter. Statistical differences ($p \leq 0.05$) are between groups labeled a and b.

C. DISCUSSION

The aim of this study was to identify the functional and mechanistic role of PAX2 in normal fallopian tube epithelium and high-grade serous ovarian cancer. Studies published so far have shown divergent roles of PAX2 depending on the tumor histotype[49, 59, 76, 80]. PAX2 is lost in HGSC and endometrial carcinomas[49, 59, 77] whereas it is overexpressed in mucinous and clear cell histotype of epithelial ovarian cancer[76]. Consistent with pathological observations, published microarray data showed that PAX2 was significantly downregulated in STIC and HGSC tumor tissues compared to tissues from normal fallopian tube epithelium[148] **(Fig. 11A)**. These data corroborated with another microarray study that showed significantly increased overall survival in HGSC patients that had high PAX2 expression compared to those with lower PAX2 **(Fig. 11B)**. Interestingly, in the TCGA database, a small subset of patients that presented with amplification in the PAX2 gene, had a longer disease-free interval before relapse, compared to patients that did not have an alteration in PAX2 **(Fig. 11C)**. The present study has utilized murine fallopian tube (oviductal) epithelial (MOE) cells that were genetically altered to knockdown PAX2 and express mutation of *TP53*. Although, PAX2 loss alone did not have a significant effect on MOE characteristics, combining it with mutation of *TP53* resulted in functional changes *in vitro*. Re-expression of PAX2 in HGSC models reduced tumor burden suggesting that PAX2 has the potential to be exploited as a therapeutic target.

Several studies have convincingly demonstrated that the fallopian tube is one of the sources of origin of majority HGSC[35, 60-62, 64, 156]. However, most of these models use SV40 to stabilize p53, therefore making it difficult to tease apart the effect of *TP53* mutation on FTE[35, 62]. Additionally, no models of SCOUTs or of fallopian tube cells lacking PAX2 have been reported. Loss of PAX2 by itself did not

have any effect on fallopian tube cells, however, when combined with *TP53* mutation, led to significant functional changes *in vitro*. The lack of tumorigenicity *in vivo* resonated with their benign pathological designation. Combining PAX2 knockdown with *TP53* mutation increased proliferation, migration and colony formation; however the effect on migration was likely due to mutation in *TP53* alone[66]. Serial passaging (aging) of the MOE cells harboring both the alterations resulted in further increase in all functional characteristics. These data are consistent with previous study performed in serially passaged fallopian tube cells that indicate that aging is sufficient to induce changes that can result in functional alterations[61]. In contrast to the tumorigenic model of serially passaging MOE cells on a CD1 background[61], the current model with PAX2 knocked down and p53 mutated did not form tumors after serial passaging. These data suggest that the loss of PAX2 and mutation of *TP53* are not sufficient to drive tumorigenesis but instead they present us with valuable models that recapitulate early benign lesions that warrant further investigation. In addition, it suggests that a latency period exists between SCOUTs and p53 signatures and tumor formation that may allow for intervention of prevention.

Gene expression analysis of MOE cells harboring altered PAX2 and *TP53* expression revealed *stathmin, fut8* and *mme* to be likely targets downstream of PAX2 in the fallopian tube epithelium. A recent publication identified that a subset of human SCOUTs (Type II) share expression profile that is similar to HGSC[146]. Our results suggest that serially passaged MOE cells with PAX2 knockdown and *TP53* mutation resemble Type II SCOUTs. The similarity between the present models and benign SCOUTs may further explain the lack of tumorigenicity seen *in vivo*. Stathmin is a microtubule destabilizing protein that is overexpressed in HGSC[56]. Consistent

with stathmin's established role in influencing migration in other tumor types, knockdown of stathmin in MOE cells with PAX2 loss + mutant *TP53* and it's "aged" variant, significantly reduced migration[157, 158]. Investigators have shown that stathmin knockdown has significant anti-tumorigenic effects in animal models, making it a favorable drug target in several tumor types[159, 160]. As per the TCGA, patients with *STMN1* gene amplification demonstrated a significantly lower overall survival compared to patients without the alteration[161]. Very little is known about fut8[162] and mme[163] in HGSC. In agreement with the TCGA data, mme and fut8 are amplified in serially passaged MOE: $PAX2^{shRNA\text{-}1}$+$p53^{mut}$. Fut8 protein is highly expressed in MOE: $Pax2^{shRNA\text{-}1}$ cells and this increased expression is progressively inhibited when combined with *TP53* mutation. Further investigation of aberrant pathway modulation downstream of PAX2 can assist to inform upon benign to malignant transformation.

Re-expression of PAX2 in murine and human tumorigenic models showed decrease in tumor burden. Joint loss of PAX2 and PTEN has been reported in endometrial carcinomas[77]. Consistent with published study, MOE cells harboring PTEN loss formed high-grade carcinomas[60] and expressed significantly lower PAX2. Stable re-expression of PAX2 in PTEN-lacking MOE cells not only reduced proliferation and migration *in vitro*, but also reduced tumor burden that is otherwise induced by PTEN loss. One study has reported that re-introduction of PAX2 in OVCA432 and OVCAR3 cells reduced cell viability[76], similar to what is shown in our study using OVCAR4, OVSAHO, OVCAR3 cells. Interestingly, multiple attempts to create a stable HGSC cell line with PAX2 overexpression led to cell death indicating that PAX2 could be inducing apoptosis in these cells. Intriguingly, the ability to successfully develop stable PAX2 variants in MOE cell line harboring PTEN loss in

contrast to HGSC cell line, suggests that additional mutations that occur in human tumors contribute to the toxic effects when PAX2 is re-expressed or there is a species difference. Transient PAX2 overexpression in HGSC cells confirmed that PAX2 expression induces apoptosis, which has not been reported so far in HGSC. Future studies may focus on whether strategies to restore PTEN may contribute to reduced tumor burden partially through enhanced expression of PAX2.

If early putative lesions of FTE-derived HGSC lose PAX2, and PAX2 continues to be lost in many tumor samples, then re-expression of PAX2 might result in cell death or other mechanisms that block tumor growth. Bioinformatics analysis of the TCGA data indicates that PAX2 is not methylated as a mechanism for repression in HGSC and that it is rarely mutated[50]. Using a cell-based screening assay and an FDA-approved compound library, luteolin was identified to be a potential "hit" that can stimulate PAX2 expression in MOE cells. Luteolin is a flavonoid that has anti-cancer properties and reduces proliferation of several tumorigenic cell lines as well as has the potential to slow tumor growth *in vivo*[164, 165]. The ability of luteolin to increase PAX2 mRNA and protein expression as well as decrease migration and proliferation in fallopian tube epithelial cells provides preliminary evidence for it's potential. Mechanistically, luteolin is known to inhibit NFκB transcription and activate c-Jun[166]. NFκB has putative binding sites on the PAX2 promoter whereas c-Jun phosphorylates PAX2 and is shown to increase PAX2-dependent transcription[167].

Co-transfection of wild type or mutant p53 along with the PAX2 promoter construct in MOE cells revealed that wild-type p53 was able to activate whereas mutant p53 repressed PAX2 promoter activity. Similar results were reported in mouse embryonic kidney cells where a ChIP-Seq analysis revealed multiple peaks of

p53 occupancy on the PAX2 promoter[145]. In light of these results, what is unclear is whether elimination of repression from mutant p53 is critical to enhance PAX2. It may be particularly interesting to combine luteolin with a mutant p53-repressing and/or wild-type p53 restoring molecule (e.g. NSC59984)[168] to observe its additive effect on PAX2 activation. Future studies will be focused on developing a robust and efficient high-throughput screening strategy that can assay large compound libraries for targets that are known to be deregulated at benign stages.

D. CONCLUSION

In summary, this is the first study to outline the molecular and genetic regulation of PAX2 in the fallopian tube epithelium and HGSC. Combining mutant p53 with PAX2 loss was critical to observe functional changes, which could explain how early lesions form in the FTE before progressing to serous tumors. Our data also revealed that PTEN loss contributes to loss of PAX2. These data suggest a dynamic feedback between PTEN, PAX2 and p53 manifested in the fixed tissue staining. These findings also imply that strategies to restore PTEN may contribute to reduced tumor burden partially through enhanced expression of PAX2. To detect the disease at a benign stage, significant progress must be made in terms of development of novel serum biomarkers as well as powerful distal tube imaging technologies. A novel proof-of-concept small molecule screen, that could block pre-neoplastic lesions or replace key proteins lost during progression, such as PAX2, is presented here. Overall, understanding the molecular basis of precursor lesion development is critical to detect the disease at benign stages and halt serous cancer progression.

V. TARGETING OF FOLLICLE STIMULATING HORMONE PEPTIDE-CONJUGATED DENDRIMERS TO OVARIAN CANCER CELLS

(Reprinted with permission from *Nanoscale, 6*(5), 2812-2820, doi:10.1039/c3nr05042d, in collaboration with Dr. Seungpyo Hong's group)

A. INTRODUCTION

A combination of cytoreductive surgery and chemotherapy are the conventional methods to treat patients that present with advanced-stage disease. Despite an initial response to the first line of drug therapy, most cases present with a recurrent disease. Additionally, as it is often the case with chemotherapeutic drugs, those indicated for ovarian cancer such as paclitaxel and cisplatin are frequently associated with severe side effects due to nonspecific biodistribution to healthy tissues. A patient diagnosed with ovarian cancer undergoing standard intraperitoneal (i.p.) injection of carboplatin/paclitaxel may not tolerate the full-recommended dose as a result of the toxic side effects experienced due to high local concentrations of chemotherapy[169, 170]. Therefore, it is highly desirable to design effective therapies that selectively target tumor cells, which can greatly reduce the systemic side effects and improve the therapeutic index of most chemotherapeutic agents.

Follicle stimulating hormone (FSH) is synthesized by the anterior pituitary gland and serves as a ligand that binds to and activates the follicle stimulating hormone receptor (FSHR). In the ovary, FSH plays a significant role in maturation of immature follicles to Graafian follicles[109]. The primordial follicles are the most immature follicles in the ovary and do not express FSHR[107, 171, 172]. Therefore, a drug carrier that selectively targets the FSHR should spare a cohort of follicles from the toxic effects of chemotherapy and potentially allow for fertility preservation in younger women diagnosed with ovarian cancer. The tissue of origin of ovarian

cancer is not known, but the potential progenitor cells are the ovarian surface epithelium (OSE) and fallopian tubal epithelium (FTE), which both express FSHR[54]. In addition, several investigators have demonstrated elevated expression of FSHR in ovarian cancers[171, 173]. Some reports have shown that FSHR also stimulates proliferation of cancer cells and its overexpression is considered oncogenic[22, 105, 174, 175]. Therefore antagonists of this receptor have the potential to reduce cancer proliferation and improve survival.

Targeting the FSHR can be achieved using peptide sequences modeled after the binding domains of FSH. Among those, the peptide derived from amino acids 33-53 (FSH33) exhibits the strongest binding affinity to FSHR[176]. This peptide has recently been employed as a targeting ligand to ovarian tumor tissue using paclitaxel-encapsulated polymeric nanoparticles (NPs) of polyethylene glycol-b-polylactide (PEG-PLA)[177]. These NPs and other types of nanocarriers such as liposomes and micelles have been widely investigated for targeted drug delivery to tumors[178-182]. Their controlled particle size (typically 50-200 nm) enables them to passively accumulate in tumor tissues through the enhanced permeability and retention (EPR) effect that is characteristic of tumor biology[183]. However, some of the limitations associated with the use of polymeric NPs include their limited diffusivity, which leads to inefficient distribution of drug payloads within the tumor mass[184]. Several studies have shown that efficient tumor penetration is largely dependent on size, with nanocarriers smaller than 20 nm having superior tissue diffusivity and penetration properties[184, 185].

Dendrimers are nanometer-sized, hyperbranched, highly monodisperse, multifunctional macromolecules that have been widely explored for a variety of biomedical applications[186-188]. Polyamidoamine (PAMAM) dendrimers are among

the most widely investigated family of dendrimers for targeted drug delivery[189]. The primary amine groups on their surface enable functionalization with targeting ligands as well as drug molecules and imaging agents, resulting in multifunctional nanodevices that have shown promising preclinical targeted drug delivery potential[190-192]. Due to their hyperbranched structure, along with high molecular flexibility and deformability, conjugation of multiple targeting moieties to the outer surface of the dendrimers has been shown to enhance their targeting efficacy due to the multivalent binding effect[193]. More importantly, their molecular flexibility combined with the small size (5-10 nm) imparts favorable tissue penetration and diffusivity properties compared to the more rigid structure of polymeric NPs[91, 194, 195].

For these reasons, a novel FSH33-targeted dendrimer-based nanocarrier was designed as a potential delivery platform targeted to ovarian cells expressing FSHR. Using generation 5 (G5) PAMAM dendrimers labeled with fluorescein, we hypothesized that conjugation with FSH33 peptide would produce a multifunctional dendritic nanocarrier that selectively targets FSHR-expressing ovarian cancer cells, while sparing immature primordial follicles. The receptor selectivity of the FSH33-targeted dendrimers was validated in 2D cell culture using two ovarian cancer cell lines, the OVCAR-3 cells that express FSHR ($FSHR^+$) and the SKOV-3 cells that are FSHR negative ($FSHR^-$). In addition, the receptor antagonistic effect of FSH33-targeted dendrimers was investigated in OVCAR-3 cells by measuring survivin expression. Survivin, an anti-apoptotic protein, is known to be downstream of FSH signaling in the OSE[23] and is overexpressed in serous cancer[196]. We also employed normal mouse 3D ovarian organ cultures grown in an alginate hydrogel, which has been previously reported to allow the successful growth of OSE cells while retaining their normal architecture and biomarkers[95]. The *in vitro* 3D organ culture system

serves as a tool for investigating the effects of the nanocarrier on ovarian cells, such as the OSE and ovarian follicles, cultured within a microenvironment that mimics physiological conditions. The targeting efficacy of the nanocarrier was further validated *in vivo* following an i.p. injection of the conjugates. This paper represents a proof-of-concept study validating the design of a novel FSH33-targeted dendritic nanocarrier with high selectivity to ovarian cancer cells and normal cells expressing FSHR, which also has the potential to provide an option for fertility preservation.

B. RESULTS

Preparation and characterization of FSH33-targeted G5 PAMAM dendrimer conjugates

A general overview of the preparation of the dendrimer conjugates is illustrated in **Fig. 25**. FITC-labeled, FSH33-targeted G5 PAMAM dendrimers were prepared by sequential conjugation with FITC and FSH33, using sulfo-SMCC as a linker, followed by full acetylation of the remaining primary amine groups, resulting in G5-Ac-FITC-FSH. Conjugation of FITC and FSH33 to the dendrimers and successful end-capping of the amine groups was confirmed using UV/Vis. The numbers of FITC and FSH33 molecules per dendrimer were calculated to be approximately 5.5 and 10.3 FITC and FSH33 molecules per dendrimer, respectively. Similarly, ^{1}H NMR characterization of G5-Ac-Cy5.5-FSH revealed 2.1 and 2.3, Cy5.5 and FSH molecules per dendrimer, respectively.

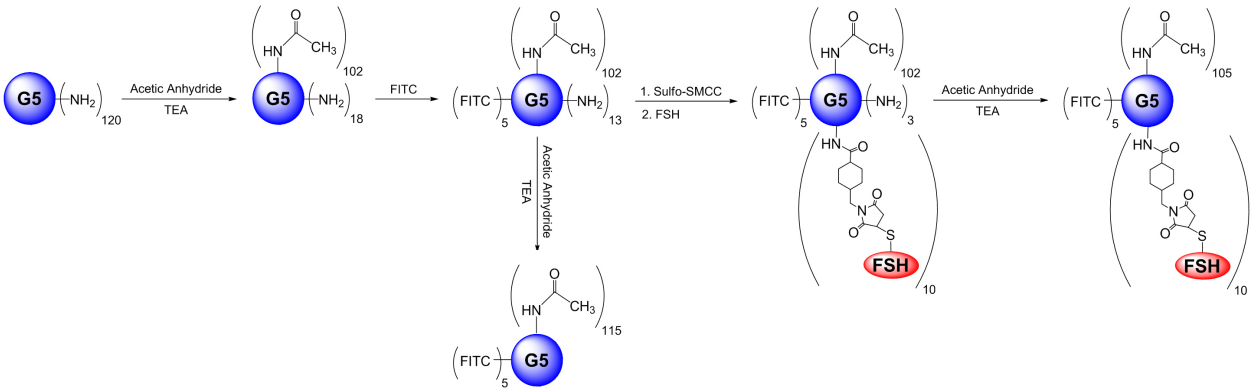

Figure 25: Overview of the preparation of FSH33-targeted G5 PAMAM dendrimer conjugates. (Data and figure generated by Dr. Suhair Sunoqrot)

G5-Ac-FITC-FSH specifically targets ovarian cancer cells expressing FSHR in 2D cell culture

Receptor selectivity of the FSH33-targeted dendrimer conjugates was investigated in OVCAR-3 and SKOV-3 cells. Western blot analysis of FSHR expression in the OVCAR-3 and SKOV-3 cell lines used in this study confirmed that OVCAR-3 cells express the receptor, while SKOV-3 cells do not, consistent with previous reports **(Fig. 26A)**[173, 177]. The SKOV-3 cell line thus served as a negative control in the 2D cell culture experiments **(Fig. 26B)**. Receptor selectivity of the FSH33-targeted conjugates was further validated by pre-treating OVCAR-3 cells with an excess amount of free FSH33, which should block the FSHR and prevent binding and uptake of the FSH33-targeted dendrimers[177]. As shown in **Fig. 27A**, the targeted G5-Ac-FITC-FSH conjugates demonstrated significant uptake by OVCAR-3 cells, as indicated by the green fluorescence signals coming from inside the cytosol. This interaction was highly selective, as evidenced by the lack of FITC fluorescence in OVCAR-3 cells following pre-treatment with free FSH33, which blocked the FSHR binding sites. The lack of positive green fluorescence signal from inside OVCAR-3 cells following treatment with the control conjugate, G5-Ac-FITC, further confirmed the selectivity of the FSH33-targeted conjugates. SKOV-3 cells treated with equivalent concentrations of G5-Ac-FITC-FSH conjugates did not exhibit any significant uptake, providing further evidence of FSHR selectivity of the G5-Ac-FITC-FSH.

Flow cytometry analysis was performed to quantify the selective uptake of G5-Ac-FITC-FSH by OVCAR-3 cells. Consistent with confocal observations, cells incubated with G5-FITC-FSH demonstrated a significantly higher fluorescence count compared to untreated cells (~8-fold increase, **Fig. 27B**), which was diminished by

pre-treating the cells with free FSH33 peptide and upon treatment with G5-Ac-FITC. Overall, these results indicate that G5-Ac-FITC-FSH selectively interacted with the OVCAR-3 ($FSHR^+$) cells, but not SKOV-3 ($FSHR^-$) cells, and could be competed away from the receptors when incubated with an excess amount of free FSH33 peptide. Additionally, OVCAR-3 cells treated with the dendrimer conjugates up to 5 μM for 24 h did not demonstrate significant cytotoxicity when compared to the untreated cells **(Fig. 28)**.

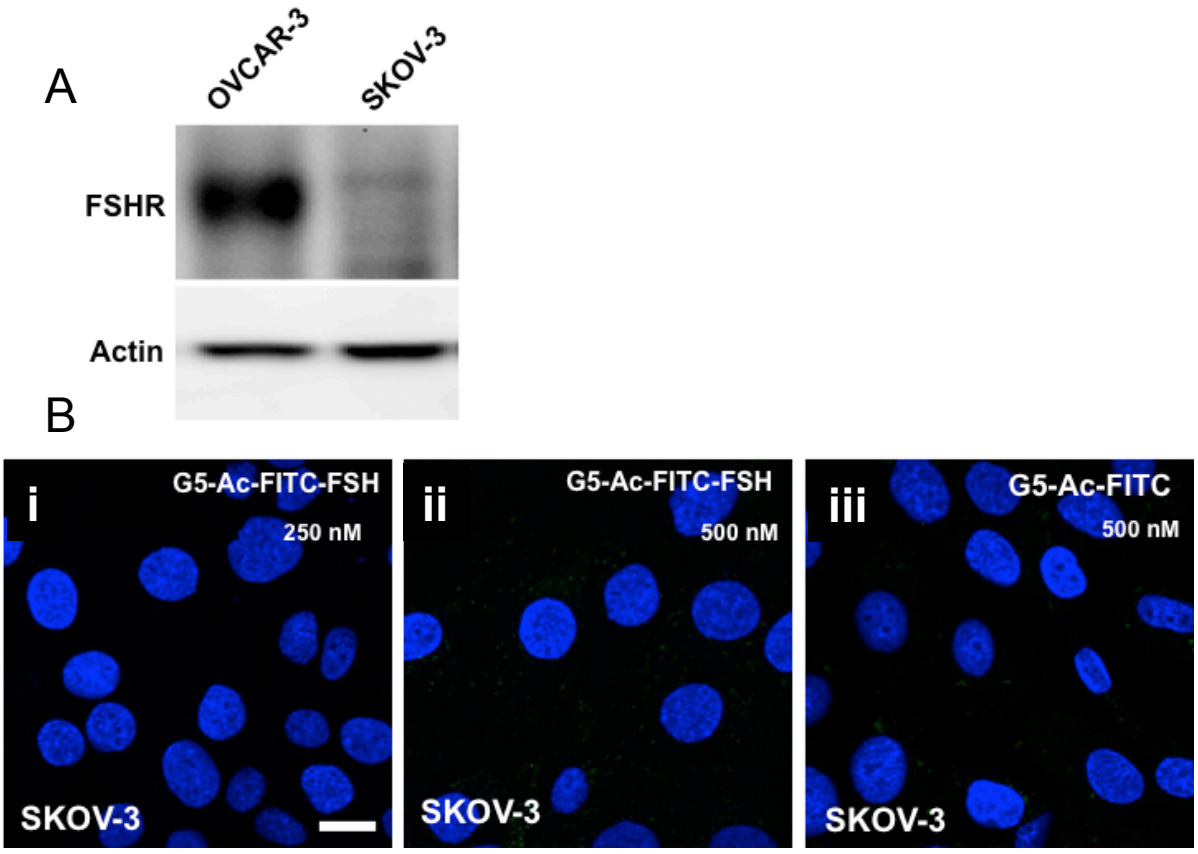

Figure 26: Receptor selectivity of the FSH33-targeted conjugates in OVCAR-3 cells. A) Expression of FSHR protein in human ovarian cancer cell lines; OVCAR-3 and SKOV-3 by western blot. Size of FSHR is ~78 kDa. **B)** Uptake of G5-Ac-FITC-FSH (i. 250 nM and ii. 500 nM) and iii. 500 nM G5-Ac-FITC in SKOV-3 cells (FSHR-) after 5 h incubation, showing minimal cellular interaction compared to OVCAR-3 cells (Fig. 27A). Blue: cell nuclei stained by DAPI, green: FITC-labeled dendrimers, scale bar: 20 µm.

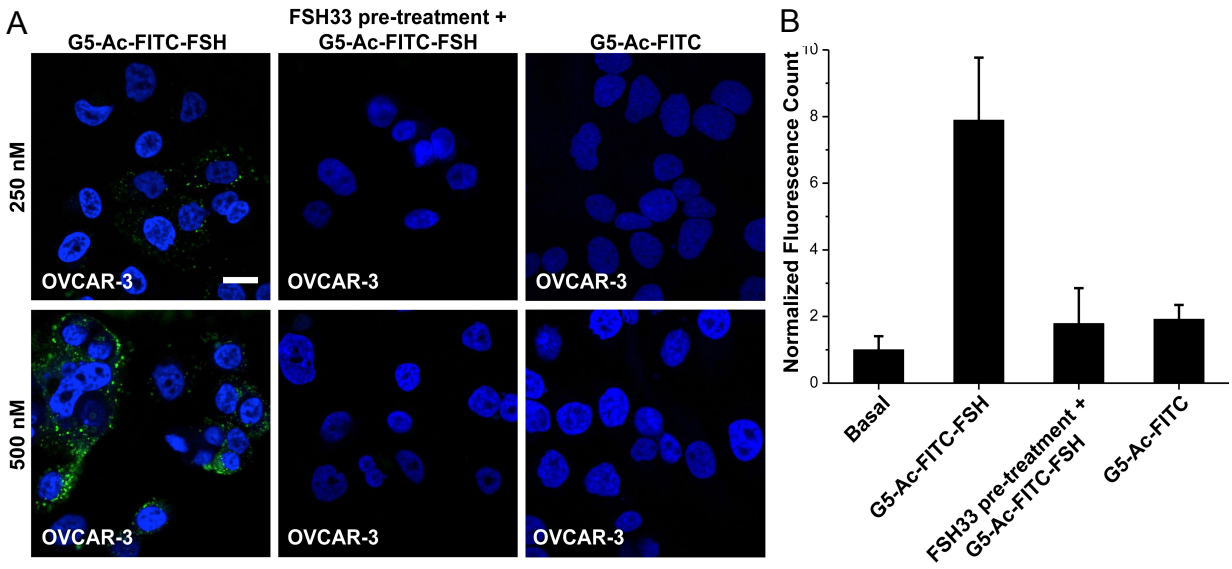

Figure 27: G5-Ac-FITC-FSH specifically targets ovarian cancer cells expressing FSHR in 2D cell culture. **A)** Confocal microscopy images of OVCAR-3 cells following treatment with 250 and 500 nM of G5-Ac-FITC-FSH for 5 h, with or without pre-treatment with 100 µM free FSH33 for 2 h, blue: cell nuclei stained by DAPI, green: FITC-labeled dendrimers, scale bar: 20 µm. FSHR selectivity of G5-Ac-FITC-FSH is demonstrated by the strong, concentration-dependent green fluorescence signals from OVCAR-3 cells, which were diminished by pre-treatment with free FSH33. No significant uptake was observed in OVCAR-3 cells following incubation with the control conjugate, G5-Ac-FITC, and in SKOV-3 cells. **B)** Normalized fluorescence count of OVCAR-3 measured by flow cytometry following treatment with 500 nM of the conjugates. Cells treated with G5-Ac-FITC-FSH showed significantly higher cell-associated fluorescence than the control groups, further supporting FSHR selectivity.

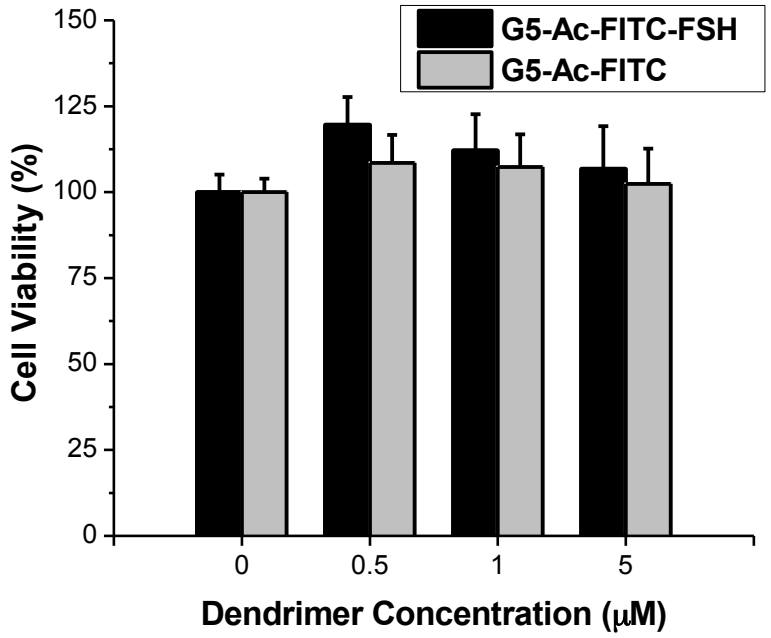

Figure 28: Cytotoxicity of the dendrimer conjugates prepared in this study in OVCAR-3 cells after 24 h incubation. The conjugates were well tolerated and did not show any cytotoxicity up to micromolar concentrations. (Data and figure generated by Dr. Suhair Sunoqrot)

FSHR antagonistic activity of G5-Ac-FITC-FSH revealed by survivin downregulation

In order to identify whether G5-Ac-FITC-FSH was an agonist or an antagonist to the FSHR, western blot analysis was performed to determine the effect of dendrimers on survivin expression. Birc5, also known as survivin, is an anti-apoptotic protein that is previously demonstrated to be a downstream target of FSH when bound to FSHR[113]. OVCAR-3 cells incubated with FSH hormone (10 mIU/mL, 24 h) demonstrated elevated levels of survivin. Whereas G5-Ac-FITC-FSH (500 nM) with and without FSH hormone, significantly downregulated survivin expression in OVCAR-3 cells **(Fig. 29)**.

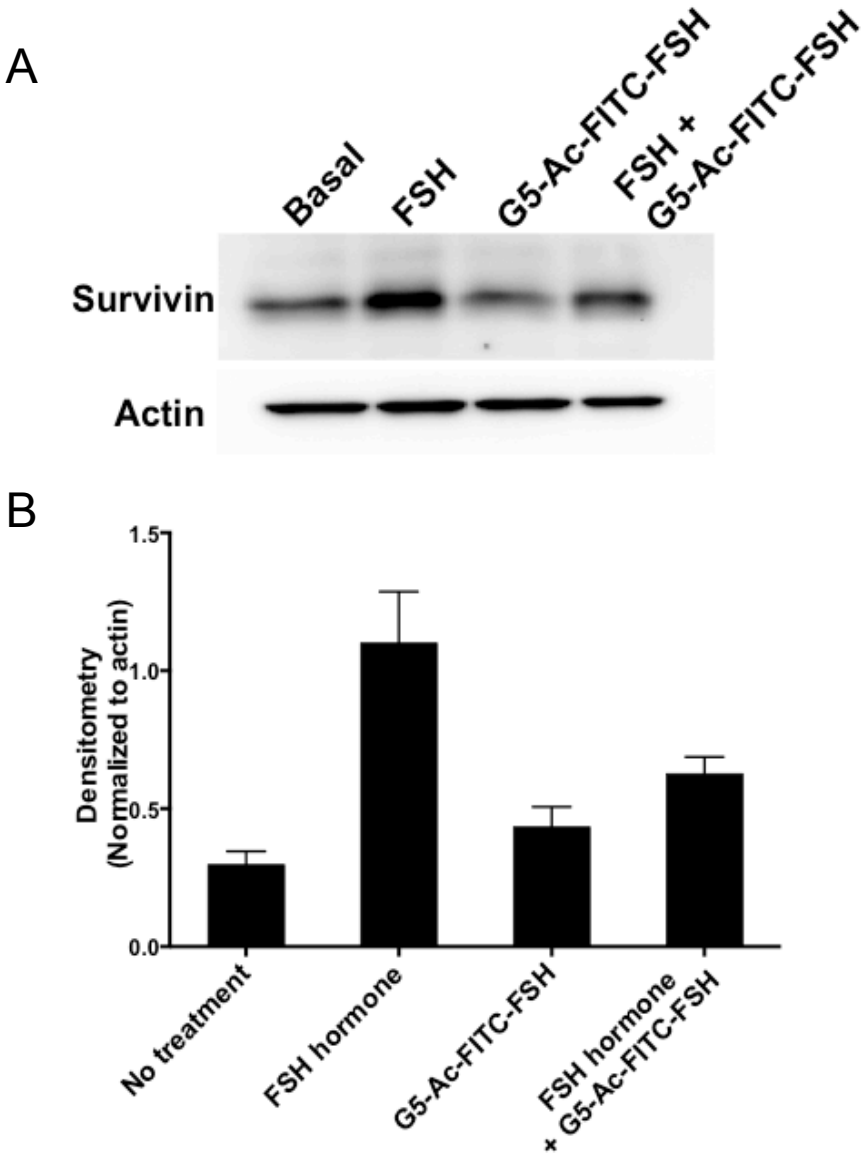

Figure 29: FSHR antagonistic activity of G5-Ac-FITC-FSH revealed by survivin downregulation A) Expression of survivin in OVCAR-3 cells when after incubation for 24 h with G5-Ac-FITC-FSH (500 nM), FSH hormone (10 mIU/mL), and FSH hormone in the presence of G5-Ac-FITC-FSH. **B)** Survivin expression relative to actin. Survivin expression is upregulated upon treatment with FSH, but is downregulated following G5-Ac-FITC-FSH treatment, revealing a potential antagonistic effect for FSH33-targeted dendrimers.

G5-Ac-FITC-FSH selectively binds to OSE cells in 3D mouse ovarian organ cultures

To validate if the targeted nanocarrier, G5-Ac-FITC-FSH, specifically binds to OSE cells expressing the FSHR, a mouse ovarian 3D organ culture system was employed to more closely mimic in vivo conditions[95]. This is particularly important since OSE cells are known to give rise to ovarian cancers, and if the progenitor cells could be targeted without negatively impacting ovarian follicles, then it might be possible to use such nanocarriers for cancer prevention as well. Ovarian organoids were cultured with the nanocarriers prior to encapsulation in alginate hydrogel. Control organoids were cultured in basal media **(Fig. 30b)**. Upon incubation of the organoids with G5-Ac-FITC-FSH (500 nM for 5 h), the ovarian surface cells stained positive for FITC, indicating successful targeting of G5-Ac-FITC-FSH to the OSE cells, which are known to express FSHR **(Fig. 30c)**[177]. A second set of organoids was pre-treated with 100 μM FSH33 for 2 h, followed by adding 500 nM G5-Ac-FITC-FSH for 5 h. Immunostaining against FITC revealed that FSH33 was successful in competitively blocking G5-Ac-FITC-FSH from accumulating in FSHR-expressing OSE[23]. As a result, G5-Ac-FITC-FSH was unable to target the OSE **(Fig. 30d)**. A third set of organoids was incubated with G5-Ac-FITC for 5 h **(Fig. 30e)**. Organoids were also treated for 2 h with 100 μM FSH33, followed by 5 h incubation with 500 nM G5-Ac-FITC **(Fig. 30f)**. Regardless of FSH33 pre-treatment, anti-FITC positive staining was seen on the OSE as well as in the stroma and some granulosa cells of the organoids **(Fig. 30e and 30f)**, demonstrating its lack of specificity. Taken together, these results suggest that the targeted G5-Ac-FITC-FSH conjugates selectively bound to cells expressing FSHR on the ovarian surface, validating their use as a targeted nanocarrier to ovarian cells expressing FSHR.

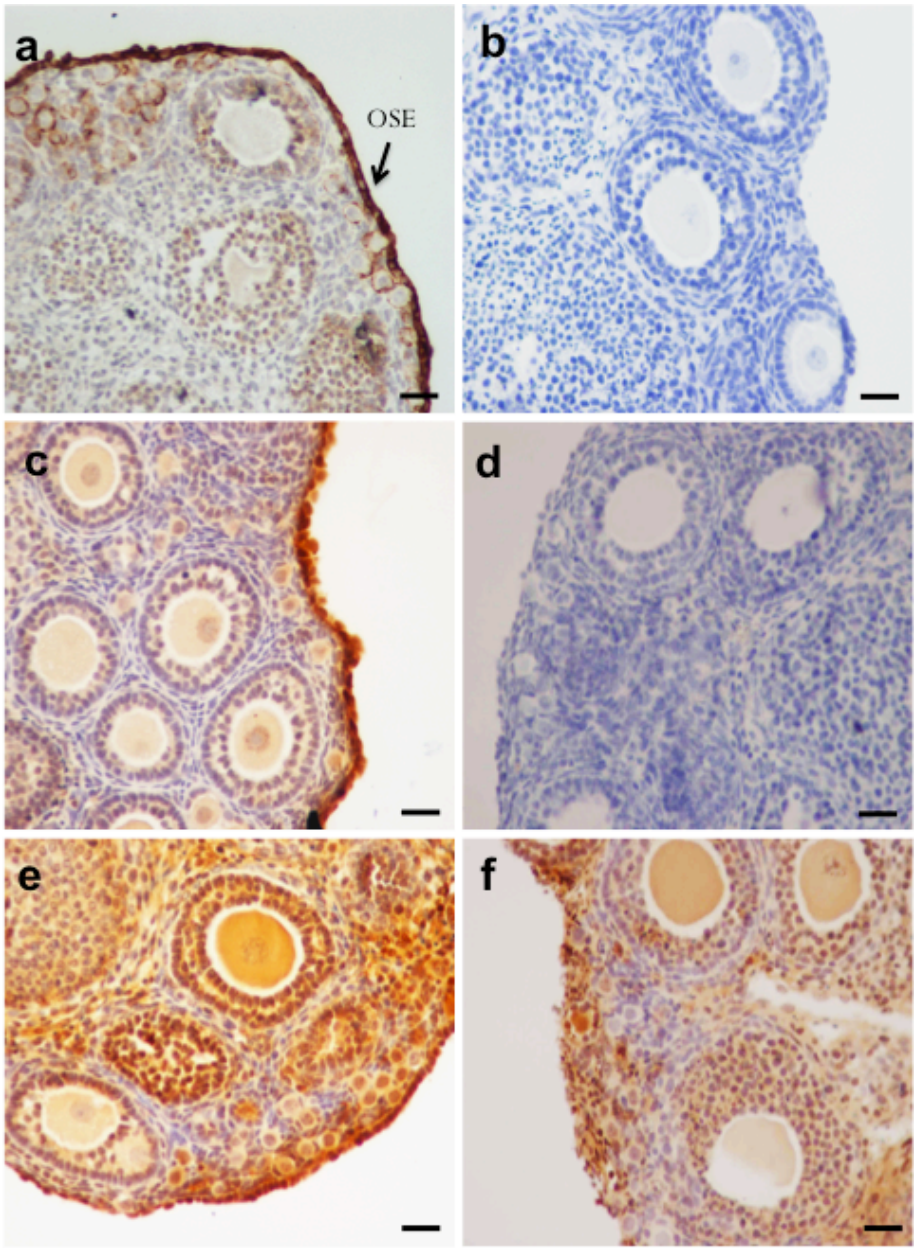

Figure 30: Uptake of G5-Ac-FITC-FSH in 3D normal mouse ovarian organ culture revealed by IHC staining. Ovarian organoids were stained with anti-FITC antibody following treatment with: **a)** OSE labeled by CK8 stain, **b)** basal media (5 h), **c)** G5-Ac-FITC-FSH (500 nM, 5 h), **d)** FSH33 (100 μM, 2 h) followed by G5-Ac-FITC-FSH (500 nM, 5 h), **e)** G5-Ac-FITC (500 nM, 5 h) **f)** FSH33 (100 μM, 2 h) followed by G5-Ac-FITC (500 nM, 5 h). Scale bar: 50 μm.

G5-Ac-Cy5.5-FSH selectively accumulates in the mouse ovary and oviduct *in vivo*

To investigate whether the targeted dendrimer, G5-Ac-Cy5.5-FSH, selectively accumulates in tissues that express the FSHR as compared to its non-targeted counterpart, an *in vivo* efficacy study was performed using female BALB/c mice. This study is particularly critical in assessing the ability of the proposed system to deliver drugs to specific sites with minimal off-target effects. Note that Cy5.5 was employed for this *in vivo* study as it is known to exhibit enhanced photostability and tissue penetration of its fluorescence signal[197]. Mice (n = 6/group) were given an i.p dose of either G5-Ac-Cy5.5-FSH or the non-targeted control, G5-Ac-Cy5.5. As shown in **Fig. 31**, the targeted conjugate, G5-Ac-Cy5.5-FSH, achieved significantly higher fluorescence intensities in the ovary and oviduct compared to the group treated with G5-Ac-Cy5.5, which are the tissues with the highest FSHR expression levels. The fluorescence count was also significantly higher than the levels measured in the uterus and kidney in both groups. Overall, these preliminary results demonstrate successful accumulation of the FSH33-targeted dendrimers in the ovary and oviduct that are the two putative sites of origin of serous ovarian cancer.

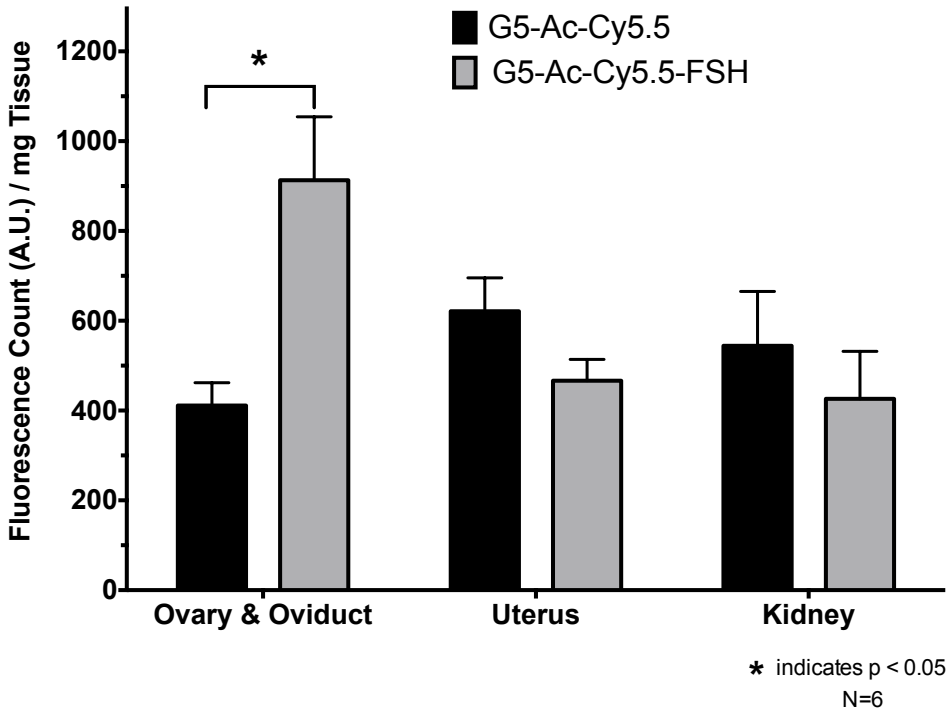

Figure 31: Accumulation of G5-Ac-Cy5.5-FSH and G5-Ac-Cy5.5 dendrimers in ovary, oviduct, uterus and kidney tissue homogenates of 6-8 week old female BALB/c mice. Six animals per group were injected IP with 15 mg/kg dendrimer solutions. At 6 h post-injection, organs were harvested, weighed, homogenized and fluorescence was measured. * indicates $p < 0.05$.

C. DISCUSSION

About 95% of the newly developed potential therapeutics have poor pharmacokinetic and biopharmaceutical properties[198]. Therefore, there is an urgent need to develop effective drug delivery systems that specifically target the active site without affecting the surrounding healthy tissues. This is particularly important in diseases such as ovarian cancer, which require rigorous treatment regimens with drugs that have low therapeutic indices and are toxic to normal tissues. In addition, development of resistance to the existing chemotherapeutic drugs occurs in most cases. As a result, treating recurring cases of ovarian cancer is challenging[199]. Over the past few decades, nanotechnology has provided a plethora of platforms that have enabled the selective delivery of payloads to target tissues and organs through passive and active targeting[183]. PAMAM dendrimers, having proven to be highly effective active targeting mediators, were chosen in this study as a potential delivery platform to selectively target ovarian cancer cells through the FSHR.

Our target of choice, FSHR, has a number of advantages. First, FSHR is expressed by the OSE and the FTE as well as overexpressed in ovarian cancer cells[171, 200]. Second, FSH33 is available as an FSHR-specific ligand that exhibits low immunogenicity and high affinity to the FSHR[177]. Third, the FSHR-targeting nanocarrier system could potentially block the cascade of oncogenic signaling pathways that are activated by FSHR upon FSH ligand binding[23, 174]. Forth, primordial follicles do not express the FSHR, which would potentially allow for fertility preservation while providing effective therapy. Other ovarian cancer targets such as the folic acid receptor (FAR) and the epithelial growth factor receptor (EGFR) have been explored for targeted drug delivery to ovarian cancer cells[201, 202]. However, these receptors can also be expressed by nonmalignant ovarian tissues and other

healthy tissues, which may result in nonspecific uptake and potential side effects[203, 204]. The FSHR is uniquely overexpressed by ovarian cancer cells, making it an excellent target for selective delivery of chemotherapeutic agents to ovarian tumors.

Preliminary validation studies in 2D cell culture using the $FSHR^+$ OVCAR-3 cell line confirmed that the FSH33-targeted dendrimers are highly selective to cells expressing FSHR and may demonstrate minimal off-target effects. Survivin is known to be upregulated in serous ovarian cancer[118]. OVCAR-3 cells incubated with FSH hormone demonstrated elevated survivin levels, supporting the potential role of hormonal influence in early events of ovarian cancer formation. However, downregulation of survivin expression when incubated with FSH hormone in presence of the G5-Ac-FITC-FSH peptide suggests that the dendrimer may be acting as an antagonist to the FSHR. In addition to selective delivery of chemotherapeutic drugs to the ovarian tissue, FSH33-targeted dendrimers thus have the potential to block the cascade of FSH signaling pathways, potentially augmenting their therapeutic effect.

Investigations into therapies that preserve fertility and selectively kill the epithelium that causes cancer are usually performed *in vivo*. The 3D *ex vivo* organ culture system offers the advantage to examine several incubation times and concentrations, while maintaining the architecture of the ovary. The targeting efficiency of the dendrimer conjugates was thus validated in a 3D organ culture system. G5-Ac-FITC-FSH targeted the FSHR on the ovarian surface epithelium and spared the primordial follicles that do not express the FSHR, as revealed by IHC. Interestingly, the non-targeted conjugate, G5-Ac-FITC, did not bind to OSE, but was able to penetrate through the ovarian surface into the stroma and the follicles, while the targeted conjugate did not. This could be attributed to the high affinity binding of

G5-Ac-FITC-FSH to OSE, which prevented its penetration into the organoids. The neutral charge and lack of targeting ligand on G5-Ac-FITC may have promoted its diffusion through the interstitium, resulting in deeper penetration[205]. These observations necessitate suitable optimization of FSH33 density on the surface of the dendrimer conjugates, to maintain receptor selectivity without hindering their tissue penetration ability, which will be the subject of our future investigations.

A preliminary *in vivo* efficacy study performed in female mice demonstrated successful targeting of FSH33-targeted dendrimers to tissues that express the FSHR. Significantly higher fluorescence counts were observed in the ovary and oviduct homogenates from the G5-Ac-Cy5.5-FSH-treated animals, compared to the group treated with non-targeted conjugates. While both dendrimer conjugates were detected in the uterus, the selective accumulation of the targeted nanocarrier was not higher than the non-targeted control, likely because the uterus does not express FSHR. Similarly, both conjugates were likely eliminated through the kidney and showed no significant difference in accumulation, due to the lack of FSHR in this negative control tissue. These findings demonstrate a strong potential for the dendrimer-based platform to deliver chemotherapeutic drugs that can effectively target ovarian cancer cells.

Taken together, the specific binding of G5-Ac-FITC-FSH to the ovarian surface, along with the lack of nonspecific uptake of G5-Ac-FITC by OSE, strongly suggest that the dendrimer-based FSH33-targeted nanocarrier can efficiently bind to cells expressing FSHR. Additionally, increased accumulation of G5-Ac-Cy5.5-FSH in mouse ovary and oviduct suggests targeted uptake in cells expressing FSHR *in vivo*. These proof-of-concept results, both *in vitro* and *in vivo* systems, provide evidence that this novel system can potentially be employed to deliver

chemotherapeutic agents to malignant cells in the ovary, while sparing healthy ones and thus allowing fertility preservation. Although FSH-targeted polymeric NPs have been previously reported[177]. The current system has the advantage of combining high receptor selectivity with the small size scale (one order of magnitude smaller than the reported NPs), which imparts superior tissue penetration and distribution properties compared to the larger more rigid NPs[185, 194, 195].

D. CONCLUSION

The current study reports on a novel dendrimer-based nanocarrier delivery system that targets to ovarian cancer cells and OSE cells expressing FSHR with high receptor selectivity. FSH33-targeted dendrimers demonstrated efficient uptake by OVCAR-3 cells in 2D cell culture, and OSE cells in 3D organ culture, sparing the primordial follicles and allowing for fertility preservation. *In vivo*, FSHR-specific nanocarriers demonstrated significant accumulation in the mouse ovary and oviduct, suggesting its potential for use in therapeutic drug targeting. This delivery system has the potential to be employed for targeted delivery of chemotherapeutic drugs used in ovarian cancer, which warrants further investigation.

VI. DISCUSSION AND FUTURE DIRECTIONS

Overall, this project helped to i) inform upon the influence of gonadotropins on ovarian cancer initiation and progression. ii) This thesis developed *in vitro* models that mimic the early precursor lesions identified in the fallopian tubes of women that were genetically predisposed to getting high-grade serous cancer identical to those found in serous tumors. iii) Lastly, efforts were focused on identifying nanocarriers that can be used for therapeutic intervention or as preventive measures while protecting women from serous cancer initiation.

Implication of our findings and scope of study

A. Gonadotropins and Ovarian Cancer

Even though most serous cancers are predicted to originate in the fallopian tube, the bulk of the tumor is often found on or surrounding the ovary. In most cases, the ovary is involved. Blocking ovulation is associated with reducing the risk of ovarian cancers. Therefore it is critical to investigate the effects of wound repair and ovulation on the OSE cells. The physiological mechanism of FSH and LH signaling in normal cells that gives rise to ovarian tumors was not well characterized. A unique aspect to our study was the use of a three-dimensional (3D) organ culture system, which is superior to the traditionally used 2D *in vitro* cell culture because it can retain the original architecture of the organ and more effectively simulate physiological conditions as many cellular processes are occurring *in vivo*[206]. Our data illustrates that gonadotropins regulate proliferative properties, migration and colony formation in the OSE cells[23]. FSH and LH alter several key pathways in the OSE that are commonly known to be regulated in serous cancer[23, 50]. Some of those molecular pathways include the EGFR, Akt, PI3K and the cyclin-dependent kinases.

Most studies demonstrate the effect of FSH or LH on the OSE cells, but this was the first study to evaluate the biological effects of administering both at the same time. During ovulation and in post-menopausal women, FSH and LH are almost always circulating together, at different levels depending on the menstrual cycle. It may be beneficial to understand the effects of FSH and LH at specific time points but it is challenging to mimic the exact ratio experimentally.

Mounting evidence convincingly demonstrates that most serous cancers originate from the FTE[5, 35, 46, 51, 52, 54, 63, 138, 207]. Therefore, it is important to evaluate the insults of ovulation on the FTE cells as well. The normal FTE cells did not respond to FSH and LH. Possibly, the role of FSH and LH concentrations in postmenopausal women that coincide with the time when most women are diagnosed with ovarian cancer is due to specific genetic changes like *TP53* mutation or deletion of PAX2 and PTEN in the FTE. Although FSH and LH do not activate the same oncogenic pathways in the FTE as they do in the OSE, they might regulate PAX2 expression by affecting phosphorylation of PTEN or GATA4, both of which are known to regulate PAX2 expression in the FTE. In the ovary, FSH is known to increase GATA4 phosphorylation and rapidly activate the PI3K/AKT pathway, which is negatively regulated by PTEN[208]. It remains to be determined if FSH and LH have additional proliferative or transformative properties in the FTE cells after oxidative stress to mimic spontaneous transformation and when *TP53* is mutated and/or PTEN is functionally eliminated. An interesting approach to circumvent the issue about the cell of origin would be to exploit a polymer nanocarrier system that delivers a therapeutic drug to selectively kill cells overexpressing a specific receptor, such as the FSHR. FSHR is overexpressed in ovarian cancer cells. The nanocarrier will be designed such that it could be used as a therapeutic agent, irrespective of the tissue

of origin of serous cancer.

B. Modeling Early Precursor Lesions of Serous Cancer

One of the major challenges in ovarian cancer is that most tumors are detected at late stage and there are currently no reliable serum biomarkers or imaging strategies for early detection. In addition, there are very few prevention options with the exception of salpingo-oophorectomy or birth control pills. Our project was therefore focused on defining specific precursor lesions that can identify the disease at an early stage and unraveling new mechanistic pathways to reverse or prevent progression. We addressed this proposed progression by generating murine oviductal cell lines with specific genetic alterations as demonstrated in the human FTE tissue samples. We demonstrated a possible mechanism of PAX2 loss, which is reported in all precursors and serous tumors. Based on fixed tissue samples it appears that SCOUTs precedes p53 signatures (where p53 is stabilized). Our data revealed that mutation in *TP53* and PTEN loss contributes to loss of PAX2 in FTE cells. PTEN loss and mutation in *TP53* are commonly observed genetic alterations in serous tumors. Loss of PTEN is sufficient to drive tumorigenesis *in vivo*. These data suggest a dynamic feedback between PTEN, PAX2 and p53 manifested in the fixed tissue staining. Re-expression of PAX2 in PTEN silenced cells reduced tumorigenicity *in vivo*. In the future, RNA-sequencing experiment will compare gene expression profile between FTE cells with scrambled shRNA, $PTEN^{shRNA}$ and $PTEN^{shRNA}$ with PAX2 overexpression. These data will identify the pathways activated by PAX2 expression when PTEN is lost that contributes to slower migration and proliferation. In addition, these data suggest that strategies to restore PTEN and/or reverse mutation of *TP53* may contribute to reduced tumor

burden partially through enhanced expression of PAX2.

A series of events occur that stimulates the benign lesions to progress into malignant ones that are widely disseminated into the peritoneal cavity. The events that define these changes are unknown. Preliminary comparative analysis of gene signature profiles between human SCOUTs [146] and our *in vitro* models of SCOUTs and p53 signatures revealed *stathmin, mme* and *fut8* as the target genes regulated by PAX2 in the FTE. It would be interesting to study their functional significance in driving tumorigenesis, by silencing or overexpressing the target genes, in presence or absence of mutant *TP53* combined with PAX2 loss. Since we have developed a model system, with much less heterogeneity and with only PAX2 silenced or mutant *TP53*, we plan to follow up by performing an RNA-sequencing experiment to compare global changes in transcription between PAX2 loss, *TP53* mutation, and the combination.

PAX2, being a developmental regulatory protein provides the locus for epigenetic modifications during development. PAX2 can modify methylation through interaction with PTIP. PTIP is also involved in the DNA damage response pathway. In the present study, we demonstrate that wild-type p53 directly regulates transcriptional activity of PAX2 whereas mutant p53 represses p53-mediated activation of the PAX2 promoter. Researchers have shown that WT-1 inversely regulates PAX2 activity in kidney cells. Future experiments will aim at performing a Chromatin Immunoprecipitation (ChIP) – Sequencing experiment to validate PAX2 occupancy on the genome and also profile changes in the RNA Polymerase II (Pol II) occupancy in fallopian tube epithelial cells. Overlapping data from both the ChIP-Seq experiments (PAX2 interacting sites and Pol II occupancy) will reveal important direct downstream targets of PAX2 in the fallopian tube epithelium. Modulating expression

of those targets might improve our understanding about early precursor lesion formation from the FTE.

Development of *in vitro* models (Chapter IV) that mimic early precursors of HGSC are a valuable resource to the scientific community because these can lead to improved understanding of the molecular changes required for disease initiation and progression. Evidence shows that SCOUTs and p53 signatures are present in women without genetic predisposition to serous cancer, which brings into question the reliability of these lesions as true "precursors". Molecular and genetic studies have revealed several pathways that are deregulated in serous tumors, mutation in *TP53* being the most frequently reported alteration. Previous reports have demonstrated that mutant *TP53* is insufficient to drive tumorigenesis unless combined with a second genetic insult. Combination of PAX2 loss and mutation in *TP53* altered *in vitro* characteristics but was insufficient to drive tumorigenicity. Therefore, further investigation is warranted to determine the fundamental molecular aberrations that are essential for formation of benign lesions and those that are required for progression to malignant cancer. The TCGA shows that 51% HGSC cases had a defect in the homologous recombination pathway, 33% cases had a mutation or methylation in BRCA1/2 whereas altered PI3K/RAS signaling was reported in 47% cases[50]. A few additional genes that are known to be associated with serous cancer are Cyclin E, c-Myc and ARID1A. Future studies will be focused on combining some of these with PAX2 loss and mutant *TP53* to find the genes that increase tumor potential. The key to unraveling these drivers of tumorigenesis is developing robust genetically engineered mouse models. These specific markers can eventually serve as cancer therapeutic targets.

C. Prevention Strategies

Currently, women that are genetically predisposed to getting HGSC are offered the most effective method of prevention and early detection – risk-reducing salpingo-oophorectomy. High-grade serous ovarian cancer is often detected at late stages when the disease has spread to the peritoneal cavity and therefore, when diagnosed, the 5-year survival rate is extremely low. Emerging data from research studies implies that early detection of precursor lesions rather than serous cancer may be a more realistic goal for screening, but the clinical feasibility of this strategy is yet to be determined.

Early putative lesions of FTE-derived HGSC lose PAX2, and PAX2 continues to be lost in many tumor samples. Re-expression of PAX2 resulted in cell death and inhibited proliferation and migration of serous cancer cells. An important translational question in HGSC is whether a small molecule can be identified that would allow for transcriptional re-expression of PAX2. To address this question, we developed and validated a new bioassay to screen for molecules that can activate PAX2 in normal FTE cells. Identifying molecules that amplify the PAX2 promoter activity in normal FTE cells will help define mechanisms for re-expressing PAX2 and could potentially be modified or studied as a novel prevention strategy. After multiple biological screens, luteolin was found to increase PAX2 mRNA and protein levels in the FTE cells.

Luteolin is a flavonoid with anticancer properties that is naturally present in some fruits and vegetables such as celery, parsley, artichoke and carrots. Luteolin has both, anti- and pro-oxidant properties. Reports suggest that luteolin's oxidation behavior is highly dependent on the concentration and source of free radicals[209]. Flavonoids are reported to possess poor oral bioavailability. Structurally, the

flavonoids rapidly metabolized to a quinoine, which significantly reduces their bioavailability.

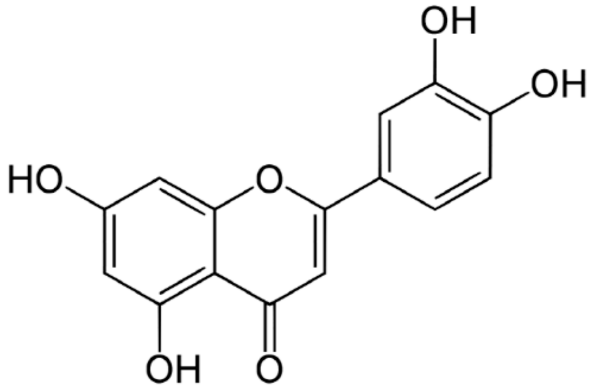

Figure 32: Chemical structure of luteolin[210].

A prospective epidemiological study demonstrated that dietary intake of luteolin, significantly reduced incidence of epithelial ovarian cancer[211]. Although luteolin has previously been shown to inhibit cell growth and reduce tumor burden in multiple cancer models[212, 213], the precise molecular mechanism is unclear. In a hepatocarcinoma model, luteolin decreased tumor burden by increasing AMPK activation via inhibition of NFκB[214]. Interestingly, NFκB has a putative binding site on the PAX2 promoter. Luteolin is also known to inhibit pro-inflammatory mediators such as iNOS and TNFα[215]. Researchers have shown that luteolin activates phosphorylation of JNK, which activates the PAX2 promoter. Whether this mechanism of PAX2 activation is true in the fallopian tube epithelium, is yet to be experimentally validated.

As luteolin is already approved by the FDA, future studies will be focused on combining luteolin with standard chemotherapy to test for cytotoxicity. Since loss of PTEN and mutant *TP53* can negatively regulate the promoter in normal fallopian tube cells, experimental studies will target the PTEN and p53 pathway in combination with molecules that re-activate PAX2 to explore the anti-cancer potential of luteolin. Even though the PAX2 promoter is not methylated in cancer, it will be

interesting to combine luteolin with strategies to change the genome, such as methylation inhibitors and HDAC inhibitors. Long-term goal is to generate photo-activateable probes that crosslink with protein targets. These complexes can be pulled down with a biotin-avidin complex and subjected to proteomics analysis to identify targets in the cell. Robust preclinical investigation is necessary to determine the exact mechanism of luteolin induced PAX2 expression and its anti-tumor effects in high-grade serous cancer.

D. Targeted Delivery

The lack of effective prevention options and the frequent chemoresistance of tumors have contributed to the high rate of mortality for women with serous ovarian cancer. Our research aimed at designing, synthesizing and biologically validating a novel dendron-based nanocarrier system that will potentially provide both prevention and treatment for ovarian cancer. We demonstrated that the targeted nanocarrier killed only the cells that expressed a specific receptor, often overexpressed in serous cancer, while sparing the other cells of the "off-target" effects. Continued investigation is warranted to determine whether the nanocarrier can effectively encapsulate chemotherapeutic drugs and specifically target the cancer cells while sparing the healthy cells. Experimental studies are required to determine if cancer cells become resistant to the nanocarrier as they do to the standard chemotherapeutic agents that are currently being used in the clinic. Our study showed accumulation of the nanocarrier in the ovary and oviduct as opposed to other organs re-enforcing the targeted nature of this delivery system. Our *in vitro* and 3D organ culture experiments involved the ovary but not the FTE. In light of recent evidence that most serous cancers originate from the FTE, it will be valuable

in determining whether the nanocarrier can effectively target the fallopian tube cells. If so, the existing polymer nanocarrier presents us with a novel system where modifications can be introduced to improve the targeting efficiency, especially as it becomes clear what genetic players are frequently altered in serous cancer compared to normal FTE cells.

Interestingly, a recent report encapsulated luteolin in a dendrimer-based polymer nanocarrier system to circumvent the problem of poor solubility and bioavailability of this naturally occurring flavone[216]. The nano-luteolin demonstrated superior *in vivo* anti-tumor activity in a lung cancer and squamous cell carcinoma head and neck cancer xenograft model compared to pure luteolin. Long-term goal is to encapsulate luteolin in the FSHR-targeted nanocarrier system to determine whether the polymer complex has better targeting and anti-cancer activity compared to pure luteolin in an ovarian cancer xenograft model. The dendrimer complex has the potential to act as a therapeutic agent by specifically targeting cancer cells, which presents a unique system to re-activate PAX2 in cancer cells.

High-grade serous cancer is a complex and deadly disease, with significant cellular and molecular diversity. There is a large unmet need to discover the key players involved in serous tumor initiation and progression. Tremendous amount of efforts are focused on improving the rate of diagnosis, reducing incidence and increasing the overall survival. Each of our findings contributes by advancing our knowledge about the pathogenesis of this deadly disease. Currently, the key focus areas of the research community includes developing efficient animal models, identifying key players in precursor lesion development, exploiting immune responses and interactions with the microenvironment, understanding clonal diversity, utilizing known genetic information and applying it to stratify clinical trials of

serous cancer subsets. Therefore, it is important to strategically prioritize experimental approaches for improving outcomes in HGSC.

APPENDICES

APPENDIX A: Insulin and Insulin-Like Growth Factor Signaling Increases Proliferation and Hyperplasia of the Ovarian Surface Epithelium and Decreases Follicular Integrity Through Upregulation of the PI3-Kinase Pathway

APPENDIX B: Copyright permission to reprint material from published manuscripts

APPENDIX C: Animal protocol approval letter

APPENDIX A

INSULIN AND INSULIN-LIKE GROWTH FACTOR SIGNALING INCREASES PROLIFERATION AND HYPERPLASIA OF THE OVARIAN SURFACE EPITHELIUM AND DECREASES FOLLICULAR INTEGRITY THROUGH UPREGULATION OF THE PI3-KINASE PATHWAY

(Reprinted with permission from *J Ovarian Res, 6*(1), 12, doi:10.1186/1757-2215-6-12)

A. INTRODUCTION

The ovarian surface epithelium (OSE) is a single layer of squamous-to-cuboidal cells surrounding the ovary that exhibits both epithelial and mesenchymal characteristics[217]. During monthly ovulations, the primary function of the OSE is to remodel the ovarian surface and underlying extracellular matrix to allow for rupture of a mature follicle. Following oocyte extrusion, the OSE proliferates to heal the wound in the surface of the ovary[13]. OSE have receptors for steroid hormones and growth factors, both of which are found in abundance in follicular fluid released during ovulation[218]. In particular, the OSE has been shown to express insulin receptor (IR) and insulin-like growth factor receptors (IGF1Rs); additionally, at high concentrations insulin can signal through IGF1R or through hybrid receptors of IR and IGF1R[219, 220]. Activation of IR or IGF1R by ligand binding activates downstream signaling pathways including the phosphatidylinositiol 3-kinase (PI3K) and mitogen-activated protein kinase (MAPK) pathways. In turn, proliferative and anti-apoptotic pathways are activated, including Akt, glycogen synthase kinase 3 β (GSK3β), Bcl2, and Bad[221].

In immortalized OSE cell lines and many primary cell cultures, insulin is a critical component of the culture medium required for propagation of the cells; however, the ovary is not a classically insulin-responsive tissue[222, 223]. Crosstalk can occur between IR and IGF1R signaling when high concentrations of insulin initiate signaling through IGF1R[224]. Interestingly, IGF-I is secreted into follicular fluid by granulosa cells, providing a local source for this cytokine[225]. While it is known that insulin and IGF are proliferative in immortalized OSE cell lines[217], it is unknown whether these growth factors may exhibit additional changes in cell growth when the ovary is cultured in three dimensions (3D). By growing normal OSE as a component of ovarian organoids cultured within alginate hydrogels[95, 206], the effects of insulin and IGF on tissue architecture can be determined. The use of alginate hydrogels for organ culture permits growth of tissues in their normal three-dimensional architecture without disruption of signaling pathways downstream of extracellular matrix, as can be observed with other culture materials such as Matrigel[226].

In America, 64% of adult women are considered obese, and this negatively influences reproductive health and fertility[227]. High circulating levels of insulin and IGFs are associated with obesity and diabetes; in the female reproductive system, increased levels of these growth factors are associated with polycystic ovary syndrome (PCOS) and ovarian cancer[31]. For example, PCOS is a leading cause of infertility that affects 5-10% of reproductive-aged women and is diagnosed when patients exhibit at least two of the three following symptoms: anovulation, hyperinsulinemia, and hyperandrogenism[228]. Ovarian cancer is the deadliest gynecological malignancy affecting American women, and obesity and diabetes are associated with a worse prognosis due in part to the effects of elevated levels of

insulin and IGF on cancer cells[229, 230]. Primary cell lines established from ovarian carcinomas demonstrate that the components of the IGF pathway are present in ovarian cancer, including secreted IGF-I and IGF-II, IGFR-I and IGFR-II, and IGFBPs[231, 232]. IGF-II is overexpressed in ovarian cancer cells compared to normal OSE[233]. IGF signaling exerts a pro-proliferative, anti-apoptotic effect on ovarian cancer cells and has also been shown to play a role in mediating cisplatin resistance[234, 235].

The current study examines the effects of high insulin and IGF levels on the OSE and ovarian follicles using an alginate hydrogel culture system. High proliferation rates in the OSE following culture with insulin or IGF were observed as described in previous studies[119, 218, 236]; however, by utilizing a 3D organ culture system, the present study demonstrates that high levels of insulin and IGF induce hyperplasia and formation of multiple cell layers in the OSE. Treatment of organ cultures with the IR/IGF1R inhibitor tyrphostin AG1024 restored the OSE to a single layer of epithelium and reduced proliferation to basal rates. Both the MAPK and PI3K pathways were involved in OSE hyperplasia, as small molecule inhibitors for these pathways inhibited insulin or IGF-induced hyperplasia and proliferation. Upon further examination of ovarian organ cultures, insulin and IGF reduced proliferation of granulosa cells, decreased Müllerian inhibiting substance (MIS) expression, and altered collagen deposition, which were restored upon blockage of IR/IGF1R function with tyrphostin AG1024. In summary, this study highlights the use of a 3D tissue culture system in demonstrating the differential effects that insulin and IGF signaling have on the ovarian surface and follicles.

B. RESULTS

Insulin and IGF-I induce OSE hyperplasia and multilayering

Culture of ovarian organoids in alginate hydrogels permits analysis of normal OSE growth in the context of its normal microenvironment without the requirement for immortalization with viral antigens[95]. To analyze the effects of specific growth factors on different cell types in the tissue, the culture medium can be supplemented with growth factors, cytokines, steroid hormones, or other factors which are able to diffuse freely across the alginate gel[237]. Organoids were cultured for 7d in basal medium (no serum or growth factors) or medium supplemented with 5 μg/ml insulin or IGF-I, a concentration which was functionally active for both insulin and IGF-1 **(Fig. 34A, 34B)** and which is comparable to insulin supplementation in standard cell culture media. Morphology of the OSE was analyzed by hematoxylin and eosin (H&E) staining or immunohistochemistry for cytokeratin 8 (CK8). To measure proliferation, 5-bromodeoxyuridine (BrdU) was added to the cultures 24h prior to fixation. Organoids cultured in basal medium exhibited a single layer of squamous OSE with few proliferating OSE **(Fig. 33A)**. Inclusion of insulin **(Fig. 33B)** or IGF-I **(Fig. 33C)** in the culture medium resulted in formation of a hyperplastic layer of OSE, approximately 4-6 cell layers thick around the outer surface of the ovary. Primordial and primary follicles were frequently observed trapped within this layer of OSE **(Fig. 33B, 33C, arrow)**.

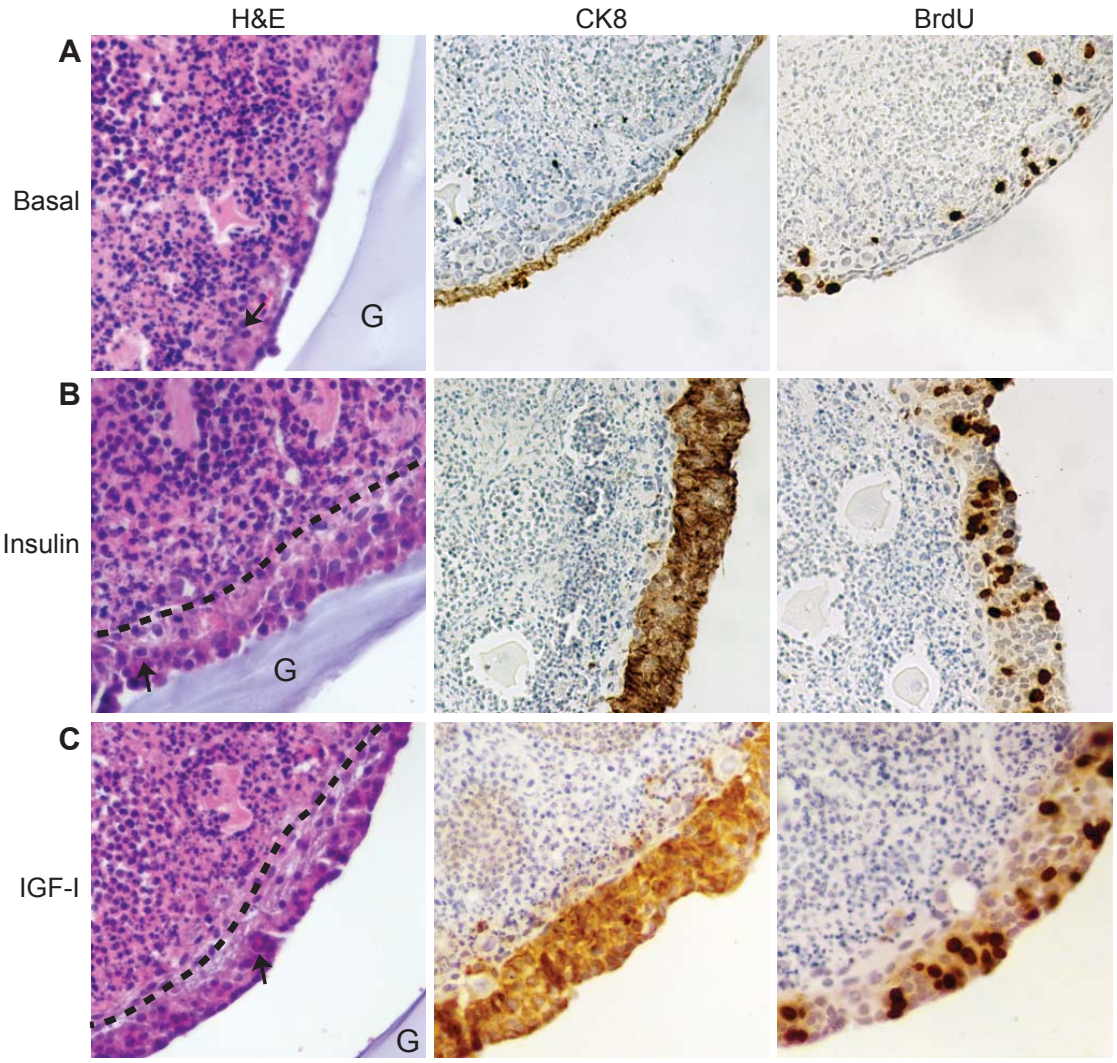

Figure 33: Insulin and IGF-I induce OSE hyperplasia and proliferation. Ovarian organoids were cultured in alginate hydrogels in basal media **(A)** or media supplemented with 5 µg/ml insulin **(B)** or IGF-I for 7d **(C)**. BrdU was added 24h prior to fixation to label dividing cells. Tissues were stained with hematoxylin and eosin (H&E) to evaluate morphology. Arrow indicates primordial follicle. Dashed line is representative of the field of OSE expansion. Alginate hydrogel stains lightly with hematoxylin and is marked by G. Serial sections were stained with antibodies against cytokeratin 8 (CK8) to mark OSE or antibodies against BrdU to mark dividing cells. All images are 400X.

Insulin and IGF-I induce OSE proliferation in a dose- and time-dependent manner

To quantify the proliferative effects of insulin and IGF and determine the relative potency of each ligand in the OSE, organoids were cultured for 7d with increasing concentrations of insulin **(Fig. 34A)** or IGF-I **(Fig. 34B)**. BrdU was added 24h prior to fixation, and serial sections stained for CK8 and BrdU were analyzed to determine the percentage of proliferating OSE (labeled with BrdU and CK8) relative to the total number of OSE (labeled only with CK8). By d7 of culture, only about 8% of OSE cultured in basal medium were proliferating. Addition of 5 μg/ml insulin or 1 μg/ml IGF-I to the culture medium increased the percentage of proliferating OSE to approximately 41% or 47% respectively, demonstrating that a higher dose of insulin was required to achieve the same proliferative effects of IGF-I. Unless otherwise noted, experiments were completed using the 5 μg/ml dose to reflect commonly used media supplements and the dose that significantly increased proliferation for both insulin and IGF-I.

The percentage of proliferating OSE was highest at d1 for all treatment groups, with 44% of OSE from organoids cultured in basal media exhibiting proliferation as measured by BrdU incorporation following a 24h label **(Fig. 34C)**. Addition of insulin to the media increased this percentage to 74%, and IGF-I increased the percent of proliferating OSE to 83%. The percent of proliferating OSE declined over 14d in culture, but at d3 and d7, OSE cultured with insulin or IGF exhibited increased percentages of proliferating OSE as compared to OSE cultured in basal media. By d14, 34% of OSE cultured with insulin were still proliferating, compared to 8% of OSE cultured with IGF and 6% of OSE cultured in basal medium **(Fig. 34C)**.

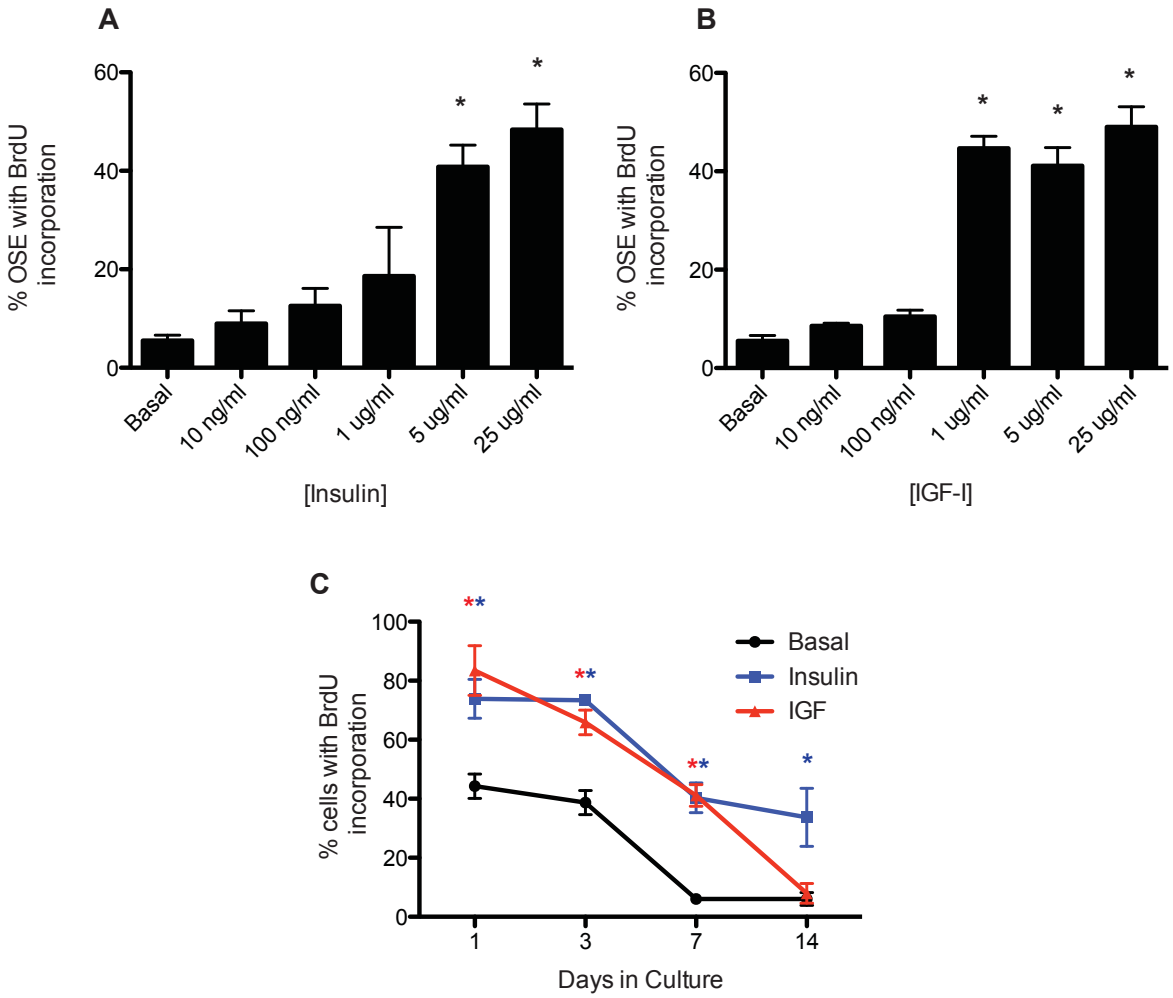

Figure 34: Insulin and IGF-I increase OSE proliferation in a dose- and time-dependent manner. Ovarian organoids were cultured for 7d with increasing concentrations of insulin **(A)** or IGF-I **(B)** and analyzed for CK8 and BrdU expression. The percentage of OSE with BrdU incorporation was determined by dividing the number of cells positive for CK8 and BrdU by the total number of CK8-positive cells. **C**, Organoids were cultured for 1, 3, 7, or 14d in basal media (black line), media with 5 µg/ml insulin (blue line), or 5 µg/ml IGF-I (red line) and assessed for the percentage of OSE with BrdU incorporation as described above. All images are 400X. Data shown represent SEM. * indicates $P<0.05$.

APPENDIX A (continued)

Inhibition of IR/IGF1R function restores OSE morphology

To validate that signaling through IR or IGF1R mediated OSE hyperplasia and proliferation, the receptor tyrosine kinase inhibitor tyrphostin AG1024, which is a small molecule inhibitor of IR and IGF1R phosphorylation, was incubated with the organ cultures[238]. Culture of ovarian organoids with 10 μM AG1024 alone resulted in a single layer of OSE with 6% of OSE proliferating, which was not statistically different from organoids cultured in basal medium **(Fig. 35A, 35B)**. Addition of AG1024 to media containing 5 μg/ml insulin or IGF-I reduced OSE hyperplasia to a single layer of cells as determined by CK8 staining, which marks the OSE **(Fig. 35A)**. AG1024 also reduced insulin-mediated or IGF-mediated proliferation to 4% or 3% respectively **(Fig. 35B)**, indicating that the increased proliferation of OSE following culture with insulin or IGF was due to signaling through IR and IGF1R.

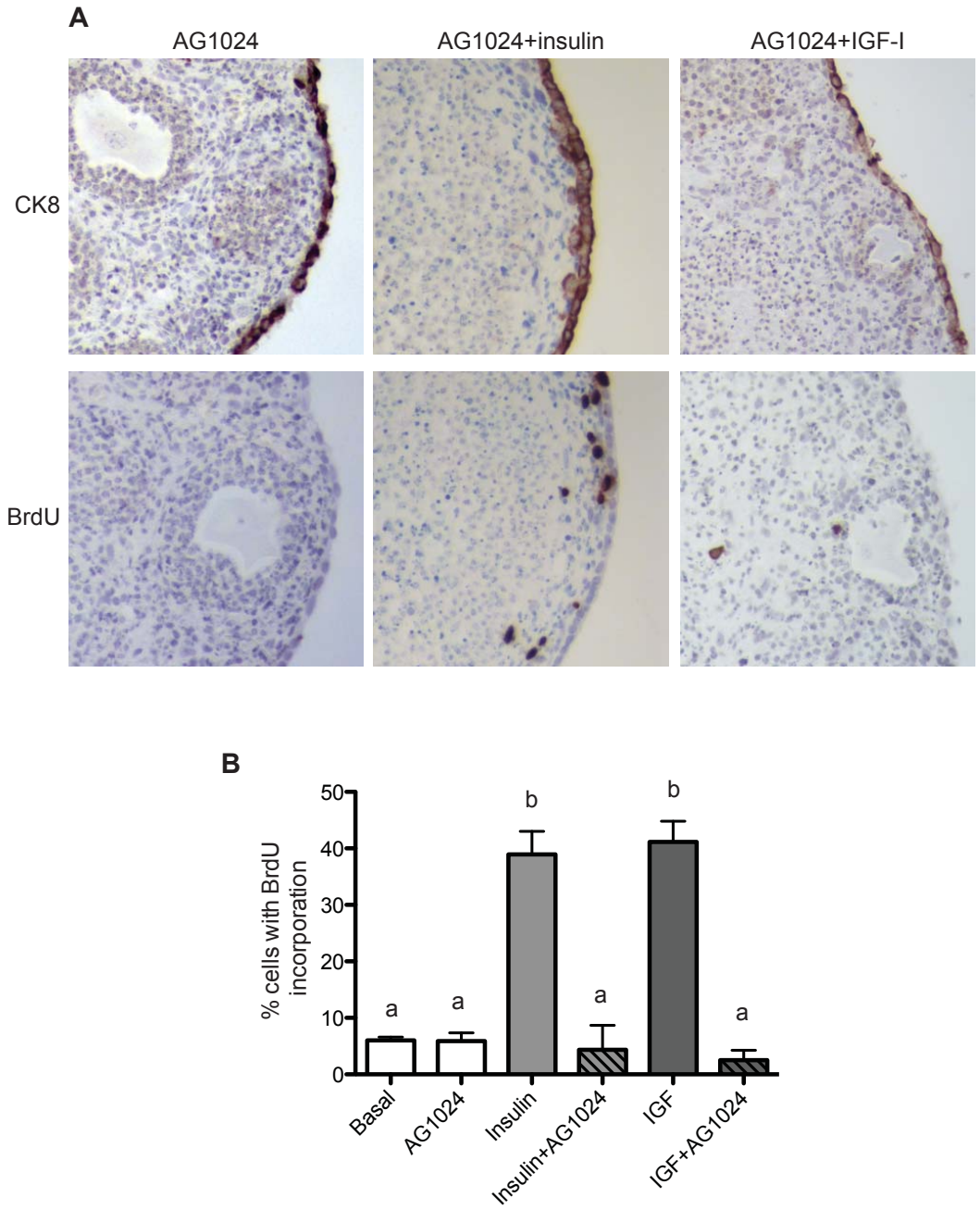

Figure 35: Inhibition of IR/IGF1R function restores OSE morphology. Ovarian organoids were cultured 7d with 10 μM AG1024, 10 μM AG1024 plus 5 μg/ml insulin, or 10 μM AG1024 plus 5 μg/ml IGF-I. Tissues were stained with antibodies against CK8 and BrdU **(A)** and the percentage of proliferating OSE was quantified **(B)** All images are 400X. Data shown represent SEM. Statistical differences ($P<0.05$) are between groups labeled a and b.

APPENDIX A (continued)

Transcription changes in the OSE in response to insulin or IGF

Few studies have investigated the transcriptional targets downstream of IR/IGF1R signaling in normal OSE. To evaluate changes in gene expression in the OSE following culture with insulin or IGF-I, OSE were collected from organoids after 3d in culture to maximize the possibility of monitoring gene changes occurring as the OSE were undergoing high rates of proliferation and cell growth. Insulin increased expression of insulin-receptor associated proteins, including insulin-like 1 (Insl1; 2.31-fold increase relative to basal) and insulin-like 3 (Insl3; 4.38-fold increase) **(Table V)**. As evidence of a negative feedback loop, insulin repressed expression of Igfr1 (-2.00) and Igf2 (-2.37). IGF also increased expression of insulin-receptor associated proteins, with a 2.73-fold increase in growth factor receptor-bound protein 10 (Grb10) and a 4.01-fold decrease in Igf2 expression **(Table V)**. As expected, insulin and IGF both regulated genes involved in metabolism, including an increase in low-density lipoprotein receptor (LDLR: 2.67-fold increase for insulin and 3.81-fold increase for IGF) **(Table V)**. Gene expression changes downstream of the mitogenic PI3K and MAPK pathways were also evaluated. At the level of transcriptional changes, insulin and IGF repressed subunits of PI3K as well as Akt1 and Akt2 **(Table V)**. Overall, components of the Ras/Raf pathway downstream of MAPK/Erk were repressed as well by insulin and IGF **(Table V)**; however, this likely represents negative feedback regulation of the pathway and is not reflective of activated phosphorylated proteins in the signaling cascade.

APPENDIX A (continued)

TABLE V
CHANGES IN GENE EXPRESSION IN THE OSE INDUCED BY 5 MG/ML INSULIN OR 5 MG/ML IGF-I

Gene symbol	Insulin	IGF
Insulin-Receptor associated proteins		
Dok1	−1.24	−4.22
Dok2	−2.17	−1.13
Dok3	−1.79	−14.41
Eif4ebp1	1.63	2.21
Gab1	−1.17	−2.71
Grb10	1.44	2.73
Igf1r	−2.00	−2.08
Igf2	−2.37	−4.01
Igfbp1	1.01	−2.13
Insl1	2.31	1.18
Insl3	4.38	−2.89
Irs2	−1.73	−7.06
Nck1	−1.41	−2.15
Ppp1ca	−1.18	−2.83
Ptpn1	−1.05	−3.25
PI3K Pathway		
Akt1	−1.26	−4.65
Akt2	−1.16	−3.19
Dusp14	−1.93	−3.11
G6pc	2.31	1.18
Hk2	1.75	2.38
Mtor	−1.38	−3.62
Pik3ca	−1.21	−2.66
Pik3r1	−1.49	−3.16
Pik3r2	−1.16	−3.23
Serpine1	3.02	2.66
Ucp1	2.31	1.18
MAPK Pathway		
Braf	−1.24	−3.76
Fos	−1.22	2.36
Hras1	−1.04	−2.26
Kras	−1.85	3.09
Nos2	−2.11	−21.53
Rps6ka1	−1.55	−4.44
Rras	2.07	2.65
Rras2	−1.58	2.55
Sos1	−1.09	2.80
Metabolism		
Cebpa	1.25	−5.08
Cebpb	1.21	2.48
Fbp1	−2.08	1.10
Gpd1	−1.03	−6.32
Gsk3b	1.19	2.59
Ldlr	2.67	3.81
Lep	2.14	1.09
Pparg	1.26	2.25
Slc27a4	−1.14	−4.55
Other Pathways		
Cfd	1.02	3.10
Retn	1.14	−20.16
Npy	−1.52	−2.98

Organoids were cultured for 3d in basal media or supplemented with insulin or IGF. RNA was isolated from collected OSE and reverse transcribed for analysis by cDNA transcription array. Data shown represent fold changes relative to insulin (n=2) after normalization to housekeeping genes.

IGF-I increases pGSK3β signaling in the OSE

To validate that changes in PI3K or MAPK signaling occurred along with proliferative changes in the OSE, organ cultures treated with insulin or IGF-I were assessed for phospho-glycogen synthase kinase 3 beta (pGSK3β) and total GSK3β expression by immunohistochemistry. Akt activation induces phosphorylation of GSK3β at serine 9, leading to inhibition of the kinase function of the protein, progression through the cell cycle, and inhibition of apoptotic pathways[239]. From gene expression data, IGF-I induced a 2.59-fold increase in Gsk3b, while insulin induced a 1.19-fold change in Gsk3b **(Table V)**. Expression of pGSK3β(Ser9) was increased in the OSE of organ cultures treated with IGF-I relative to basal cultures, in agreement with the gene expression data **(Fig. 36A)**. This increase in pGSK3βwas redistributed with the AG1024 IR/IGF1R inhibitor into a punctate diffuse pattern; additionally, AG1024 reduced expression of total GSK3β **(Fig. 36A, 36B)**.

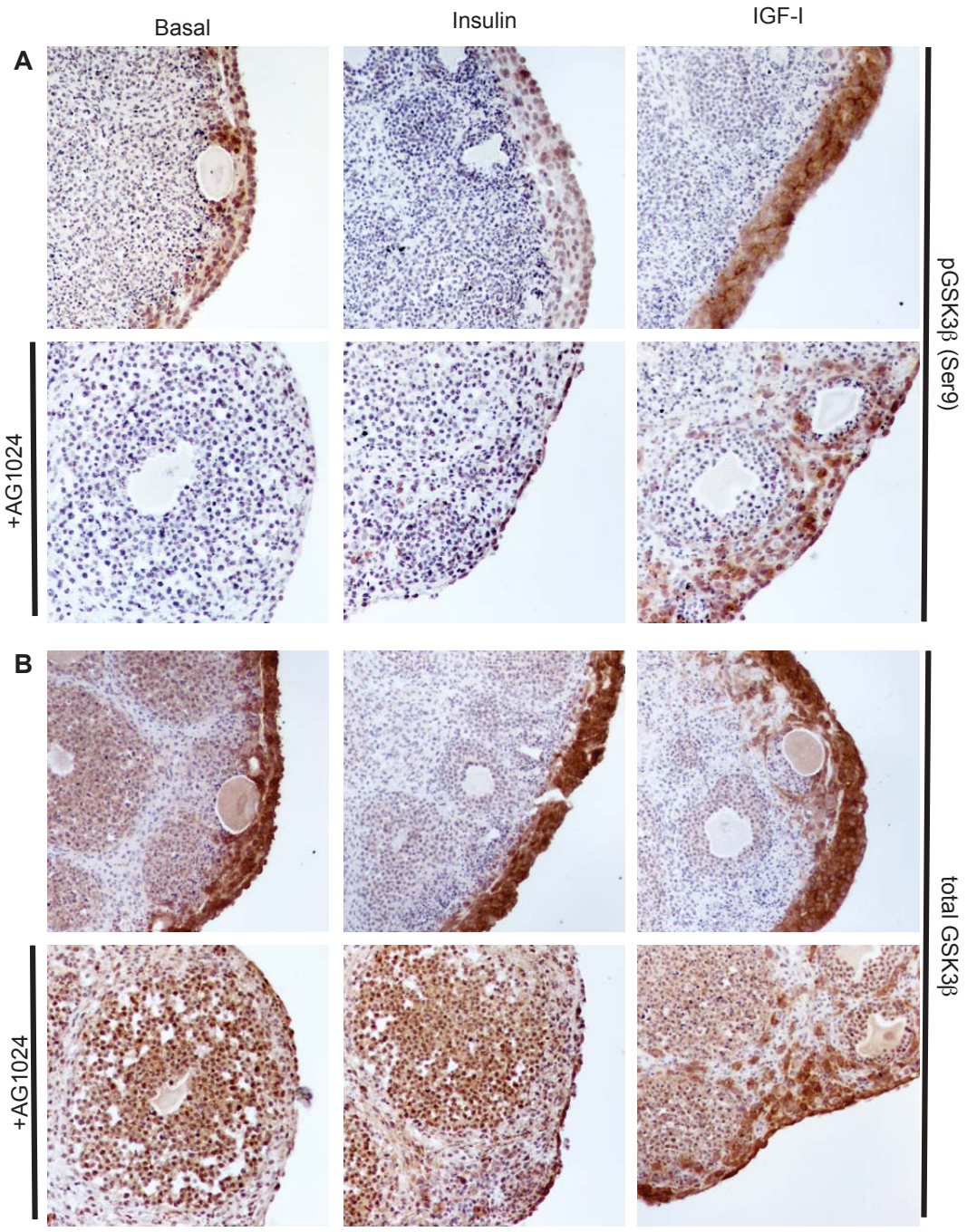

Figure 36: IGF-I increases pGSK3β signaling in the OSE. Organoids were cultured 7d in basal media or media containing 5 μg/ml insulin or IGF-I, with or without the addition of 10 μM AG1024. Tissues were stained for expression of GSK3β phosphorylated at Ser9 **(A)** or total GSK3β protein **(B)** All images are 400X.

Inhibition of MAPK/Erk signaling reduces insulin-induced OSE hyperplasia

Activation of the MAPK pathway is known to occur downstream of IR/IGF1R signaling, leading to increased transcription and cell proliferation[223]. Components of the MAPK pathway were regulated by insulin and IGF in the OSE by transcription array **(Table V)**. To determine if this signaling pathway was involved in OSE hyperplasia and proliferation, ovarian organoids were cultured with the MEK1/2 inhibitor UO126. When organoids were cultured with UO126 alone, a single layer of OSE was observed with 8% of OSE proliferating, which was similar to organoids cultured in basal media **(Fig. 37A, 37B)**. To determine if inhibition of MAPK signaling by UO126 could reduce the OSE hyperplasia and proliferation induced by insulin, organoids were cultured with both UO126 and insulin. A single layer of OSE was observed, with 13% of OSE proliferating, which was not significantly different from basal rates **(Fig. 37B)**. However, organoids cultured with UO126 and IGF-I exhibited several layers of OSE, although the thickness of the OSE was reduced as compared to that induced by IGF-I alone **(Fig. 37A, 33C)**. Addition of UO126 to the culture media reduced the percentage of proliferating OSE to 7%, as compared to 41% for IGF-I alone **(Fig. 37B)**.

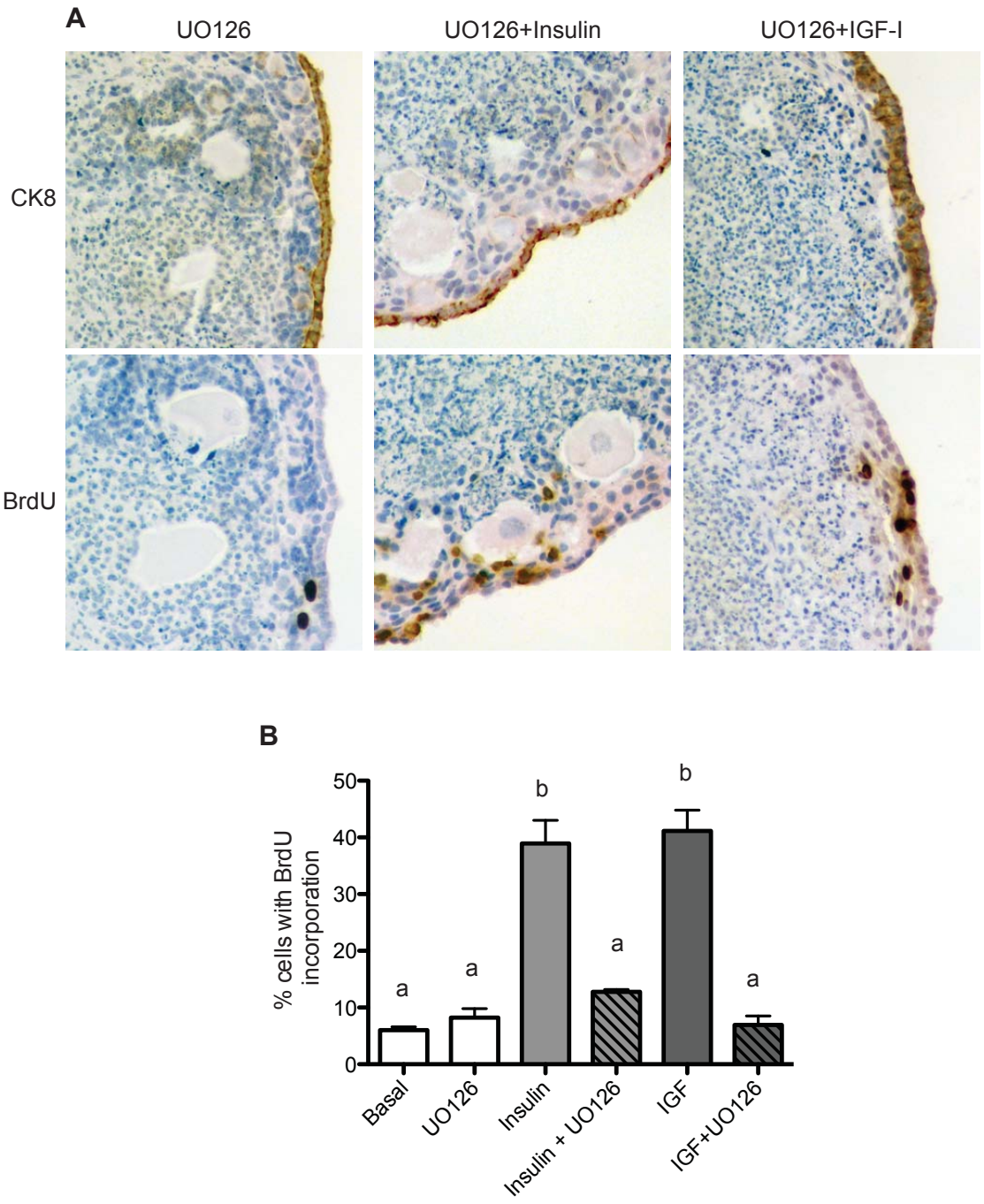

Figure 37: Inhibition of MAPK/Erk signaling reduces insulin-induced OSE hyperplasia. Organoids were cultured 7d in media containing the MEK1/2 inhibitor 10 μM UO126, 10 μM UO126 plus 5 μg/ml insulin, or 10 μM UO126 plus 5 μg/ml IGF-I. Tissues were stained for expression of CK8 and BrdU **(A)** and the percentage of proliferating OSE was quantified **(B)** All images are 400X. Data shown represent SEM. Statistical differences ($P<0.05$) are between groups labeled a and b.

Insulin- and IGF-induced OSE hyperplasia and proliferation requires PI3K signaling

Another pathway downstream of IR/IGF1R is the PI3K pathway, which plays a role in cell proliferation, regulation of apoptosis, and directional cell growth[223]. Activation of the PI3K pathway alters orientation of the cytoskeleton through the Rho/Rac/Cdc42 GTPases, as well as affecting other components required for cell polarity and migration[240]. Targets of the PI3K pathway were altered in response to insulin and IGF **(Table V)** and the OSE exhibited altered morphology, hyperplasia, and multilayering in response to insulin and IGF, indicating that activation of the PI3K pathway may be involved in this phenotype. Organoids cultured with 10 μM LY294002, a PI3K inhibitor, exhibited a single layer of OSE with only 1% of OSE proliferating **(Fig. 38A, 38B)**. To determine if LY294002 could effectively block insulin- or IGF-induced hyperplasia and proliferation, organoids were cultured with LY294002 and insulin or IGF. Culture of organoids with insulin plus LY294002 or IGF-I plus LY294002 resulted in growth of a single layer of OSE **(Fig. 38A)**, unlike organoids cultured with UO126, which only completely blocked insulin-induced OSE hyperplasia **(Fig. 37A)**. LY294002 reduced insulin-induced OSE proliferation from 41% to 10%, and reduced IGF-induced OSE proliferation from 41% to 4% **(Fig. 38B)**.

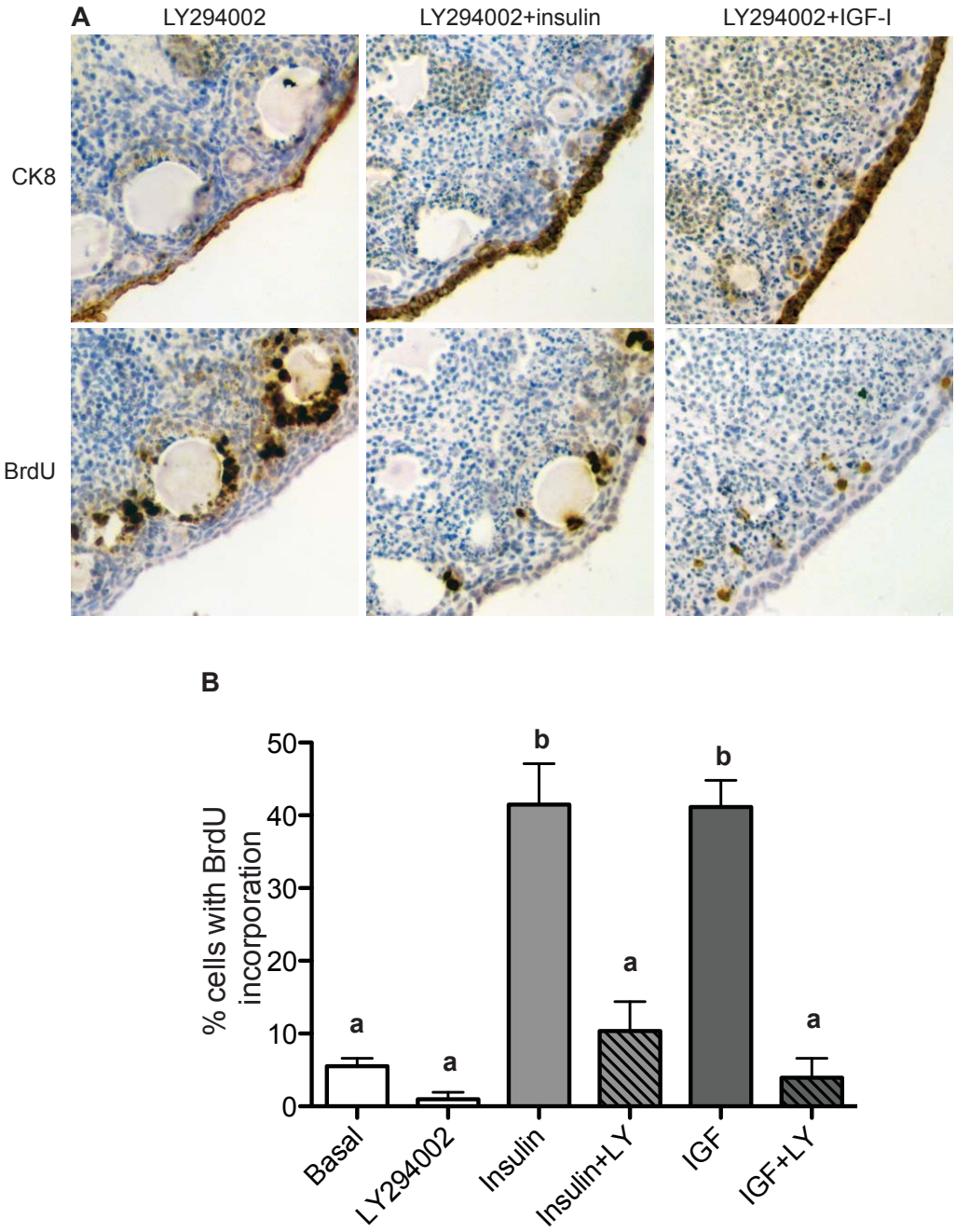

Figure 38: Insulin- and IGF-induced OSE hyperplasia and proliferation requires PI3K signaling. Organoids were cultured 7d in media containing the PI3K inhibitor 10 μM LY294002, 10 μM LY294002 plus 5 μg/ml insulin, or 10 μM LY294002 plus 5 μg/ml IGF-I. Tissues were stained for expression of CK8 and BrdU **(A)** and the percentage of proliferating OSE was quantified **(B)** All images are 400X. Data shown represent SEM. Statistical differences ($P<0.05$) are between groups labeled a and b.

High levels of insulin and IGF-I decrease secondary follicle MIS expression

In the mouse ovary, immature primordial and primary follicles are located in the cortex close to the surface of the ovary, with maturing follicles found in the medulla and perimedullary zone[241]. As follicles become activated and begin to mature into secondary and preantral follicles, granulosa cells proliferate to form multiple cell layers around the oocyte and begin to secrete Müllerian Inhibiting Substance (MIS)[241]. IGF secreted by granulosa cells is required for follicle maturation beyond the antral stage[225]; however, high levels of insulin or IGF can be detrimental to follicle development, resulting in polyovular follicles, ovarian cysts, and poor oocyte quality[242-244]. To determine if insulin or IGF affected the follicles as well as the OSE, the expression of MIS by the secondary follicles was analyzed. All organoids exhibited localization of MIS to the ovarian surface as expected, with organoids cultured with insulin or IGF exhibiting several cell layers of OSE expressing MIS, providing a second marker indicating expansion of this cell type in response to insulin and IGF signaling **(Fig. 39)**. Secondary follicles were classified morphologically based on the appearance of at least 2 layers of granulosa cells surrounding the oocyte. In basal-cultured organoids, most secondary follicles exhibited MIS expression; however, addition of insulin or IGF to the culture media resulted in reduced expression of MIS in secondary follicles, which could be rescued by addition of tyrphostin AG1024 to the media to block IR and IGF1R signaling **(Fig. 39)**. Inhibitors of the MAPK and PI3K pathway did not equivalently restore MIS expression following treatment with insulin or IGF-I, as culture of organoids with UO126 restored MIS expression when organoids were cultured with insulin, but LY294002 restored expression of MIS when organoids were cultured with IGF-I.

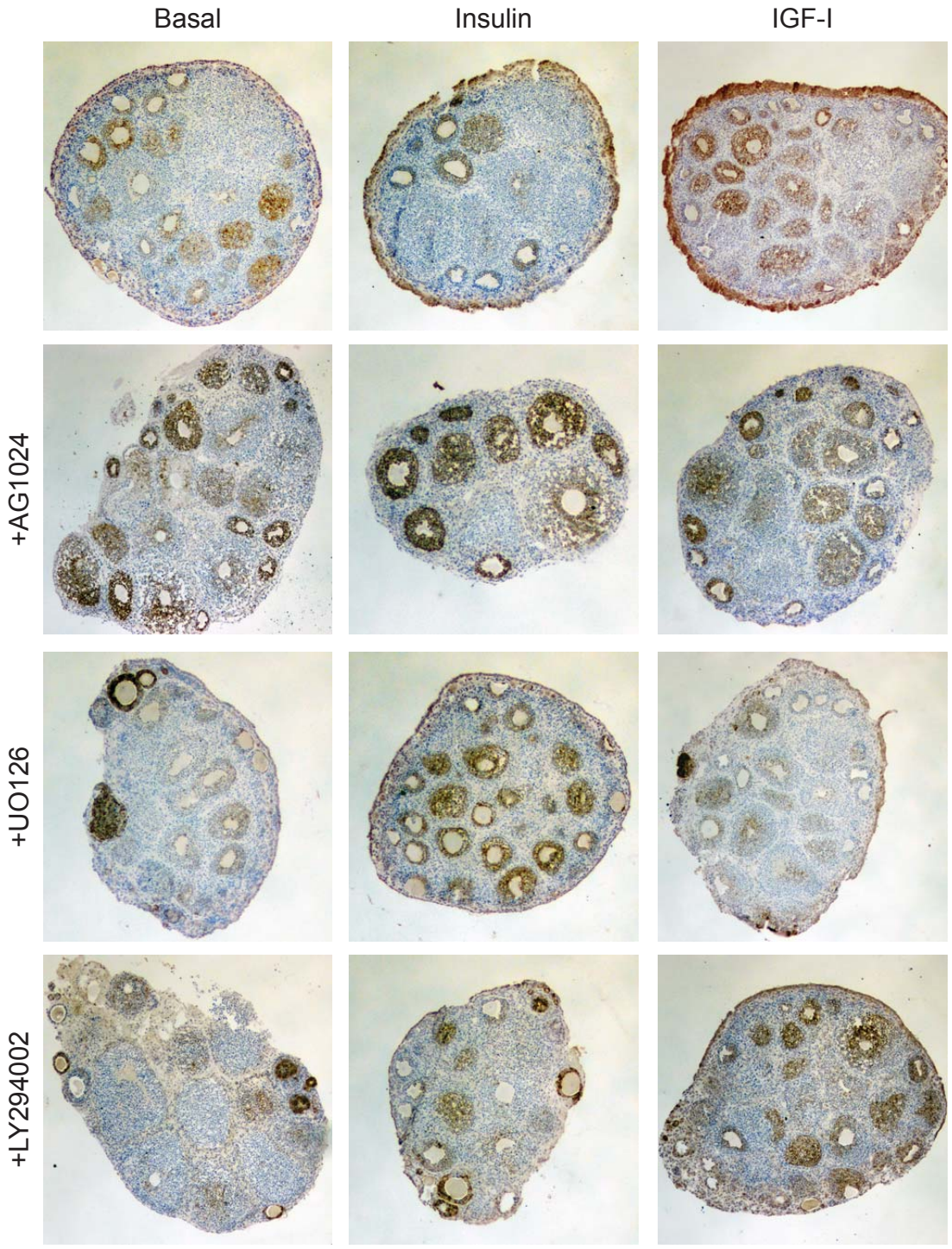

Figure 39: High levels of insulin and IGF-I decrease secondary follicle MIS expression. Organoids were cultured for 7d in the indicated media. Tissues were stained for expression of MIS. All images are 100X.

APPENDIX A (continued)

Culture of organoids with insulin or IGF-I disorders collagen-IV organization

Inclusion of high levels of insulin or IGF-I in ovarian organoid culture medium resulted in hyperplastic OSE and reduced follicle MIS expression (Figure 1 and Figure 7). Recent work suggests that the mechanical forces within the ovary may be involved in follicle maturation and ovulation[245]. Expression of extracellular matrix proteins (ECM) in the ovary has been well characterized, with collagen IV expressed abundantly in the OSE and theca cells, with very low levels in the granulosa cells and stroma[246]. To determine if culture of organoids with insulin or IGF-I resulted in altered ECM deposition or organization, organoids were analyzed for localization of collagen IV. Organoids cultured in basal medium exhibited strong expression of collagen IV in the OSE and theca, but collagen IV was also detected in the granulosa cells **(Fig. 40)**. Addition of insulin to the medium resulted in a dramatic increase in collagen IV expression in the granulosa cells, with little expression observed in the theca. Organoids cultured with IGF-I exhibited a similar expression pattern as basal-cultured organoids, with collagen IV expressed primarily in the OSE and theca, with low expression in the granulosa cells. Abrogation of IR and IGF1R signaling byAG1024 alone altered the deposition of collagen such that the follicles were surrounded with collagen and very little expression was detected in the granulosa cells which was a phenotype that resembled uncultured ovaries and was different than basal organs. The resulting phenotype from AG1024 alone suggested antagonizing endogenous IGF resulted in collagen deposition more similar to uncultured ovaries. AG1024 in combination with insulin also resulted in collagen IV expression restricted to the OSE and theca, resembling normal, uncultured ovaries[246]. However, addition of AG1024 to organoids cultured with exogenous IGF did not alter the collagen IV distribution back to resembling uncultured ovaries, suggesting that 10 μM of the inhibitor could not effectively block all the endogenous and exogenous IGF. Although inhibition of MAPK by UO126 did not rescue collagen IV localization (data not shown), inhibition of the PI3K pathway by LY294002 reduced granulosa cell expression of collagen IV to those of organoids cultured with AG1024 alone, indicating that the PI3K pathway may play a central role in altered collagen synthesis and deposition downstream of insulin and IGF signaling **(Fig. 40)**.

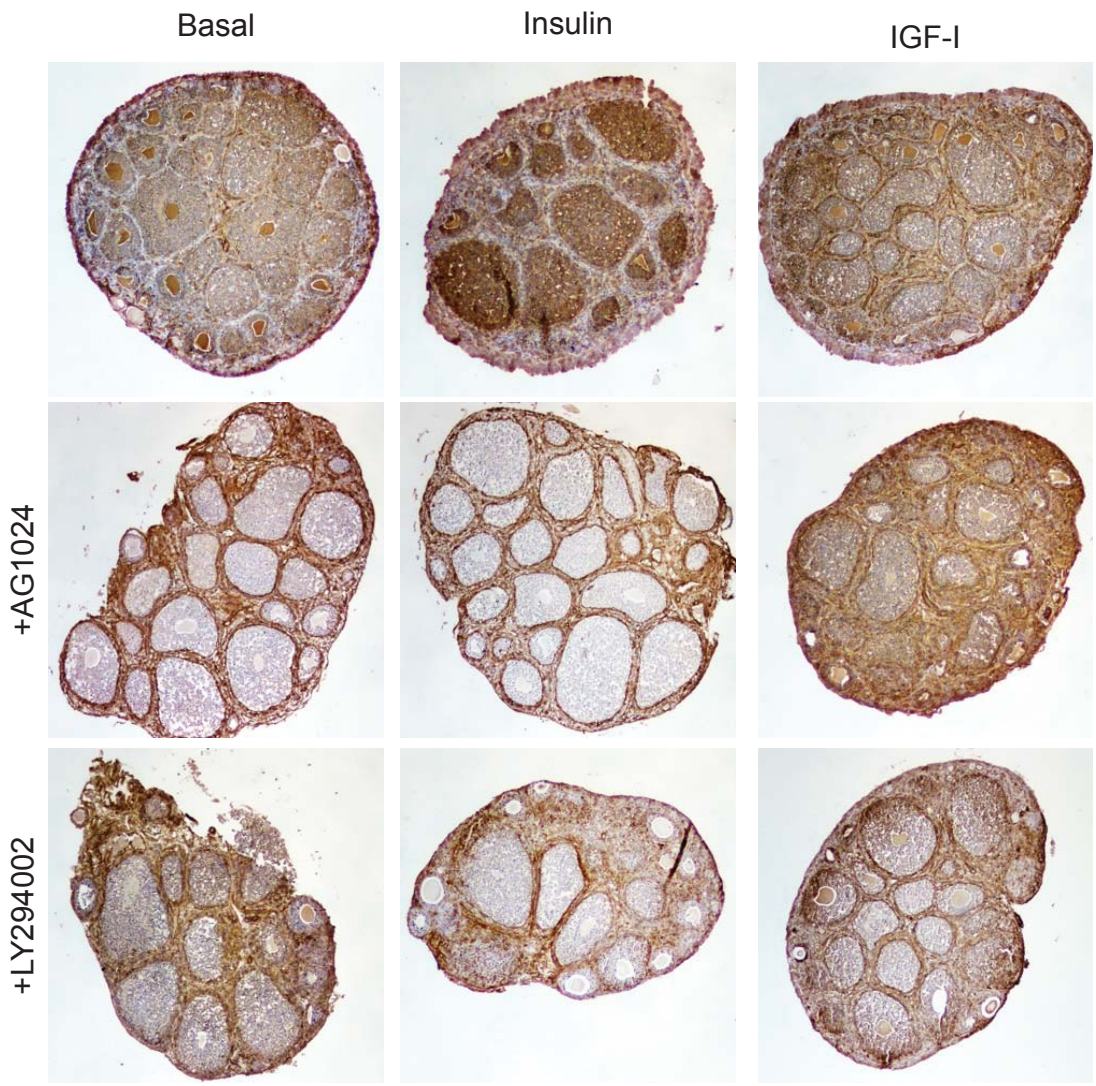

Figure 40: Culture of organoids with insulin or IGF-I disorders collagen-IV organization. Organoids were cultured for 7d in the indicated media. Tissues were stained for expression of collagen IV. All images are 100X.

C. DISCUSSION

In vitro culture of primary human or mouse OSE often requires inclusion of insulin in the media to induce proliferation[121, 222]. Although insulin and the related growth factor IGF-I have been shown to alter epithelial polarity and directional cell growth[240], little is known about how these growth factors may affect directional growth of the OSE. Normal OSE grows on the outer surface of the ovary as a single layer of squamous-to-cuboidal epithelium; however, at concentrations routinely used for culture of primary cells, insulin and IGF-I induced formation of hyperplastic OSE 4-6 cell layers thick likely due to a dramatic increase in the percentage of OSE undergoing proliferation **(Fig. 33, 34).** Importantly, the concentrations used in the present study and in typical cell culture media are higher than circulating levels or levels found in follicular fluid. Physiological concentrations in the ovary range from 0.5-10 ng/mL insulin and 100-500ng/mL IGF[247]. Previously IGF1 at 100 ng/mL was reported to increase OSE proliferation[218, 248]. The signaling pathway primarily responsible for this hyperplasia was the PI3K pathway, as inclusion of the PI3K inhibitor LY294002 restored growth of the OSE to a single cell layer **(Fig. 39)**. The PI3K pathway plays an important role in cell polarity through regulation of the actin cytoskeleton. Activation of PI3K at the plasma membrane in turn leads to activation of Akt, which plays a critical role in chemotaxis and migration of many normal as well as cancerous cell types[249]. Activation of this pathway may also repress expression of E-cadherin, a component of the epithelial cell tight junction that functions to establish and maintain cell polarity that is often altered in ovarian cancer cells to permit increased metastasis[250]. While no universally accepted precursor lesion exists for ovarian cancer originating in the OSE, menopausal ovaries and some mouse models of ovarian cancer exhibit hyperplasia of the OSE, formation of papillary structures, and inclusion cysts[251, 252]. Insulin and IGF-I did not induce transformative changes in OSE as measured by growth in soft agar (data not shown); however, it is possible that if levels of insulin and IGF accumulate enough locally in disease they might act on early stages of ovarian cancer to increase proliferation and alter cell polarity to encourage hyperplasia.

The OSE is able to secrete its own ECM, which may play a role in wound healing following ovulation[253]. In particular, OSE express collagen I and collagen IV in the basement membrane that delineates the OSE from the stroma[246]. Since insulin and IGF-I induced formation of hyperplastic OSE **(Fig. 33)**, the effects of insulin and IGF-I on collagen IV expression and localization were analyzed to determine if the hyperplasia included changes in cell polarity. Organoids cultured in basal media exhibited strong collagen expression in the OSE and theca cells as expected, with low levels observed in the granulosa cells **(Fig. 40).** However, insulin dramatically increased collagen IV expression in the granulosa cells, which may correlate with reduced expression of MIS in secondary follicles **(Fig. 39).** Inhibition of IR/IGF1R function with tyrphostin AG1024 resulted in collagen IV expression restricted to the OSE and theca as well as increased MIS expression in granulosa cells **(Fig. 39, 40)**. Studies from the Woodruff lab have demonstrated that altered cortical rigidity can disrupt folliculogenesis, as a more rigid environment favors androgen secretion and

reduced follicle growth[237, 245]. As high levels of insulin cause hyperplastic OSE and increased collagen deposition in the OSE and granulosa cells, this may possibly increase cortical tension on the ovarian follicles to restrict their growth and reduce MIS expression. The detrimental effects of high levels of insulin or IGF on follicle growth may be also be mediated directly by increased MAPK and PI3K signaling.

The MAPK and PI3K pathways are canonical signaling pathways downstream of IR and IGF1R activation[221]. Ovarian organoids cultured with inhibitors of the insulin/IGF pathway appeared to have more MIS expression in the granulosa cells indicating that the ovary has endogenous production of IGF that in *ex vivo* 3D culture is detrimental to the tissue. In the current study, inhibition of the MAPK pathway more effectively blocked insulin-induced OSE hyperplasia and follicular degeneration and was less effective at attenuating the effects of IGF-I. When the MAPK inhibitor UO126 was included along with insulin in the culture medium, the OSE grew as a single layer of cells and the secondary follicles produced MIS **(Fig. 37, 39)**. However, collagen IV expression was still detected in the granulosa cells (data not shown), indicating that additional signaling pathways may be involved in the process of altered ECM deposition in response to insulin. The PI3K inhibitor LY294002 effectively reduced OSE multilayering and proliferation induced by either insulin or IGF-I **(Fig. 38)** as well as restoring MIS expression **(Fig. 39)**. This correlated with expression of collagen IV being restricted to the OSE and theca cells similar to when organoids were cultured with the IR/IGF1R inhibitor AG1024 (**Fig. 40)**, indicating that PI3K signaling may control collagen IV synthesis or deposition in the ovary, although future work is necessary to delineate the role of each of these pathways in the OSE.

Use of an alginate hydrogel 3D culture system facilitates observation of how different cell types in the ovary interact with one another when stimulated with insulin or IGF-I. As an example, IGF-I is produced locally from the granulosa cells [225] and may be responsible for the low levels of collagen IV observed in basal-cultured organoids **(Fig. 40)** while inhibition of endogenous IGF signaling by AG1024 was able to restore collagen to the appearance of uncultured ovaries. It is unknown whether high levels of insulin and IGF directly or indirectly affect follicle health through expansion of the OSE, resulting in a restricted growth environment as all conditions that enhanced MIS expression also reduced OSE multilayering. Increased collagen deposition has been observed in the stroma of PCOS patients[254] and although PCOS is a complex syndrome involving many different tissues type, this culture system provides an interesting new model of chronic exposure to insulin and IGF that resulted in a thickened ovarian surface layer and aberrant collagen deposition that could impede follicular rupture.

D. CONCLUSIONS

In this study, an alginate hydrogel culture system was used to investigate the effects of high levels of insulin and IGF-I on normal ovarian surface epithelium. Insulin and IGF-I induced OSE proliferation and hyperplasia resulting in formation of multiple cell layers of OSE, which could be reversed by inhibition of the PI3K pathway. Granulosa cell health as assessed by MIS expression was reduced following culture of organoids with insulin or IGF-I. Inhibition of the MAPK pathway effectively restored MIS expression in organoids cultured with insulin, while inhibition of PI3K signaling restored increased MIS expression in organoids cultured with IGF-I. Therefore, the OSE responds to insulin and IGF-I by proliferating and altering the deposition of collagen, which cannot be discerned in traditional 2D systems. By culturing the ovarian surface in three-dimensions with the stroma and ovarian follicles intact, a new phenotype was discovered suggesting that high levels of insulin and IGF signaling promote hyperplasia of the ovarian surface and encourage changes in collagen deposition that impair granulosa cell function.

APPENDIX B

Permission for reprinting Chapter III

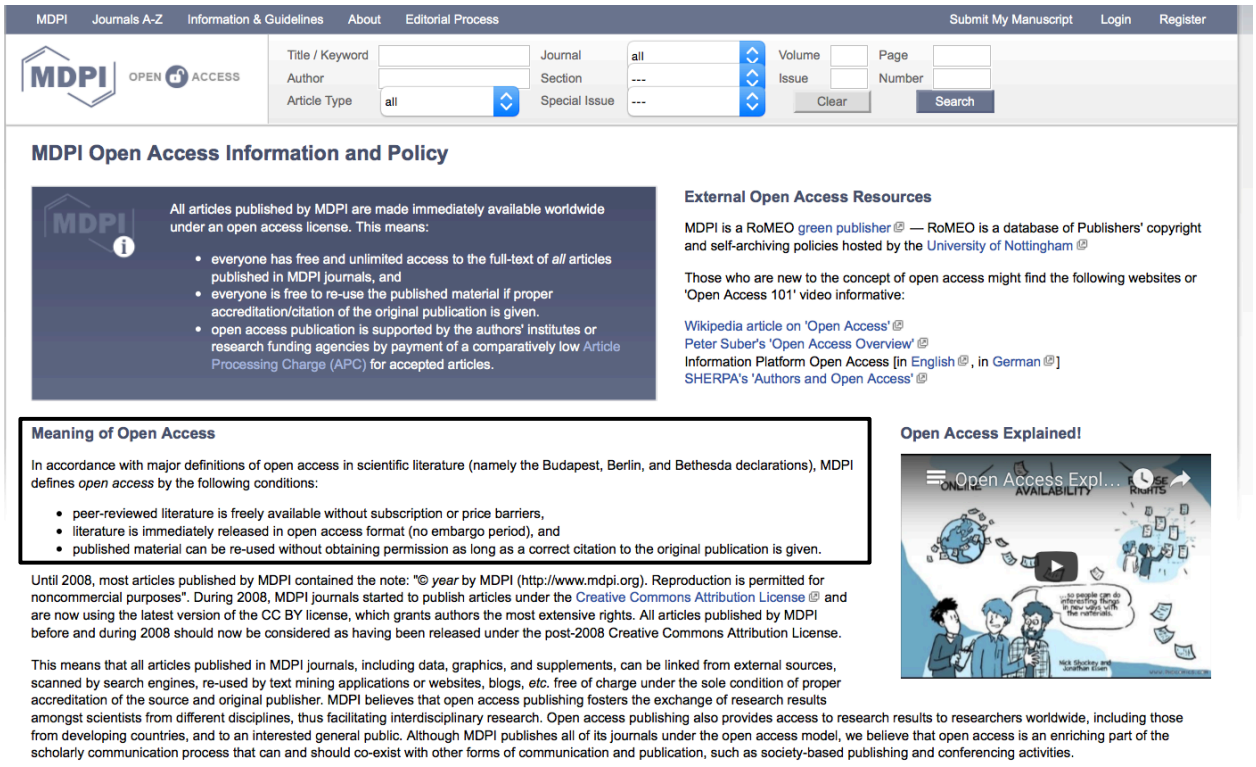

MDPI Journals A-Z Information & Guidelines About Editorial Process Submit My Manuscript Login Register

MDPI OPEN ACCESS

Title / Keyword Journal all Volume Page
Author Section --- Issue Number
Article Type all Special Issue --- Clear Search

MDPI Open Access Information and Policy

All articles published by MDPI are made immediately available worldwide under an open access license. This means:

- everyone has free and unlimited access to the full-text of *all* articles published in MDPI journals, and
- everyone is free to re-use the published material if proper accreditation/citation of the original publication is given.
- open access publication is supported by the authors' institutes or research funding agencies by payment of a comparatively low Article Processing Charge (APC) for accepted articles.

External Open Access Resources

MDPI is a RoMEO green publisher — RoMEO is a database of Publishers' copyright and self-archiving policies hosted by the University of Nottingham

Those who are new to the concept of open access might find the following websites or 'Open Access 101' video informative:

Wikipedia article on 'Open Access'
Peter Suber's 'Open Access Overview'
Information Platform Open Access [in English, in German]
SHERPA's 'Authors and Open Access'

Meaning of Open Access

In accordance with major definitions of open access in scientific literature (namely the Budapest, Berlin, and Bethesda declarations), MDPI defines *open access* by the following conditions:

- peer-reviewed literature is freely available without subscription or price barriers,
- literature is immediately released in open access format (no embargo period), and
- published material can be re-used without obtaining permission as long as a correct citation to the original publication is given.

Open Access Explained!

Until 2008, most articles published by MDPI contained the note: "© *year* by MDPI (http://www.mdpi.org). Reproduction is permitted for noncommercial purposes". During 2008, MDPI journals started to publish articles under the Creative Commons Attribution License and are now using the latest version of the CC BY license, which grants authors the most extensive rights. All articles published by MDPI before and during 2008 should now be considered as having been released under the post-2008 Creative Commons Attribution License.

This means that all articles published in MDPI journals, including data, graphics, and supplements, can be linked from external sources, scanned by search engines, re-used by text mining applications or websites, blogs, *etc.* free of charge under the sole condition of proper accreditation of the source and original publisher. MDPI believes that open access publishing fosters the exchange of research results amongst scientists from different disciplines, thus facilitating interdisciplinary research. Open access publishing also provides access to research results to researchers worldwide, including those from developing countries, and to an interested general public. Although MDPI publishes all of its journals under the open access model, we believe that open access is an enriching part of the scholarly communication process that can and should co-exist with other forms of communication and publication, such as society-based publishing and conferencing activities.

Permission for reprinting CHAPTER V

Author reusing their own work published by the Royal Society of Chemistry

You do not need to request permission to reuse your own figures, diagrams, etc, that were originally published in a Royal Society of Chemistry publication. However, permission should be requested for use of the whole article or chapter except if reusing it in a thesis. If you are including an article or book chapter published by us in your thesis please ensure that your co-authors are aware of this.

Reuse of material that was published originally by the Royal Society of Chemistry must be accompanied by the appropriate acknowledgement of the publication. The form of the acknowledgement is dependent on the journal in which it was published originally, as detailed in 'Acknowledgements'.

Material published by the Royal Society of Chemistry to be used in another of our publications

Authors contributing to our publications (journal articles, book or book chapters) do not need to formally request permission to reproduce material contained in another Royal Society of Chemistry publication. However, permission should be requested for use of a whole article or chapter. For all cases of reproduction the correct acknowledgement of the reproduced material should be given. The form of the acknowledgement is dependent on the journal in which it was published originally, as detailed in the 'Acknowledgements' section.

Dimple Modi

903 S. Ashland Avenue Apt 1018B • Chicago, IL 60607 • Phone: 925-980-7027 • dmodi2@uic.edu

Date: February 2, 2016

Shelby King, PhD
Senior Research Scientist
Organovo, Inc.
San Diego, CA 92121

I am writing to request permission to use the following material from your publication (Insulin And Insulin-Like Growth Factor Signaling Increases Proliferation and Hyperplasia of the Ovarian Surface Epithelium and Decreases Follicular Integrity Through Upregulation of the PI3-Kinase Pathway, 2013, Journal of Ovarian Research) in my thesis. This material will appear as originally published. Unless you request otherwise, I will use the conventional style of the Graduate College of the University of Illinois at Chicago as acknowledgment.

A copy of this letter is included for your records. Thank you for your kind consideration of this request.

Sincerely,

Dimple Modi
903 S. Ashland Avenue Apt 1018B,
Chicago IL 60607

The above request is approved.

Approved by: Shelby King Shelby King
Date: 2/16/16

APPENDIX C

UIC UNIVERSITY OF ILLINOIS AT CHICAGO

Office of Animal Care and
Institutional Biosafety Committees (MC 672)
Office of the Vice Chancellor for Research
206 Administrative Office Building
1737 West Polk Street
Chicago, Illinois 60612-7227

January 14, 2015

Joanna Burdette
Medicinal Chemistry & Pharmacognosy
M/C 781

Dear Dr. Burdette:

The protocol indicated below was reviewed at a convened ACC meeting in accordance with the Animal Care Policies of the University of Illinois at Chicago on **11/18/2014**. *The protocol was not initiated until final clarifications were reviewed and approved on* **1/12/2015**. *The protocol is approved for a period of* ***3*** years with annual continuation.

Title of Application: Akt Transformation of Ovarian Surface and Oviductal Cells

ACC Number: 14-180

Initial Approval Period: 1/12/2015 to 11/18/2015

Current Funding: ***Portions of this protocol are supported by the funding sources indicated in the table below.***
Number of funding sources: 1

Funding Agency	**Funding Title**			**Portion of Proposal Matched**
ACS- American Cancer Society	*AKT Transformation of Ovarian and Fallopian Cells*			*Protocol is linked to form G*
				14-181
Funding Number	**Current Status**	**UIC PAF NO.**	**Performance Site**	**Funding PI**
RSG-12-230-01-TBG	*Funded*	*201201837*	*UIC*	*Joanna Burdette*

This institution has Animal Welfare Assurance Number A3460.01 on file with the Office of Laboratory Animal Welfare (OLAW), NIH. **This letter may only be provided as proof of IACUC approval for those specific funding sources listed above in which all portions of the funding proposal are matched to this ACC protocol.**

In addition, all investigators are responsible for ensuring compliance with all federal and institutional policies and regulations related to use of animals under this protocol and the funding sources listed on this protocol. Please use OLAW's "*What Investigators Need to Know about the Use of Animals*" (http://grants.nih.gov/grants/olaw/InvestigatorsNeed2Know.pdf) as a reference guide. Thank you for complying with the Animal Care Policies and Procedures of UIC.

Phone (312) 996-1972 • Fax (312) 996-9088 • www.research.uic.edu

UIC UNIVERSITY OF ILLINOIS AT CHICAGO

Office of Animal Care and Institutional
Biosafety Committee (OACIB) (M/C 672)
Office of the Vice Chancellor for Research
206 Administrative Office Building
1737 West Polk Street
Chicago, Illinois 60612

11/18/2015

Joanna Burdette
Medicinal Chemistry & Pharmacognosy
M/C 781

Dear Dr. Burdette:

The protocol indicated below was reviewed in accordance with the Animal Care Policies and Procedures of the University of Illinois at Chicago and **renewed on 11/18/2015.**

Title of Application: **Akt Transformation of Ovarian Surface and Oviductal Cells**
ACC NO: **14-180**
Original Protocol Approval: **1/12/2015 (3 year approval with annual continuation required).**
Current Approval Period: **11/18/2015 to 11/18/2016**

Funding: ***Portions of this protocol are supported by the funding sources indicated in the table below.***
Number of funding sources: 1

Funding Agency	**Funding Title**			**Portion of Funding Matched**
ACS- American Cancer Society	*AKT Transformation of Ovarian and Fallopian Cells*			*Protocol is linked to form G 14-181*
Funding Number	**Current Status**	**UIC PAF NO.**	**Performance Site**	**Funding PI**
RSG-12-230-01-TBG	*Funded*	*2012-01837*	*UIC*	*Joanna Burdette*

This institution has Animal Welfare Assurance Number A3460.01 on file with the Office of Laboratory Animal Welfare, NIH. **This letter may only be provided as proof of IACUC approval for those specific funding sources listed above in which all portions of the grant are matched to this ACC protocol.**

Thank you for complying with the Animal Care Policies and Procedures of the UIC.

Sincerely,

John P. O'Bryan, PhD
Chair, Animal Care Committee
JPO/*kg*
cc: BRL, ACC File, Daniel Lantvit

Phone (312) 996-1972 • Fax (312) 996-9088

CITED LITERATURE

1. Siegel RL, Miller KD, Jemal A. Cancer statistics, 2016. CA Cancer J Clin. 2016;66: 7-30.
2. Society AC. Cancer Facts & Figures 2015. Atlanta: American Cancer Society. 2015.
3. Siegel RL, Miller KD, Jemal A. Cancer statistics, 2015. CA Cancer J Clin. 2015;65: 5-29.
4. Romero I, Bast RC, Jr. Minireview: human ovarian cancer: biology, current management, and paths to personalizing therapy. Endocrinology. 2012;153: 1593-1602.
5. Kurman RJ, Shih Ie M. Molecular pathogenesis and extraovarian origin of epithelial ovarian cancer--shifting the paradigm. Hum Pathol. 2011;42: 918-931.
6. Alsop K, Fereday S, Meldrum C, et al. BRCA mutation frequency and patterns of treatment response in BRCA mutation-positive women with ovarian cancer: a report from the Australian Ovarian Cancer Study Group. J Clin Oncol. 2012;30: 2654-2663.
7. Hennessy BT, Timms KM, Carey MS, et al. Somatic mutations in BRCA1 and BRCA2 could expand the number of patients that benefit from poly (ADP ribose) polymerase inhibitors in ovarian cancer. J Clin Oncol. 2010;28: 3570-3576.
8. Risch HA, McLaughlin JR, Cole DE, et al. Prevalence and penetrance of germline BRCA1 and BRCA2 mutations in a population series of 649 women with ovarian cancer. Am J Hum Genet. 2001;68: 700-710.
9. Bowtell DD. The genesis and evolution of high-grade serous ovarian cancer. Nat Rev Cancer. 2010;10: 803-808.
10. Risch HA, McLaughlin JR, Cole DE, et al. Population BRCA1 and BRCA2 mutation frequencies and cancer penetrances: a kin-cohort study in Ontario, Canada. J Natl Cancer Inst. 2006;98: 1694-1706.
11. Roa BB, Boyd AA, Volcik K, Richards CS. Ashkenazi Jewish population frequencies for common mutations in BRCA1 and BRCA2. Nat Genet. 1996;14: 185-187.
12. Janavicius R. Founder BRCA1/2 mutations in the Europe: implications for hereditary breast-ovarian cancer prevention and control. EPMA J. 2010;1: 397-412.
13. Fathalla MF. Incessant ovulation--a factor in ovarian neoplasia? Lancet. 1971;2: 163.
14. Bristow RE, Karlan BY. Ovulation induction, infertility, and ovarian cancer risk. Fertil Steril. 1996;66: 499-507.
15. Franceschi S, La Vecchia C, Booth M, et al. Pooled analysis of 3 European case-control studies of ovarian cancer: II. Age at menarche and at menopause. Int J Cancer. 1991;49: 57-60.
16. Holschneider CH, Berek JS. Ovarian cancer: epidemiology, biology, and prognostic factors. Semin Surg Oncol. 2000;19: 3-10.
17. Purdie D, Green A, Bain C, et al. Reproductive and other factors and risk of epithelial ovarian cancer: an Australian case-control study. Survey of Women's Health Study Group. Int J Cancer. 1995;62: 678-684.
18. King SM, Hilliard TS, Wu LY, Jaffe RC, Fazleabas AT, Burdette JE. The impact of ovulation on fallopian tube epithelial cells: evaluating three hypotheses connecting ovulation and serous ovarian cancer. Endocr Relat Cancer. 2011;18: 627-642.
19. Yang-Hartwich Y, Gurrea-Soteras M, Sumi N, et al. Ovulation and extra-ovarian origin of ovarian cancer. Sci Rep. 2014;4: 6116.
20. Murdoch WJ. Ovulatory factor in ovarian carcinogenesis. Adv Exp Med Biol. 2008;622: 119-128.
21. Collaborative Group on Epidemiological Studies of Ovarian C, Beral V, Doll R, Hermon C, Peto R, Reeves G. Ovarian cancer and oral contraceptives: collaborative reanalysis of data from 45 epidemiological studies including 23,257 women with ovarian cancer and 87,303 controls. Lancet. 2008;371: 303-314.

22. Choi JH, Wong AS, Huang HF, Leung PC. Gonadotropins and ovarian cancer. Endocr Rev. 2007;28: 440-461.
23. Hilliard TS, Modi DA, Burdette JE. Gonadotropins activate oncogenic pathways to enhance proliferation in normal mouse ovarian surface epithelium. Int J Mol Sci. 2013;14: 4762-4782.
24. Burdette JE, Kurley SJ, Kilen SM, Mayo KE, Woodruff TK. Gonadotropin-induced superovulation drives ovarian surface epithelia proliferation in CD1 mice. Endocrinology. 2006;147: 2338-2345.
25. Davies BR, Finnigan DS, Smith SK, Ponder BA. Administration of gonadotropins stimulates proliferation of normal mouse ovarian surface epithelium. Gynecol Endocrinol. 1999;13: 75-81.
26. Stewart SL, Querec TD, Gruver BN, O'Hare B, Babb JS, Patriotis C. Gonadotropin and steroid hormones stimulate proliferation of the rat ovarian surface epithelium. J Cell Physiol. 2004;198: 119-124.
27. Terry KL, Karageorgi S Fau - Shvetsov YB, Shvetsov Yb Fau - Merritt MA, et al. Genital powder use and risk of ovarian cancer: a pooled analysis of 8,525 cases and 9,859 controls. Cancer prevention research (Philadelphia, Pa.).
28. Yang HS, Yoon C, Myung SK, Park SM. Effect of obesity on survival of women with epithelial ovarian cancer: a systematic review and meta-analysis of observational studies. Int J Gynecol Cancer. 2011;21: 1525-1532.
29. Nagle CM, Bain CJ, Webb PM. Cigarette smoking and survival after ovarian cancer diagnosis. Cancer Epidemiol Biomarkers Prev. 2006;15: 2557-2560.
30. Lueth NA, Anderson KE, Harnack LJ, Fulkerson JA, Robien K. Coffee and caffeine intake and the risk of ovarian cancer: the Iowa Women's Health Study. Cancer Causes Control. 2008;19: 1365-1372.
31. Schildkraut JM, Schwingl PJ, Bastos E, Evanoff A, Hughes C. Epithelial ovarian cancer risk among women with polycystic ovary syndrome. Obstet Gynecol. 1996;88: 554-559.
32. Risch HA, Howe GR. Pelvic inflammatory disease and the risk of epithelial ovarian cancer. Cancer Epidemiol Biomarkers Prev. 1995;4: 447-451.
33. Brinton LA, Gridley G, Persson I, Baron J, Bergqvist A. Cancer risk after a hospital discharge diagnosis of endometriosis. Am J Obstet Gynecol. 1997;176: 572-579.
34. Ng A, Barker N. Ovary and fimbrial stem cells: biology, niche and cancer origins. Nat Rev Mol Cell Biol. 2015;16: 625-638.
35. Karst AM, Levanon K, Drapkin R. Modeling high-grade serous ovarian carcinogenesis from the fallopian tube. Proc Natl Acad Sci U S A. 2011;108: 7547-7552.
36. Piek JM, van Diest PJ, Zweemer RP, et al. Dysplastic changes in prophylactically removed Fallopian tubes of women predisposed to developing ovarian cancer. J Pathol. 2001;195: 451-456.
37. Medeiros F, Muto MG, Lee Y, et al. The tubal fimbria is a preferred site for early adenocarcinoma in women with familial ovarian cancer syndrome. Am J Surg Pathol. 2006;30: 230-236.
38. Piek JM, van Diest PJ, Zweemer RP, Kenemans P, Verheijen RH. Tubal ligation and risk of ovarian cancer. Lancet. 2001;358: 844.
39. Piek JM, Verheijen RH, Kenemans P, Massuger LF, Bulten H, van Diest PJ. BRCA1/2-related ovarian cancers are of tubal origin: a hypothesis. Gynecol Oncol. 2003;90: 491.
40. Callahan MJ, Crum CP, Medeiros F, et al. Primary fallopian tube malignancies in BRCA-positive women undergoing surgery for ovarian cancer risk reduction. J Clin Oncol. 2007;25: 3985-3990.

41. Carcangiu ML, Radice P, Manoukian S, et al. Atypical epithelial proliferation in fallopian tubes in prophylactic salpingo-oophorectomy specimens from BRCA1 and BRCA2 germline mutation carriers. Int J Gynecol Pathol. 2004;23: 35-40.
42. Colgan TJ, Murphy J, Cole DE, Narod S, Rosen B. Occult carcinoma in prophylactic oophorectomy specimens: prevalence and association with BRCA germline mutation status. Am J Surg Pathol. 2001;25: 1283-1289.
43. Finch A, Shaw P, Rosen B, Murphy J, Narod SA, Colgan TJ. Clinical and pathologic findings of prophylactic salpingo-oophorectomies in 159 BRCA1 and BRCA2 carriers. Gynecol Oncol. 2006;100: 58-64.
44. Kindelberger DW, Lee Y, Miron A, et al. Intraepithelial carcinoma of the fimbria and pelvic serous carcinoma: Evidence for a causal relationship. Am J Surg Pathol. 2007;31: 161-169.
45. Paley PJ, Swisher EM, Garcia RL, et al. Occult cancer of the fallopian tube in BRCA-1 germline mutation carriers at prophylactic oophorectomy: a case for recommending hysterectomy at surgical prophylaxis. Gynecol Oncol. 2001;80: 176-180.
46. Przybycin CG, Kurman RJ, Ronnett BM, Shih Ie M, Vang R. Are all pelvic (nonuterine) serous carcinomas of tubal origin? Am J Surg Pathol. 2010;34: 1407-1416.
47. Shaw PA, Rouzbahman M, Pizer ES, Pintilie M, Begley H. Candidate serous cancer precursors in fallopian tube epithelium of BRCA1/2 mutation carriers. Mod Pathol. 2009;22: 1133-1138.
48. Chen EY, Mehra K, Mehrad M, et al. Secretory cell outgrowth, PAX2 and serous carcinogenesis in the Fallopian tube. J Pathol. 2010;222: 110-116.
49. Quick CM, Ning G, Bijron J, et al. PAX2-null secretory cell outgrowths in the oviduct and their relationship to pelvic serous cancer. Mod Pathol. 2012;25: 449-455.
50. Cancer Genome Atlas Research N. Integrated genomic analyses of ovarian carcinoma. Nature. 2011;474: 609-615.
51. Folkins AK, Jarboe EA, Saleemuddin A, et al. A candidate precursor to pelvic serous cancer (p53 signature) and its prevalence in ovaries and fallopian tubes from women with BRCA mutations. Gynecol Oncol. 2008;109: 168-173.
52. Lee Y, Miron A, Drapkin R, et al. A candidate precursor to serous carcinoma that originates in the distal fallopian tube. J Pathol. 2007;211: 26-35.
53. Leeper K, Garcia R, Swisher E, Goff B, Greer B, Paley P. Pathologic findings in prophylactic oophorectomy specimens in high-risk women. Gynecol Oncol. 2002;87: 52-56.
54. Jarboe E, Folkins A, Nucci MR, et al. Serous carcinogenesis in the fallopian tube: a descriptive classification. Int J Gynecol Pathol. 2008;27: 1-9.
55. Sehdev AS, Kurman RJ, Kuhn E, Shih Ie M. Serous tubal intraepithelial carcinoma upregulates markers associated with high-grade serous carcinomas including Rsf-1 (HBXAP), cyclin E and fatty acid synthase. Mod Pathol. 2010;23: 844-855.
56. Karst AM, Levanon K, Duraisamy S, et al. Stathmin 1, a marker of PI3K pathway activation and regulator of microtubule dynamics, is expressed in early pelvic serous carcinomas. Gynecol Oncol. 2011;123: 5-12.
57. Kuhn E, Meeker A, Wang TL, Sehdev AS, Kurman RJ, Shih Ie M. Shortened telomeres in serous tubal intraepithelial carcinoma: an early event in ovarian high-grade serous carcinogenesis. Am J Surg Pathol. 2010;34: 829-836.
58. Carlson JW, Miron A, Jarboe EA, et al. Serous tubal intraepithelial carcinoma: its potential role in primary peritoneal serous carcinoma and serous cancer prevention. J Clin Oncol. 2008;26: 4160-4165.

59. Roh MH, Yassin Y, Miron A, et al. High-grade fimbrial-ovarian carcinomas are unified by altered p53, PTEN and PAX2 expression. Mod Pathol. 2010;23: 1316-1324.
60. Eddie SL, Quartuccio SM, E Oh, et al. Tumorigenesis and peritoneal colonization from fallopian tube epithelium. Oncotarget. 2015;6: 20500-20512.
61. Endsley MP, Moyle-Heyrman G, Karthikeyan S, et al. Spontaneous Transformation of Murine Oviductal Epithelial Cells: A Model System to Investigate the Onset of Fallopian-Derived Tumors. Front Oncol. 2015;5: 154.
62. Jazaeri AA, Bryant JL, Park H, et al. Molecular requirements for transformation of fallopian tube epithelial cells into serous carcinoma. Neoplasia. 2011;13: 899-911.
63. Perets R, Wyant GA, Muto KW, et al. Transformation of the fallopian tube secretory epithelium leads to high-grade serous ovarian cancer in Brca;Tp53;Pten models. Cancer Cell. 2013;24: 751-765.
64. Kim J, Coffey DM, Creighton CJ, Yu Z, Hawkins SM, Matzuk MM. High-grade serous ovarian cancer arises from fallopian tube in a mouse model. Proc Natl Acad Sci U S A. 2012;109: 3921-3926.
65. Sherman-Baust CA, Kuhn E, Valle BL, et al. A genetically engineered ovarian cancer mouse model based on fallopian tube transformation mimics human high-grade serous carcinoma development. J Pathol. 2014;233: 228-237.
66. Quartuccio SM, Karthikeyan S, Eddie SL, et al. Mutant p53 expression in fallopian tube epithelium drives cell migration. Int J Cancer. 2015;137: 1528-1538.
67. Shan W, Mercado-Uribe I, Zhang J, et al. Mucinous adenocarcinoma developed from human fallopian tube epithelial cells through defined genetic modifications. Cell Cycle. 2012;11: 2107-2113.
68. Bopp D, Burri M, Baumgartner S, Frigerio G, Noll M. Conservation of a large protein domain in the segmentation gene paired and in functionally related genes of Drosophila. Cell. 1986;47: 1033-1040.
69. Dahl E, Koseki H, Balling R. Pax genes and organogenesis. Bioessays. 1997;19: 755-765.
70. Robson EJ, He SJ, Eccles MR. A PANorama of PAX genes in cancer and development. Nat Rev Cancer. 2006;6: 52-62.
71. Eberhard D, Jimenez G, Heavey B, Busslinger M. Transcriptional repression by Pax5 (BSAP) through interaction with corepressors of the Groucho family. EMBO J. 2000;19: 2292-2303.
72. Torres M, Gomez-Pardo E, Dressler GR, Gruss P. Pax-2 controls multiple steps of urogenital development. Development. 1995;121: 4057-4065.
73. Torres M, Gomez-Pardo E, Gruss P. Pax2 contributes to inner ear patterning and optic nerve trajectory. Development. 1996;122: 3381-3391.
74. Tong GX, Chiriboga L, Hamele-Bena D, Borczuk AC. Expression of PAX2 in papillary serous carcinoma of the ovary: immunohistochemical evidence of fallopian tube or secondary Mullerian system origin? Mod Pathol. 2007;20: 856-863.
75. Tung CS, Mok SC, Tsang YT, et al. PAX2 expression in low malignant potential ovarian tumors and low-grade ovarian serous carcinomas. Mod Pathol. 2009;22: 1243-1250.
76. Song H, Kwan SY, Izaguirre DI, et al. PAX2 Expression in Ovarian Cancer. Int J Mol Sci. 2013;14: 6090-6105.
77. Monte NM, Webster KA, Neuberg D, Dressler GR, Mutter GL. Joint loss of PAX2 and PTEN expression in endometrial precancers and cancer. Cancer Res. 2010;70: 6225-6232.

78. Strissel PL, Ellmann S, Loprich E, et al. Early aberrant insulin-like growth factor signaling in the progression to endometrial carcinoma is augmented by tamoxifen. Int J Cancer. 2008;123: 2871-2879.
79. Martins FC, Santiago I, Trinh A, et al. Combined image and genomic analysis of high-grade serous ovarian cancer reveals PTEN loss as a common driver event and prognostic classifier. Genome Biol. 2014;15: 526.
80. Al-Hujaily EM, Tang Y, Yao DS, Carmona E, Garson K, Vanderhyden BC. Divergent Roles of PAX2 in the Etiology and Progression of Ovarian Cancer. Cancer Prev Res (Phila). 2015;8: 1163-1173.
81. Muratovska A, Zhou C, He S, Goodyer P, Eccles MR. Paired-Box genes are frequently expressed in cancer and often required for cancer cell survival. Oncogene. 2003;22: 7989-7997.
82. Daniel L, Lechevallier E, Giorgi R, et al. Pax-2 expression in adult renal tumors. Hum Pathol. 2001;32: 282-287.
83. Hueber PA, Iglesias D, Chu LL, Eccles M, Goodyer P. In vivo validation of PAX2 as a target for renal cancer therapy. Cancer Lett. 2008;265: 148-155.
84. Hueber PA, Waters P, Clark P, Eccles M, Goodyer P. PAX2 inactivation enhances cisplatin-induced apoptosis in renal carcinoma cells. Kidney Int. 2006;69: 1139-1145.
85. Khoubehi B, Kessling AM, Adshead JM, Smith GL, Smith RD, Ogden CW. Expression of the developmental and oncogenic PAX2 gene in human prostate cancer. J Urol. 2001;165: 2115-2120.
86. Ueda T, Ito S, Shiraishi T, et al. Hyper-expression of PAX2 in human metastatic prostate tumors and its role as a cancer promoter in an in vitro invasion model. Prostate. 2013;73: 1403-1412.
87. Buttiglieri S, Deregibus MC, Bravo S, et al. Role of Pax2 in apoptosis resistance and proinvasive phenotype of Kaposi's sarcoma cells. J Biol Chem. 2004;279: 4136-4143.
88. Schimmenti LA. Renal coloboma syndrome. Eur J Hum Genet. 2011;19: 1207-1212.
89. Modi DA, Sunoqrot S, Bugno J, Lantvit DD, Hong S, Burdette JE. Targeting of follicle stimulating hormone peptide-conjugated dendrimers to ovarian cancer cells. Nanoscale. 2014;6: 2812-2820.
90. Sunoqrot S, Bae JW, Pearson RM, et al. Temporal control over cellular targeting through hybridization of folate-targeted dendrimers and PEG-PLA nanoparticles. Biomacromolecules. 2012;13: 1223-1230.
91. Sunoqrot S, Liu Y, Kim DH, Hong S. In vitro evaluation of dendrimer-polymer hybrid nanoparticles on their controlled cellular targeting kinetics. Mol Pharm. 2013;10: 2157-2166.
92. King SM, Modi DA, Eddie SL, Burdette JE. Insulin and insulin-like growth factor signaling increases proliferation and hyperplasia of the ovarian surface epithelium and decreases follicular integrity through upregulation of the PI3-kinase pathway. J Ovarian Res. 2013;6: 12.
93. King SM, Quartuccio SM, Vanderhyden BC, Burdette JE. Early transformative changes in normal ovarian surface epithelium induced by oxidative stress require Akt upregulation, DNA damage and epithelial-stromal interaction. Carcinogenesis. 2013;34: 1125-1133.
94. Mitra AK, Davis DA, Tomar S, et al. In vivo tumor growth of high-grade serous ovarian cancer cell lines. Gynecol Oncol. 2015;138: 372-377.
95. Jackson KS, Inoue K, Davis DA, Hilliard TS, Burdette JE. Three-dimensional ovarian organ culture as a tool to study normal ovarian surface epithelial wound repair. Endocrinology. 2009;150: 3921-3926.

96. Vasudevan D, Hickok JR, Bovee RC, et al. Nitric Oxide Regulates Gene Expression in Cancers by Controlling Histone Posttranslational Modifications. Cancer Res. 2015;75: 5299-5308.
97. Kierny MR, Cunningham TD, Bouhenni RA, Edward DP, Kay BK. Generating Recombinant Antibodies against Putative Biomarkers of Retinal Injury. PLoS One. 2015;10: e0124492.
98. Sukerkar PA, MacRenaris KW, Townsend TR, Ahmed RA, Burdette JE, Meade TJ. Synthesis and biological evaluation of water-soluble progesterone-conjugated probes for magnetic resonance imaging of hormone related cancers2011;22: 2304-2316.
99. Majoros IJ, Myc A, Thomas T, Mehta CB, Baker JR, Jr. PAMAM dendrimer-based multifunctional conjugate for cancer therapy: synthesis, characterization, and functionality. Biomacromolecules. 2006;7: 572-579.
100. Sunoqrot S, Bae JW, Jin SE, Pearson RM, Liu Y, Hong S. Kinetically controlled cellular interactions of polymer-polymer and polymer-liposome nanohybrid systems. Bioconjugate Chem. 2011;22: 466-474.
101. Sunoqrot S, Bae JW, Pearson RM, et al. Temporal control over cellular targeting through hybridization of folate-targeted dendrimers and PEG-PLA nanoparticles. Biomacromolecules. 2012;13: 1223-1230.
102. Sunoqrot S, Liu Y, Kim D-H, Hong S. In vitro evaluation of dendrimer–polymer hybrid nanoparticles on their controlled cellular targeting kinetics. Mol. Pharm. 2013;10: 2157-2166.
103. Hong S, Bielinska AU, Mecke A, et al. Interaction of poly(amidoamine) dendrimers with supported lipid bilayers and cells: hole formation and the relation to transport. Bioconjug Chem. 2004;15: 774-782.
104. Hong S, Leroueil PR, Janus EK, et al. Interaction of polycationic polymers with supported lipid bilayers and cells: nanoscale hole formation and enhanced membrane permeability. Bioconjug Chem. 2006;17: 728-734.
105. Syed V, Ulinski G, Mok SC, Yiu GK, Ho SM. Expression of gonadotropin receptor and growth responses to key reproductive hormones in normal and malignant human ovarian surface epithelial cells. Cancer Res. 2001;61: 6768-6776.
106. Auersperg N, Woo MM, Gilks CB. The origin of ovarian carcinomas: a developmental view. Gynecol Oncol. 2008;110: 452-454.
107. Leung PC, Choi JH. Endocrine signaling in ovarian surface epithelium and cancer. Hum Reprod Update. 2007;13: 143-162.
108. Bernard DJ, Fortin J, Wang Y, Lamba P. Mechanisms of FSH synthesis: what we know, what we don't, and why you should care. Fertil Steril. 2010;93: 2465-2485.
109. Dierich A, Sairam MR, Monaco L, et al. Impairing follicle-stimulating hormone (FSH) signaling in vivo: targeted disruption of the FSH receptor leads to aberrant gametogenesis and hormonal imbalance. Proc Natl Acad Sci U S A. 1998;95: 13612-13617.
110. Hunzicker-Dunn M, Maizels ET. FSH signaling pathways in immature granulosa cells that regulate target gene expression: branching out from protein kinase A. Cell Signal. 2006;18: 1351-1359.
111. Rao MC, Midgley AR, Jr., Richards JS. Hormonal regulation of ovarian cellular proliferation. Cell. 1978;14: 71-78.
112. Parrott JA, Doraiswamy V, Kim G, Mosher R, Skinner MK. Expression and actions of both the follicle stimulating hormone receptor and the luteinizing hormone receptor in normal ovarian surface epithelium and ovarian cancer. Mol Cell Endocrinol. 2001;172: 213-222.

113. Huang Y, Hua K, Zhou X, et al. Activation of the PI3K/AKT pathway mediates FSH-stimulated VEGF expression in ovarian serous cystadenocarcinoma. Cell Res. 2008;18: 780-791.
114. Tourgeman DE, Lu JJ, Boostanfar R, Amezcua C, Felix JC, Paulson RJ. Human chorionic gonadotropin suppresses ovarian epithelial neoplastic cell proliferation in vitro. Fertil Steril. 2002;78: 1096-1099.
115. Wimalasena J, Meehan D, Cavallo C. Human epithelial ovarian cancer cell steroid secretion and its control by gonadotropins. Gynecol Oncol. 1991;41: 56-63.
116. Ivarsson K, Sundfeldt K, Brannstrom M, Hellberg P, Janson PO. Diverse effects of FSH and LH on proliferation of human ovarian surface epithelial cells. Hum Reprod. 2001;16: 18-23.
117. Slot KA, de Boer-Brouwer M, Houweling M, Vaandrager AB, Dorrington JH, Teerds KJ. Luteinizing hormone inhibits Fas-induced apoptosis in ovarian surface epithelial cell lines. J Endocrinol. 2006;188: 227-239.
118. Choi JH, Choi KC, Auersperg N, Leung PC. Gonadotropins upregulate the epidermal growth factor receptor through activation of mitogen-activated protein kinases and phosphatidyl-inositol-3-kinase in human ovarian surface epithelial cells. Endocr Relat Cancer. 2005;12: 407-421.
119. Wong AS, Leung PC. Role of endocrine and growth factors on the ovarian surface epithelium. J Obstet Gynaecol Res. 2007;33: 3-16.
120. Wright JW, Toth-Fejel S, Stouffer RL, Rodland KD. Proliferation of rhesus ovarian surface epithelial cells in culture: lack of mitogenic response to steroid or gonadotropic hormones. Endocrinology. 2002;143: 2198-2207.
121. Gamwell LF, Collins O, Vanderhyden BC. The mouse ovarian surface epithelium contains a population of LY6A (SCA-1) expressing progenitor cells that are regulated by ovulation-associated factors. Biol Reprod. 2012;87: 80.
122. Altomare DA, Wang HQ, Skele KL, et al. AKT and mTOR phosphorylation is frequently detected in ovarian cancer and can be targeted to disrupt ovarian tumor cell growth. Oncogene. 2004;23: 5853-5857.
123. Kinross KM, Montgomery KG, Kleinschmidt M, et al. An activating Pik3ca mutation coupled with Pten loss is sufficient to initiate ovarian tumorigenesis in mice. J Clin Invest. 2012;122: 553-557.
124. Gladhaug IP, Refsnes M, Christoffersen T. Regulation of hepatocyte epidermal growth factor receptors by n-butyrate and dimethyl sulfoxide: sensitivity to modulation by the tumor promoter TPA. Anticancer Res. 1989;9: 1587-1592.
125. Osterholzer HO, Johnson JH, Nicosia SV. An autoradiographic study of rabbit ovarian surface epithelium before and after ovulation. Biol Reprod. 1985;33: 729-738.
126. Bai W, Oliveros-Saunders B, Wang Q, Acevedo-Duncan ME, Nicosia SV. Estrogen stimulation of ovarian surface epithelial cell proliferation. In Vitro Cell Dev Biol Anim. 2000;36: 657-666.
127. Bellacosa A, de Feo D, Godwin AK, et al. Molecular alterations of the AKT2 oncogene in ovarian and breast carcinomas. Int J Cancer. 1995;64: 280-285.
128. Cheng JQ, Godwin AK, Bellacosa A, et al. AKT2, a putative oncogene encoding a member of a subfamily of protein-serine/threonine kinases, is amplified in human ovarian carcinomas. Proc Natl Acad Sci U S A. 1992;89: 9267-9271.
129. Sun M, Wang G, Paciga JE, et al. AKT1/PKBalpha kinase is frequently elevated in human cancers and its constitutive activation is required for oncogenic transformation in NIH3T3 cells. Am J Pathol. 2001;159: 431-437.

130. Yuan ZQ, Sun M, Feldman RI, et al. Frequent activation of AKT2 and induction of apoptosis by inhibition of phosphoinositide-3-OH kinase/Akt pathway in human ovarian cancer. Oncogene. 2000;19: 2324-2330.
131. Cristiano BE, Chan JC, Hannan KM, et al. A specific role for AKT3 in the genesis of ovarian cancer through modulation of G(2)-M phase transition. Cancer Res. 2006;66: 11718-11725.
132. Flynn MP, Maizels ET, Karlsson AB, et al. Luteinizing hormone receptor activation in ovarian granulosa cells promotes protein kinase A-dependent dephosphorylation of microtubule-associated protein 2D. Mol Endocrinol. 2008;22: 1695-1710.
133. Bull Phelps SL, Schorge JO, Peyton MJ, et al. Implications of EGFR inhibition in ovarian cancer cell proliferation. Gynecol Oncol. 2008;109: 411-417.
134. Sewell JM, Macleod KG, Ritchie A, Smyth JF, Langdon SP. Targeting the EGF receptor in ovarian cancer with the tyrosine kinase inhibitor ZD 1839 ("Iressa"). Br J Cancer. 2002;86: 456-462.
135. Psyrri A, Kassar M, Yu Z, et al. Effect of epidermal growth factor receptor expression level on survival in patients with epithelial ovarian cancer. Clin Cancer Res. 2005;11: 8637-8643.
136. Tanaka Y, Terai Y, Tanabe A, et al. Prognostic effect of epidermal growth factor receptor gene mutations and the aberrant phosphorylation of Akt and ERK in ovarian cancer. Cancer Biol Ther. 2011;11: 50-57.
137. Guo X, Liu G, Schauer IG, et al. Overexpression of the beta subunit of human chorionic gonadotropin promotes the transformation of human ovarian epithelial cells and ovarian tumorigenesis. Am J Pathol. 2011;179: 1385-1393.
138. Mehra K, Mehrad M, Ning G, et al. STICS, SCOUTs and p53 signatures; a new language for pelvic serous carcinogenesis. Front Biosci (Elite Ed). 2011;3: 625-634.
139. Dressler GR, Woolf AS. Pax2 in development and renal disease. Int J Dev Biol. 1999;43: 463-468.
140. Dressler GR, Deutsch U, Chowdhury K, Nornes HO, Gruss P. Pax2, a new murine paired-box-containing gene and its expression in the developing excretory system. Development. 1990;109: 787-795.
141. Lechner MS, Levitan I, Dressler GR. PTIP, a novel BRCT domain-containing protein interacts with Pax2 and is associated with active chromatin. Nucleic Acids Res. 2000;28: 2741-2751.
142. Patel SR, Kim D, Levitan I, Dressler GR. The BRCT-domain containing protein PTIP links PAX2 to a histone H3, lysine 4 methyltransferase complex. Dev Cell. 2007;13: 580-592.
143. Wu J, Prindle MJ, Dressler GR, Yu X. PTIP regulates 53BP1 and SMC1 at the DNA damage sites. J Biol Chem. 2009;284: 18078-18084.
144. Patel SR, Bhumbra SS, Paknikar RS, Dressler GR. Epigenetic mechanisms of Groucho/Grg/TLE mediated transcriptional repression. Mol Cell. 2012;45: 185-195.
145. Saifudeen Z, Liu J, Dipp S, et al. A p53-Pax2 pathway in kidney development: implications for nephrogenesis. PLoS One. 2012;7: e44869.
146. Ning G, Bijron JG, Yamamoto Y, et al. The PAX2-null immunophenotype defines multiple lineages with common expression signatures in benign and neoplastic oviductal epithelium. J Pathol. 2014;234: 478-487.
147. Edgar R, Domrachev M, Lash AE. Gene Expression Omnibus: NCBI gene expression and hybridization array data repository. Nucleic Acids Res. 2002;30: 207-210.
148. Yamamoto Y, Ning G, Howitt BE, et al. In vitro and in vivo correlates of physiological and neoplastic human Fallopian tube stem cells. J Pathol. 2015.

149. Gyorffy B, Surowiak P, Budczies J, Lanczky A. Online survival analysis software to assess the prognostic value of biomarkers using transcriptomic data in non-small-cell lung cancer. PLoS One. 2013;8: e82241.
150. Quartuccio SM, Karthikeyan S, Eddie SL, et al. Mutant p53 expression in fallopian tube epithelium drives cell migration2015;137: 1528-1538.
151. Novak M, Lester J, Karst AM, et al. Stathmin 1 and p16(INK4A) are sensitive adjunct biomarkers for serous tubal intraepithelial carcinoma. Gynecol Oncol. 2015;139: 104-111.
152. Ning G, Bijron JG, Yamamoto Y, et al. The PAX2-null immunophenotype defines multiple lineages with common expression signatures in benign and neoplastic oviductal epithelium2014;234: 478-487.
153. Eddie SL, Quartuccio SM, E Óh, et al. Tumorigenesis and peritoneal colonization from fallopian tube epithelium2015;6: 20500-20512.
154. Stayner CK, Cunliffe HE, Ward TA, Eccles MR. Cloning and characterization of the human PAX2 promoter. J Biol Chem. 1998;273: 25472-25479.
155. Patel SR, Dressler GR. Expression of Pax2 in the intermediate mesoderm is regulated by YY1. Dev Biol. 2004;267: 505-516.
156. Levanon K, Ng V, Piao HY, et al. Primary ex vivo cultures of human fallopian tube epithelium as a model for serous ovarian carcinogenesis. Oncogene. 2010;29: 1103-1113.
157. Baldassarre G, Belletti B, Nicoloso MS, et al. p27(Kip1)-stathmin interaction influences sarcoma cell migration and invasion. Cancer Cell. 2005;7: 51-63.
158. Liu F, Sun YL, Xu Y, Liu F, Wang LS, Zhao XH. Expression and phosphorylation of stathmin correlate with cell migration in esophageal squamous cell carcinoma. Oncol Rep. 2013;29: 419-424.
159. Alli E, Bash-Babula J, Yang JM, Hait WN. Effect of stathmin on the sensitivity to antimicrotubule drugs in human breast cancer. Cancer Res. 2002;62: 6864-6869.
160. Rana S, Maples PB, Senzer N, Nemunaitis J. Stathmin 1: a novel therapeutic target for anticancer activity. Expert Rev Anticancer Ther. 2008;8: 1461-1470.
161. Integrated genomic analyses of ovarian carcinoma2011;474: 609-615.
162. Takahashi T, Ikeda Y, Miyoshi E, Yaginuma Y, Ishikawa M, Taniguchi N. alpha1,6fucosyltransferase is highly and specifically expressed in human ovarian serous adenocarcinomas. Int J Cancer. 2000;88: 914-919.
163. Khin EE, Kikkawa F, Ino K, et al. Neutral endopeptidase/CD10 expression in the stroma of epithelial ovarian carcinoma. Int J Gynecol Pathol. 2003;22: 175-180.
164. Chiu FL, Lin JK. Downregulation of androgen receptor expression by luteolin causes inhibition of cell proliferation and induction of apoptosis in human prostate cancer cells and xenografts. Prostate. 2008;68: 61-71.
165. Samy RP, Gopalakrishnakone P, Ignacimuthu S. Anti-tumor promoting potential of luteolin against 7,12-dimethylbenz(a)anthracene-induced mammary tumors in rats. Chem Biol Interact. 2006;164: 1-14.
166. Kim JS, Jobin C. The flavonoid luteolin prevents lipopolysaccharide-induced NF-kappaB signalling and gene expression by blocking IkappaB kinase activity in intestinal epithelial cells and bone-marrow derived dendritic cells. Immunology. 2005;115: 375-387.
167. Cai Y, Lechner MS, Nihalani D, Prindle MJ, Holzman LB, Dressler GR. Phosphorylation of Pax2 by the c-Jun N-terminal kinase and enhanced Pax2-dependent transcription activation. J Biol Chem. 2002;277: 1217-1222.

168. Zhang S, Zhou L, Hong B, et al. Small-Molecule NSC59984 Restores p53 Pathway Signaling and Antitumor Effects against Colorectal Cancer via p73 Activation and Degradation of Mutant p53. Cancer Res. 2015;75: 3842-3852.
169. Cho KR. Ovarian cancer update: lessons from morphology, molecules, and mice. Arch Pathol Lab Med. 2009;133: 1775-1781.
170. Gilks CB. Molecular abnormalities in ovarian cancer subtypes other than high-grade serous carcinoma. J Oncol. 2010;2010: 740968.
171. Bose CK. Follicle stimulating hormone receptor in ovarian surface epithelium and epithelial ovarian cancer. Oncol Res. 2008;17: 231-238.
172. Leung EH, Leung PC, Auersperg N. Differentiation and growth potential of human ovarian surface epithelial cells expressing temperature-sensitive SV40 T antigen. In Vitro Cell Dev Biol Anim. 2001;37: 515-521.
173. Choi JH, Choi KC, Auersperg N, Leung PC. Overexpression of follicle-stimulating hormone receptor activates oncogenic pathways in preneoplastic ovarian surface epithelial cells. J Clin Endocrinol Metab. 2004;89: 5508-5516.
174. Ji Q, Liu PI, Chen PK, Aoyama C. Follicle stimulating hormone-induced growth promotion and gene expression profiles on ovarian surface epithelial cells. Int J Cancer. 2004;112: 803-814.
175. Li Y, Ganta S, Cheng C, Craig R, Ganta RR, Freeman LC. FSH stimulates ovarian cancer cell growth by action on growth factor variant receptor. Mol Cell Endocrinol. 2007;267: 26-37.
176. Agris PF, Guenther RH, Sierzputowska-Gracz H, et al. Solution structure of a synthetic peptide corresponding to a receptor binding region of FSH (hFSH-beta 33-53). J Protein Chem. 1992;11: 495-507.
177. Zhang XY, Chen J, Zheng YF, et al. Follicle-stimulating hormone peptide can facilitate paclitaxel nanoparticles to target ovarian carcinoma in vivo. Cancer Res. 2009;69: 6506-6514.
178. Azarmi S, Roa WH, Lobenberg R. Targeted delivery of nanoparticles for the treatment of lung diseases. Adv Drug Deliv Rev. 2008;60: 863-875.
179. Kataoka K, Harada A, Nagasaki Y. Block copolymer micelles for drug delivery: design, characterization and biological significance. Adv Drug Deliv Rev. 2001;47: 113-131.
180. Soppimath KS, Aminabhavi TM, Kulkarni AR, Rudzinski WE. Biodegradable polymeric nanoparticles as drug delivery devices. J Control Release. 2001;70: 1-20.
181. Torchilin VP. Recent advances with liposomes as pharmaceutical carriers. Nat Rev Drug Discov. 2005;4: 145-160.
182. Vasir JK, Labhasetwar V. Biodegradable nanoparticles for cytosolic delivery of therapeutics. Adv Drug Deliv Rev. 2007;59: 718-728.
183. Peer D, Karp JM, Hong S, Farokhzad OC, Margalit R, Langer R. Nanocarriers as an emerging platform for cancer therapy. Nat Nanotechnol. 2007;2: 751-760.
184. Wong C, Stylianopoulos T, Cui J, et al. Multistage nanoparticle delivery system for deep penetration into tumor tissue. Proc Natl Acad Sci U S A. 2011;108: 2426-2431.
185. Tang L, Fan TM, Borst LB, Cheng J. Synthesis and biological response of size-specific, monodisperse drug-silica nanoconjugates. ACS Nano. 2012;6: 3954-3966.
186. Cheng Y, Zhao L Fau - Li Y, Li Y Fau - Xu T, Xu T. Design of biocompatible dendrimers for cancer diagnosis and therapy: current status and future perspectives. Chem Soc Rev. 2011.
187. Lee CC, MacKay JA, Frechet JM, Szoka FC. Designing dendrimers for biological applications. Nat Biotechnol. 2005;23: 1517-1526.

188. Pearson RM, Sunoqrot S, Hsu HJ, Bae JW, Hong S. Dendritic nanoparticles: the next generation of nanocarriers? Ther Deliv. 2012;3: 941-959.
189. Esfand R, Tomalia DA. Poly(amidoamine) (PAMAM) dendrimers: from biomimicry to drug delivery and biomedical applications. Drug Discov Today. 2001;6: 427-436.
190. Kukowska-Latallo JF, Candido KA, Cao Z, et al. Nanoparticle targeting of anticancer drug improves therapeutic response in animal model of human epithelial cancer. Cancer Res. 2005;65: 5317-5324.
191. Majoros IJ, Thomas TP, Mehta CB, Baker JR, Jr. Poly(amidoamine) dendrimer-based multifunctional engineered nanodevice for cancer therapy. J Med Chem. 2005;48: 5892-5899.
192. Myc A, Kukowska-Latallo J, Cao P, et al. Targeting the efficacy of a dendrimer-based nanotherapeutic in heterogeneous xenograft tumors in vivo. Anticancer Drugs. 2010;21: 186-192.
193. Myung JH, Gajjar KA, Saric J, Eddington DT, Hong S. Dendrimer-mediated multivalent binding for the enhanced capture of tumor cells. Angew Chem Int Ed Engl. 2011;50: 11769-11772.
194. Dhanikula RS, Argaw A, Bouchard JF, Hildgen P. Methotrexate loaded polyether-copolyester dendrimers for the treatment of gliomas: enhanced efficacy and intratumoral transport capability. Mol Pharm. 2008;5: 105-116.
195. Waite CL, Roth CM. PAMAM-RGD conjugates enhance siRNA delivery through a multicellular spheroid model of malignant glioma. Bioconjug Chem. 2009;20: 1908-1916.
196. Huang Y, Jin H, Liu Y, et al. FSH inhibits ovarian cancer cell apoptosis by up-regulating survivin and down-regulating PDCD6 and DR5. Endocr Relat Cancer. 2011;18: 13-26.
197. Biffi S, Garrovo C, Macor P, et al. In vivo biodistribution and lifetime analysis of cy5.5-conjugated rituximab in mice bearing lymphoid tumor xenograft using time-domain near-infrared optical imaging. Mol Imaging. 2008;7: 272-282.
198. Koo OM, Rubinstein I, Onyuksel H. Role of nanotechnology in targeted drug delivery and imaging: a concise review. Nanomedicine. 2005;1: 193-212.
199. Bast RC, Jr., Hennessy B, Mills GB. The biology of ovarian cancer: new opportunities for translation. Nat Rev Cancer. 2009;9: 415-428.
200. Zheng W, Magid MS, Kramer EE, Chen YT. Follicle-stimulating hormone receptor is expressed in human ovarian surface epithelium and fallopian tube. Am J Pathol. 1996;148: 47-53.
201. Mendelsohn J, Baselga J. Status of epidermal growth factor receptor antagonists in the biology and treatment of cancer. J Clin Oncol. 2003;21: 2787-2799.
202. Sudimack J, Lee RJ. Targeted drug delivery via the folate receptor. Adv Drug Deliv Rev. 2000;41: 147-162.
203. Ross JF, Chaudhuri PK, Ratnam M. Differential regulation of folate receptor isoforms in normal and malignant tissues in vivo and in established cell lines. Physiologic and clinical implications. Cancer. 1994;73: 2432-2443.
204. Zimmermann M, Zouhair A, Azria D, Ozsahin M. The epidermal growth factor receptor (EGFR) in head and neck cancer: its role and treatment implications. Radiat Oncol. 2006;1: 11.
205. Yang Y, Sunoqrot S, Stowell C, et al. Effect of size, surface charge, and hydrophobicity of poly(amidoamine) dendrimers on their skin penetration. Biomacromolecules. 2012;13: 2154-2162.

206. King SM, Quartuccio S, Hilliard TS, Inoue K, Burdette JE. Alginate hydrogels for three-dimensional organ culture of ovaries and oviducts. J Vis Exp. 2011.
207. Crum CP, Drapkin R, Kindelberger D, Medeiros F, Miron A, Lee Y. Lessons from BRCA: the tubal fimbria emerges as an origin for pelvic serous cancer. Clin Med Res. 2007;5: 35-44.
208. Kwintkiewicz J, Cai Z, Stocco C. Follicle-stimulating hormone-induced activation of Gata4 contributes in the up-regulation of Cyp19 expression in rat granulosa cells. Mol Endocrinol. 2007;21: 933-947.
209. Cao G, Sofic E, Prior RL. Antioxidant and prooxidant behavior of flavonoids: structure-activity relationships. Free Radic Biol Med. 1997;22: 749-760.
210. Jeon IH, Kim HS, Kang HJ, et al. Anti-inflammatory and antipruritic effects of luteolin from Perilla (P. frutescens L.) leaves. Int J Mol Sci. 2014;19: 6941-6951.
211. Gates MA, Tworoger SS, Hecht JL, De Vivo I, Rosner B, Hankinson SE. A prospective study of dietary flavonoid intake and incidence of epithelial ovarian cancer. Int J Cancer. 2007;121: 2225-2232.
212. Lin Y, Shi R, Wang X, Shen HM. Luteolin, a flavonoid with potential for cancer prevention and therapy. Curr Cancer Drug Targets. 2008;8: 634-646.
213. Seelinger G, Merfort I, Wolfle U, Schempp CM. Anti-carcinogenic effects of the flavonoid luteolin. Molecules. 2008;13: 2628-2651.
214. Hwang JT, Park OJ, Lee YK, et al. Anti-tumor effect of luteolin is accompanied by AMP-activated protein kinase and nuclear factor-kappaB modulation in HepG2 hepatocarcinoma cells. Int J Mol Med. 2011;28: 25-31.
215. Ando C, Takahashi N, Hirai S, et al. Luteolin, a food-derived flavonoid, suppresses adipocyte-dependent activation of macrophages by inhibiting JNK activation. FEBS Lett. 2009;583: 3649-3654.
216. Majumdar D, Jung Kh Fau - Zhang H, Zhang H Fau - Nannapaneni S, et al. Luteolin nanoparticle in chemoprevention: in vitro and in vivo anticancer activity. Cancer Prev Res (Phila). 2015.
217. Auersperg N, Wong AS, Choi KC, Kang SK, Leung PC. Ovarian surface epithelium: biology, endocrinology, and pathology. Endocr Rev. 2001;22: 255-288.
218. Doyle LK, Donadeu FX. Regulation of the proliferative activity of ovarian surface epithelial cells by follicular fluid. Anim Reprod Sci. 2009;114: 443-448.
219. Kuroda H, Mandai M, Konishi I, et al. Human ovarian surface epithelial (OSE) cells express LH/hCG receptors, and hCG inhibits apoptosis of OSE cells via up-regulation of insulin-like growth factor-1. Int J Cancer. 2001;91: 309-315.
220. Soos MA, Field CE, Siddle K. Purified hybrid insulin/insulin-like growth factor-I receptors bind insulin-like growth factor-I, but not insulin, with high affinity. Biochem J. 1993;290 (Pt 2): 419-426.
221. Sandow J. Growth effects of insulin and insulin analogues. Arch Physiol Biochem. 2009;115: 72-85.
222. Auersperg N, Maines-Bandiera SL, Dyck HG, Kruk PA. Characterization of cultured human ovarian surface epithelial cells: phenotypic plasticity and premalignant changes. Lab Invest. 1994;71: 510-518.
223. Straus DS. Growth-stimulatory actions of insulin in vitro and in vivo. Endocr Rev. 1984;5: 356-369.
224. Pollak M. Insulin and insulin-like growth factor signalling in neoplasia. Nat Rev Cancer. 2008;8: 915-928.
225. Giudice LC. Insulin-like growth factors and ovarian follicular development. Endocr Rev. 1992;13: 641-669.

226. Augst AD, Kong HJ, Mooney DJ. Alginate hydrogels as biomaterials. Macromol Biosci. 2006;6: 623-633.
227. Ostchega Y, Hughes JP, Terry A, Fakhouri TH, Miller I. Abdominal obesity, body mass index, and hypertension in US adults: NHANES 2007-2010. Am J Hypertens. 2012;25: 1271-1278.
228. Matalliotakis I, Kourtis A, Koukoura O, Panidis D. Polycystic ovary syndrome: etiology and pathogenesis. Arch Gynecol Obstet. 2006;274: 187-197.
229. Jemal A, Siegel R, Ward E, Hao Y, Xu J, Thun MJ. Cancer statistics, 2009. CA Cancer J Clin. 2009;59: 225-249.
230. Kaaks R, Lukanova A. Energy balance and cancer: the role of insulin and insulin-like growth factor-I. Proc Nutr Soc. 2001;60: 91-106.
231. Beck EP, Russo P, Gliozzo B, et al. Identification of insulin and insulin-like growth factor I (IGF I) receptors in ovarian cancer tissue. Gynecol Oncol. 1994;53: 196-201.
232. Conover CA, Hartmann LC, Bradley S, et al. Biological characterization of human epithelial ovarian carcinoma cells in primary culture: the insulin-like growth factor system. Exp Cell Res. 1998;238: 439-449.
233. Sayer RA, Lancaster JM, Pittman J, et al. High insulin-like growth factor-2 (IGF-2) gene expression is an independent predictor of poor survival for patients with advanced stage serous epithelial ovarian cancer. Gynecol Oncol. 2005;96: 355-361.
234. An Y, Cai Y, Guan Y, et al. Inhibitory effect of small interfering RNA targeting insulin-like growth factor-I receptor in ovarian cancer OVCAR3 cells. Cancer Biother Radiopharm. 2010;25: 545-552.
235. Eckstein N, Servan K, Hildebrandt B, et al. Hyperactivation of the insulin-like growth factor receptor I signaling pathway is an essential event for cisplatin resistance of ovarian cancer cells. Cancer Res. 2009;69: 2996-3003.
236. Tashiro H, Katabuchi H, Begum M, et al. Roles of luteinizing hormone/chorionic gonadotropin receptor in anchorage-dependent and -independent growth in human ovarian surface epithelial cell lines. Cancer Sci. 2003;94: 953-959.
237. West ER, Xu M, Woodruff TK, Shea LD. Physical properties of alginate hydrogels and their effects on in vitro follicle development. Biomaterials. 2007;28: 4439-4448.
238. Parrizas M, Gazit A, Levitzki A, Wertheimer E, LeRoith D. Specific inhibition of insulin-like growth factor-1 and insulin receptor tyrosine kinase activity and biological function by tyrphostins. Endocrinology. 1997;138: 1427-1433.
239. Cross DA, Alessi DR, Cohen P, Andjelkovich M, Hemmings BA. Inhibition of glycogen synthase kinase-3 by insulin mediated by protein kinase B. Nature. 1995;378: 785-789.
240. Cain RJ, Ridley AJ. Phosphoinositide 3-kinases in cell migration. Biol Cell. 2009;101: 13-29.
241. Edson MA, Nagaraja AK, Matzuk MM. The mammalian ovary from genesis to revelation. Endocr Rev. 2009;30: 624-712.
242. Dyck MK, Parlow AF, Senechal JF, Sirard MA, Pothier F. Ovarian expression of human insulin-like growth factor-I in transgenic mice results in cyst formation. Mol Reprod Dev. 2001;59: 178-185.
243. Hirshfeld-Cytron JE, Duncan FE, Xu M, Jozefik JK, Shea LD, Woodruff TK. Animal age, weight and estrus cycle stage impact the quality of in vitro grown follicles. Hum Reprod. 2011;26: 2473-2485.
244. Nandi A, Wang X, Accili D, Wolgemuth DJ. The effect of insulin signaling on female reproductive function independent of adiposity and hyperglycemia. Endocrinology. 2010;151: 1863-1871.

245. Woodruff TK, Shea LD. A new hypothesis regarding ovarian follicle development: ovarian rigidity as a regulator of selection and health. J Assist Reprod Genet. 2011;28: 3-6.
246. Berkholtz CB, Lai BE, Woodruff TK, Shea LD. Distribution of extracellular matrix proteins type I collagen, type IV collagen, fibronectin, and laminin in mouse folliculogenesis. Histochem Cell Biol. 2006;126: 583-592.
247. Spicer LJ, Echternkamp SE. The ovarian insulin and insulin-like growth factor system with an emphasis on domestic animals. Domest Anim Endocrinol. 1995;12: 223-245.
248. Kirby CJ, Armstrong JD, Huff BG, et al. Changes in serum somatotropin, somatotropin mRNA, and serum and follicular insulin-like growth factor-I in response to feed restriction in cows actively immunized against growth hormone-releasing factor. J Anim Sci. 1993;71: 3033-3042.
249. Chung CY, Potikyan G, Firtel RA. Control of cell polarity and chemotaxis by Akt/PKB and PI3 kinase through the regulation of PAKa. Mol Cell. 2001;7: 937-947.
250. Lau MT, Leung PC. The PI3K/Akt/mTOR signaling pathway mediates insulin-like growth factor 1-induced E-cadherin down-regulation and cell proliferation in ovarian cancer cells. Cancer Lett. 2012;326: 191-198.
251. Romero-Aleshire MJ, Diamond-Stanic MK, Hasty AH, Hoyer PB, Brooks HL. Loss of ovarian function in the VCD mouse-model of menopause leads to insulin resistance and a rapid progression into the metabolic syndrome. Am J Physiol Regul Integr Comp Physiol. 2009;297: R587-592.
252. Tok EC, Ertunc D, Tataroglu C, Yazici G, Kanat H, Dilek S. Clinicopathologic study of the putative precursor lesions of epithelial ovarian cancer in low-risk women. Int J Gynecol Cancer. 2006;16: 501-506.
253. Auersperg N, Maclaren IA, Kruk PA. Ovarian surface epithelium: autonomous production of connective tissue-type extracellular matrix. Biol Reprod. 1991;44: 717-724.
254. Diamanti-Kandarakis E, Piperi C, Spina J, et al. Polycystic ovary syndrome: the influence of environmental and genetic factors. Hormones (Athens). 2006;5: 17-34.

VITA

EDUCATION

August 2011 - Present	**Ph.D. Candidate, Pharmacognosy** University of Illinois at Chicago, Chicago, IL, USA Thesis Advisor: Joanna E. Burdette, Ph.D.
2009 - 2011	**M.S., Pharmaceutical Sciences** University of Southern California, Los Angeles, CA, USA Thesis Advisors: Daryl L. Davies, Ph.D. and Ronald L. Alkana, PharmD, Ph.D.
2005 - 2009	**Bachelor of Pharmaceutical Sciences** University of Mumbai, Maharashtra, India

PROFESSIONAL EXPERIENCE

August 2011 - Present	**Graduate Research Assistant** University Of Illinois At Chicago, Chicago, IL, USA
June – August 2014	**Oncology Clinical Development Intern** AbbVie Inc., North Chicago, IL, USA
2009 - 2011	**Graduate Research Assistant** University Of Southern California, Los Angeles, CA, USA
June – August 2010	**Neurophysiology Intern** Genentech Inc., South San Francisco, CA, USA

PUBLICATIONS

1. **Modi DA**, Tagare RD, Davis D, Lantvit DD, Burdette JE: Investigating PAX2 as a novel target in fallopian tube-derived high grade serous ovarian cancer (In preparation) **2016**

2. Quartuccio SM, Karthikeyan S, Eddie SL, Lantvit DD, E Óh, **Modi DA**, Wei JJ, Burdette JE: Mutant p53 expression in fallopian tube epithelium drives cell migration. Int. J. Cancer **2015**, 137(7):1528-1538.

3. **Modi DA**, Sunoqrot S, Bugno J, Lantvit DD, Hong S, Burdette JE: Targeting of follicle stimulating hormone peptide-conjugated dendrimers to ovarian cancer cells. Nanoscale **2014**, 6(5):2812-2820.

4. **Modi DA**, Shepherd S: White Paper AbbVie Inc. **2014**

5. Hilliard TS, **Modi DA**, Burdette JE: Gonadotropins activate oncogenic pathways to enhance proliferation in normal mouse ovarian surface epithelium. Int. J. Mol. Sci. **2013**, 14(3):4762-4782.

6. King SM, **Modi DA**, Eddie SL, Burdette JE: Insulin and insulin-like growth factor signaling increases proliferation and hyperplasia of the ovarian surface epithelium and decreases follicular integrity through upregulation of the PI3-kinase pathway. J. of Ovarian Res. **2013**, 6(1):12.

PRESENTATIONS

Oral Presentations

November 2015	Regulation and functional significance of PAX2 in the fallopian tube epithelium and high-grade serous ovarian carcinoma. Center for Biomolecular Sciences seminar series, UIC, Chicago, IL
October 2015	Regulation of PAX2 in fallopian tube epithelium and high-grade serous ovarian carcinoma. 7th Illinois Symposium on Reproductive Sciences, University of Illinois at Urbana-Champagne, Champagne, IL
April 2014	Getting your *PAX* straight: Is loss of PAX2 the missing link in ovarian carcinogenesis? Center for Pharmaceutical Biotechnology seminar series, UIC, Chicago, IL

Poster Presentations

October 2015	Regulation of PAX2 in fallopian tube epithelium and high-grade serous ovarian carcinoma**.** American Association for Cancer Research - Ovarian Cancer, Orlando, FL
September 2014	PAX2 transcription factor regulation and function in early events of fallopian tube epithelial-derived serous cancers. American Association for Cancer Research - Ovarian Cancer, Seattle, WA
April 2014	Regulation Of Pax2 Expression In High Grade Serous Ovarian Cancer. University of Illinois Cancer Center Research Forum, Chicago, IL
October 2014	PAX2 transcription factor regulation and function in early events of fallopian tube epithelial-derived serous cancers. 6th Illinois Symposium on Reproductive Sciences, UIC, Chicago, IL
October 2013	Regulation of PAX2 expression in high-grade serous ovarian cancer. 5th Illinois Symposium on Reproductive Sciences, Southern Illinois University, Carbondale, IL

February 2013	Gonadotropins activate oncogenic pathways to enhance proliferation in normal mouse ovarian surface epithelium. UIC College of Pharmacy Research Day, Chicago, IL
October 2012	Regulation of AKT pathway in mouse ovarian surface epithelium (OSE) by gonadotropin stimulation. 4th Illinois Symposium on Reproductive Sciences, Northwestern University, Chicago, IL
February 2012	Insulin signaling in OSE proliferation and ECM deposition in a 3D model of normal ovarian Surface epithelium. UIC College of Pharmacy Research Day, Chicago, IL
November 2010	Role of His192 in mammalian intestinal oligopeptide transporter-hPepT1. American Association of Pharmaceutical Scientists Annual Meeting, New Orleans, LA
October 2010	Role of His192 in mammalian intestinal oligopeptide transporter-hPepT1. Moving Targets Symposium, University of Southern California, Los Angeles, CA

AWARDS AND HONORS

February 2016	W. E. Van Doren Scholar Award, UIC College of Pharmacy
January 2016	Graduate Student Council Travel Award for presenting research at AACR conference
December 2015	Graduate College Student Presenter Award for presenting poster at AACR conference
October 2015	Best Scientific Podium Presentation award (third place), 7th Illinois Symposium for Reproductive Sciences (ISRS)
2015 and 2013	Chancellor's Student Service and Leadership Award (CSSLA) at UIC
April 2015	Women in Science and Engineering (WISE) Graduate Research Honorable mention
March 2015	Selected for membership of Rho Chi Pharmacy honors society-Phi Chapter
September 2014	Pre-doctoral Education for Clinical and Translational Scientists Fellowship
October 2014	Best scientific poster presentation award, 6th ISRS

April 2014	Best scientific poster presentation award, University of Illinois Cancer Center Research Forum
November 2013	Chancellor's Graduate Research Fellowship, UIC
February 2013	W. E. Van Doren Scholar Award, UIC College of Pharmacy

LEADERSHIP EXPERIENCE

2013 - Present	**Secretary**, Expanding Your Horizons Chicago
2013 - 2014	**Chairperson**, American Association for Pharmaceutical Scientists - UIC Student chapter
2010 - 2011	**Chairperson** of Pharmacy Education, International Pharmaceutical Students' Federation

ACTIVE PROFESSIONAL MEMBERSHIPS

2015 - Present	American Association for Cancer Research (AACR)
2008 - Present	Indian Pharmaceutical Association (IPA)